

FRP STAY IN PLACE FORMWORK

A thesis report submitted
in partial fulfillment of the requirements
for the award of degree of
MASTER OF ENGINEERING
In
STRUCTURAL ENGINEERING

Submitted By
REEMA GOYAL
Roll No. 800822008

Under the Supervision of

DR. ABHIJIT MUKHERJEE
Director
Thapar University (Patiala)

DR. SHWETA GOYAL
Asstt. Prof. (CED)
Thapar University (Patiala)



DEPARTMENT OF CIVIL ENGINEERING
THAPAR UNIVERSITY
PATIALA-147001
2010

CERTIFICATE

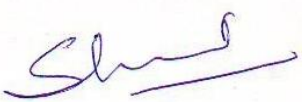
I hereby certify that the work which is being presented in this thesis entitled, "FRP Stay In Place Formwork", being, in partial fulfillment of the requirements for the award of degree of Master of Engineering in Structural Engineering submitted in Civil Engineering Department of Thapar University, Patiala, is an authentic record of my own work carried out under the supervision of Dr. Abhijit Mukherjee and Dr. Shweta Goyal and refers other researcher's works which are duly listed in the reference section.

The matter presented in this thesis has not been submitted for the award of any other degree of this or any other university.



Reema Goyal

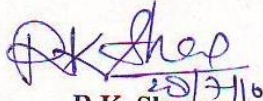
This is to certify that the above statement made by the candidate is correct and true to the best of my knowledge.


Dr. Abhijit Mukherjee
Director
Thapar University


Dr. Shweta Goyal
Asstt. Prof. (CED)
Thapar University

Countersigned by :-


Dr. Maneek Kumar
Professor and head
Civil Engineering Department
Thapar University


R.K. Sharma
Dean Academic Affairs
Thapar University

ACKNOWLEDGEMENT

I express my sincere gratitude to my guides **Dr. Abhijit Mukherjee, Director and Dr. Shweta Goyal, Asstt. Prof., Department of Civil Engineering, Thapar University, Patiala** for acting as supervisors and giving their valuable guidance during the course of this thesis.

I do not find enough words with which I express my gratitude to entire faculty and staff of **Department of Civil engineering, Thapar University, Patiala** for their help, inspiration and moral support, which went a long way in successful completion of my thesis.

I would also like to thank Vivek Singla, IInd year B.E student, Department of Civil Engineering for his support and help during the course of my thesis.

Last but not the least my family and friends for helping me complete my thesis.

DATE: 16/7/10

PLACE: Patiala

Reema
REEMA GOYAL

Abstract

The new approach for the construction of durable concrete structures is investigated in this research. The aim of this thesis is to develop a novel concept for a hybrid FRP –concrete slab system, in which FRP serves the dual purpose of stay in place formwork when concrete is in wet stage and as reinforcement when concrete has hardened. The system simplifies and accelerates construction and the non corrosive GFRP forms can replace steel rebars, thus negating the problem of steel corrosion when exposed to environment.

The purpose of this research was to conduct experimental and analytical studies on the use of GFRP section consisting of GFRP plates stiffened with GFRP channels, as stay in place formwork and reinforcement for concrete slabs. Different GFRP hand lay up sections having different layers of GFRP in plates and channels, different number and arrangement of channels (longitudinal and transverse) are investigated in this work to find out the suitable GFRP section which can satisfy the deflection and strength criteria. 1m long slabs are tested for both wet concrete loading and ultimate strength. 3m long FRP SIP was prepared using connectors which connected three 1m long GFRP forms and were tested for concrete loading to evaluate the performance of connectors.

This thesis contains the results of concrete load testing on two single span stiffened double layered forms with and without transverse stiffeners. It also includes structural and non structural testing of stiffened four layer forms. Effect of aggregate bonding to the form during structural and non structural testing was studied. One double layered and one four layered three span form was subjected to non structural testing.

It was observed that stiffened double layer forms are not suitable for their use as form work. But stiffened four layer forms satisfy both strength and deflection criteria. It was observed that aggregate bond system increases the initial crack load and the ultimate tensile strength. It was concluded that Four layer base form stiffened with four no. four layer channel section can serve the purpose of both formwork and reinforcement.

TABLE OF CONTENTS

Certificate	i
Acknowledgement	i
Abstract	iii
Table of Contents	iv
List of tables	viii
List of Figures	xii
CHAPTER 1: INTRODUCTION	1-7
1.1 Introduction	1
1.2 Origin of Project	3
1.3 Objectives	5
1.4 Scope of the Work	5
1.5 Outline of the Thesis	6
CHAPTER 2: FRP STAY IN PLACE FORMWORK	8-14
2.1 General	8
2.2.1 Fibre Reinforced Polymers	8
2.2.2 Properties of FRP Composites	8
2.2.3 Advantages of Composites	11
2.2.4 Applications of FRP	11
2.3.1 Stay In Place Formwork System	12
2.3.2 Open SIP FRP Forms	13

CHAPTER 3: LITERATURE REVIEW ON OPEN FORM SYSTEMS	15-46
3.1 General	15
3.2 Bond Mechanisms between Concrete and Structural Forms	15
3.3 Different Stay in Place Structural Open Form Systems	28
3.3.1 Hybrid FRP-Concrete Sandwich Panels	28
3.3.2 Steel-Free Composite Slab on Girder	29
3.3.3 FRP Box Girder with Concrete in the Compression Zone	30
3.4 Flexural Behaviour	33
3.5 FRP SIP Formwork in Bridges	36
CHAPTER 4: STEPS OF INVESTIGATION	46-51
4.1 Introduction	46
4.2 Material Selection Criteria	46
4.3 Analytical Work	48
4.3.1 Double Layer Base Form Stiffened with Single Layer Channel Sections	48
4.3.2 Four Layer Base Form with Four No., Four Layer Channels	49
CHAPTER 5: PREPARATION OF BASE FORM	51-64
5.1 Introduction	51
5.2 GFRP SIP Formwork	51
5.3 Channels	52
5.4 Base Forms	54

5.4.1 Double Layer Stiffened Base Form	54
5.4.1.1 Single Span Form	54
5.4.1.2 Three Span Forms	57
5.4.1.3 Form with Transverse Stiffener	60
5.4.2 Four Layer Base Form	60
5.4.2.1 Single Span Form	60
5.4.2.2. Three Span Forms	62
5.4.2.2.1 Double Layer Connectors	63
CHAPTER 6: EXPERIMENTAL PROGRAM	64-126
6.1 Introduction	64
6.2 Materials Used	64
6.3 Lab Equipments Used	66
6.4 Non-Structural Testing of Single Span Forms	66
6.4.1 Double Layer Base Form D11	67
6.4.2 Double Layer Stiffened D21 Form	69
6.4.3 Four Layer Stiffened Form F11	71
6.4.4 Four Layer Stiffened Form F21	73
6.4.5 Four Layered Stiffened Form F31	73
6.5 Non-Structural Testing of Three Span Forms	75
6.5.1 Double Layer Stiffened Three Span Form D13	75
6.5.2 Four Layered Stiffened Three Span Form F23	76
6.6 Structural Testing	78

6.6.1 F11 Slab	79
6.6.2 F21 Slab	79
6.6.3 F31 Slab	79
CHAPTER 7: RESULTS AND DISCUSSIONS	81
7.1 Introduction	81
7.2 Single Span Forms	81
7.2.1 D11 Stiffened Double Layer Base Form coated with Aggregates	81
7.2.2 D21 Double Layer Base Forms Stiffened with Longitudinal and Transverse Channels	84
7.2.3 Four layer forms stiffened with four layer channel sections (F11)	89
7.2.4 Stiffened Four Layer Base Form with Aggregates (F21)	93
7.2.5 Four Layer Stiffened Channel F31	97
7.3 Three Span Forms	99
7.3.1 Three Span Stiffened Double Layer Forms D13	99
7.3.2 Three span four layered stiffened base form (F23)	105
7.4 Structural Testing of Forms	110
7.4.1 F11 Slab	110
7.4.2 F21 Slab	118
7.4.3 F31 Slab	

CHAPTER 8: CONCLUSION AND SCOPE FOR

FURTHER STUDIES	126-127
8.1 General	126
8.2 Conclusion	126
8.3 Scope for Further Work	126
REFERENCES	127
APPENDIX A	131
APPENDIX B	134
APPENDIX C	135

List of tables

Table No.	Description	Page No.
2.1	Typical fiber properties	9
2.2	Typical matrix properties	10
2.3	Mechanical properties of CFRP and GFRP	10
3.1	Dimension of fabricated FRP plank reinforced beam Specimens	19
3.2	Summary of test matrix for slabs	25
3.3	Summary of test results for slabs	25
3.4	Summary of test matrix for girders	26
3.5	Summary of test results for girders	27
6.1	Details about the forms used	65
7.1	Deflection at various points during wet concrete loading in D11	82
7.2	Deflection of form D21 during sand loading	86
7.3	Deflection of form D21 during wet concrete loading	86
7.4	Deflection of F11 during sand testing	90

7.5	Deflection of F11 due to wet concrete loading	90
7.6	Creep deflection of form F11	91
7.7	Deflection of form F21 during sand testing	95
7.8	Deflection of form F21 during wet concrete loading	95
7.9	Deflection of form F21 taking into account creep effects	96
7.10	Deflection at various points in form F31	98
7.11	Deflections at various load levels in form D13	100
7.12	Deflection at various points on form F23 during wet concrete loading	105
7.13	Creep deflection at various points in form F23	106
7.14	Deflection at various points after removal of jacks.	110
7.15	Deflection in F11 slab during ultimate load test	111
7.16	Deflection during ultimate load test of form F21	118
7.17	Deflection during ultimate load testing of for F31	123

List of figures

Figures	Description	Page No.
2.1	Use Of FRP Composite In Civil Engineering	12
2.2	Different configurations of FRP structural forms for concrete members	14
2.3	Some commonly available FRP sections	14
3.1	Concrete and GFRP ribbed sheet hybrid section	16
3.2	Average Bond Stress with Slip	17
3.3	12 inch wide pultruded FRP plank	18
3.4	Dimension of fabricated FRP plank reinforced beam specimens	18
3.5	Specimens 1-3 and C1 after test	19
3.6	Specimens 4-5 and C2 after test	20
3.7	GFRP profile and concrete fill configuration	21
3.8	Load deflection response	22
3.9	Selection of formwork used	22
3.10	Flat pultruded FRP plates for slabs	24
3.11	Trapezoidal pultruded GFRP section used for girders	24
3.12	Test results of slabs 1 to 4	26
3.13	Load-deflection responses of girder specimens	27

3.14	Cross-section of hybrid sandwich beams	29
3.15	Steel-free composite slab-on-girder design	30
3.16	Novel FRP/concrete hybrid flexural member	31
3.17	Dimensions of girder 6 and 7	32
3.18	Dimensions of girder 8	33
3.19	Effect of flange thickness (t)	35
3.20	Moment curvature relationship	35
3.21	Moment curvature relationship	35
3.23	SIP FRP deck panels, FRP rebars, and bi-directional FRP grid during placement	38
3.24	Construction stages	39
3.25	Completed stage	39
3.26	Cross-section structural SIP forms for deck component.	40
3.27	Hybrid tube bridge system	41
3.28	Gridform reinforcement panels: longitudinal section (a) and close-up (b)	43
3.29	Gridform detailing: panel-to-panel overlap connection (a, b); anchoring to girder (c); and cutting of end panels at expansion joint (d).	43
3.30	Installation of CDS deck panels	44
3.31	SafPlank panel	44
3.32	Gridform reinforcement detail	45

3.33	Load and deflection behaviour for panel specimens.	45
5.1	WRM 450 gsm GFRP used for making forms	51
5.2	(A) single layer channel (B) four layer channel	52
5.3	Mould for making channel	53
5.4	Applying gel coat on mould	53
5.5	Applying fiber sheet on mould	53
5.6	Applying resin coating on fiber sheet	54
5.7a	Connection of channels with the base form	54
5.7b	Detailed dimensions in mm of the double layered form	55
5.8	Provision for wooden side forms	55
5.9	Applying initial resin layer on glass platform	56
5.10	Glass fiber single layer and resin coating on glass platform	56
5.11	Removing single layer sheet from glass platform	57
5.12	Prepared double layer base form with stiffener channels	57
5.13	Three 1m span forms placed adjacent to each other before connection	58
5.14	Position of joints in three span double layered base form	58
5.15	Forms after first connection layer	59
5.16	Layout of two connecting layers	59
5.17	Double layer base form with both longitudinal and transverse stiffeners	60

5.18a	Description of four layer base forms	61
5.18b	Dimensions in mm of four layered form	61
5.19	Four layer base form stiffened with channels	61
5.20	Position of joints	62
5.21	Connection arrangement using two layers	63
6.1	Form D11 coated with aggregates	67
6.2	Cross sectional area of slab to be casted	68
6.3	Test set up for form D11	68
6.4	Test set up for form D11	69
6.5	Location of points where deflection was measured	69
6.6	Position of dial gages on form D21	70
6.7a	Front view of the test set up	70
6.7b	Top view showing form within side forms	70
6.8	Sand loading test being done on form D21	71
6.9a	Position of dial gages in form F11	72
6.9b	Sand loading test on form F11	72
6.10	Slab casted on form F11	72
6.11	Aggregates bonded to form F21	73
6.12	Position of dial gages in form F31	74
6.13	Side forms around the base form	74

6.14	Use of needle vibrator	74
6.15	Slab casted on form F31	74
6.16	Test set up for three span beams	75
6.17	Position of dial gages on form D13	76
6.18	Sand test being carried out on form D13	76
6.19	Use of car jacks during testing of form F23	77
6.20	Position of dial gages if form F23	77
6.21	200mm slab casted on form F23	78
6.22	Position of dial gages during jack removal	78
6.23	Structural testing of slab on form F11 with unstiffened supports	79
7.1	Location of points where deflection was measured	82
7.2	Load deflection plot at various points in form D11	83
7.3	Excessive deflection during slab casting on form D11	84
7.4	Buckling of channels in form D11	84
7.5	Location of deflection measurement points in form D21	85
7.6	Deflection at various points during sand loading (D12)	87
7.7	Load deflection plot of form D21 during wet concrete loading	88
7.8	Excessive deflection of form D21	88
7.9	Points where deflection was measured in form F11	89

7.10	Prepared slab on form F11	91
7.11	Load deflection plot at various points for form F11 during sand testing	92
7.12	Load deflection plot for various points in form F11 during wet concrete loading	93
7.13	Points where deflection was measured in form F21	94
7.14	Load deflection plot at various points in form F21 due to sand loading	96
7.15	Load deflection plot at various points for form F21 due to wet concrete loading	97
7.16	Location of deflection measurement points in form F31	98
7.17	Load deflection plots for form F31	99
7.18	Points of deflection measurement in form D13	100
7.19	Load deflection curve for points on central pan during sand testing	101
7.20	Load deflection curve for points on side span during sand testing on form D13	102
7.21	Load deflection plot for points on side span during sand load test on form D13	103
7.22	Comparison between deflection at central form and side forms	104
7.23	Delamination of the second connector layer	104
7.24	Points where deflection measurement was taken for form F23	105
7.25	Deflections at various load levels on the central span form	105

7.26	Load deflection plot for side forms	107
7.27	Load deflection plot for side span	108
7.28	Comparison between deflection at central span and side spans	109
7.29	Deflection measurement points at the removal of jacks	110
7.30	Points where deflection was noted during ultimate load test	110
7.31	Deflection during ultimate load test	113
7.32	First crack	114
7.33	More cracks at load 150KN	114
7.34	Slight delamination at load of 210KN	115
7.35	Widening of cracks at 200KN	116
7.36	Breakage of form F11	117
7.37	Delamination of channels	117
7.38a	Deflection during ultimate load test of form F21	120
7.38b	First crack in F21 slab	121
7.39	Horizontal cracks and delamination in F21 slab	121
7.40	Delamination of form F21	122
7.41	Deflection during ultimate strength testing of form F31	124
7.42	Sudden brittle failure of form F31	125

CHAPTER 1

INTRODUCTION

1.1 INTRODUCTION

Fiber reinforced polymer (FRP) composites have an extensive history of successful use in the aerospace, defence, marine, corrosion resistant equipments and automotive sectors. However until few years back they were largely considered to be of limited value in civil infrastructure beyond use in facades, aesthetic additions and for architectural purposes. Their key advantages, such as free form and tailorable design characteristics, strength to weight ratio that significantly exceed those of conventional civil engineering materials and a high degree of chemical inertness in most civil environments were lost in high material and manufacturing costs. But now there has been growing interest in the use of composites due to advances in low cost manufacturing methods, reduced material demand in high cost areas (for example, defence), the ability to mould complex shapes, and the economic viability of composites when combined with conventional materials.

FRP composites today are used in variety of applications ranging from replacement for steel rebars and tendons used conventionally as tensile reinforcement in concrete, jackets for retrofit of column and externally bonded reinforcement for the rehabilitation of deteriorating structural systems, to use in all composite structures such as building frames and even bridge decks. Despite their relative newness, these materials (primarily using E glass and carbon reinforcing fibers), are being increasingly adopted for specific applications on part with, and even in preference to conventional materials such as steel and concrete. The attractiveness of composites is not merely based on performance attributes such as high specific strength and specific stiffness and corrosion resistance, but also due to their light weight and ease of installation in the field, tailorable anisotropy, and ability for rapid installation and potential for long term durability.

Composites have found their maximum current use as material for rapid and cost effective rehabilitation (retrofit, repair and strengthening) of deteriorated and under-strength structural concrete components. New construction with composites has also become of interest in the civil and the structural engineering areas. New construction can be with all FRP solutions or new composite FRP/concrete system. Use of FRPs in the form of Stay In

Place (SIP) structural formwork for concrete is an example of use of FRPs in new construction. Structural SIP formwork is a type of formwork which is not removed after the concrete has been cast and it acts as a formwork during plastic stage of concrete and as reinforcement when concrete has hardened. Since these forms have excellent stiffness and dimensional stability, the need for scaffolding or shoring is greatly reduced or eliminated completely. In this case, the FRP formwork can simply be rested on supports at either end of the span, and then the concrete can be poured onto the formwork. In essence, the resultant member is a concrete/FRP hybrid member in which each of these materials is utilized efficiently; the FRP resists tension, and the concrete primarily resists compression. While the initial cost of FRP stay-in-place forms is likely greater than that of conventional concrete forms fabricated from wood or steel, this additional cost would be offset by improved ease and speed of erection, and reduced life-cycle costs of the overall structure due to superior longevity and durability.

Although there is abundant research information on the use of FRP in concrete as internal or external reinforcement, the performance of FRP as formwork for concrete structure needs special attention. Though the use of FRP SIP formwork in the form of tubes for beams, columns, piers, piles and girders has gained wide popularity and are being widely used but the use of open forms as the forms for slabs, beams, bridge decks is still very limited.

In India until now there has been no use of FRPs as formwork either with open or tubular forms. But the use of FRPs as SIP formwork is now days very popular in various developed countries and research work on large scale is going on. One important example of research work in the field of FRP SIP formwork is the recent research conducted at the University of Wisconsin demonstrating the evolution of SIP reinforcing system to include FRP SIP formwork. An outcome of this research is a cost-effective, structural FRP SIP formwork system integrated with reinforcement for concrete highway bridge decks.

Parameters that effect strength and durability of FRP formwork include concrete strength, type of fibers and resin, fiber volume fraction and fiber orientation in the forms, form thickness and interfacial bond between the core and the form. Also, shape of the cross section and slenderness ratio can directly impact the confinement effectiveness of the form. There are no codes or guidelines available till now on the behaviour of FRPs as SIP formwork. Whilst a very few experimental studies have investigated the participating behaviour between FRP formwork and concrete, there are still many issues which remain

unexplored. It is essential that some basic aspects be addressed if efficient and cost effective use of FRP SIP formwork is realised. These aspects include shape optimisation, bond mechanism, bond failure behaviour, serviceability performance, ultimate limit state behaviour and finally long term durability for environmentally exposed structures. It is by the intelligent, rational and innovative use of these materials that light weight but at the same time strong and durable construction system may be achieved.

In this thesis experimental investigation has been done on the use of GFRP SIP formwork for concrete slabs. The SIP formwork used in this thesis is an open formwork in which flat GFRP (glass fiber reinforced polymer) base form is stiffened by GFRP channels. This formwork also acts as reinforcement when concrete has hardened. There has been no other steel reinforcement provided in concrete slabs. Because of the relatively short time FRP materials have been on the market and available for use in structural applications, there has not been enough time for the evolution of a prescribed design methodology for the use of FRP in reinforced concrete slabs. Therefore in general, the purpose of this thesis is to evaluate different proposed GFRP SIP formwork systems structural performance and determine if it can satisfy some critical general strength and serviceability requirement for concrete slab designs through laboratory testing and use of some analytical tools.

1.2 ORIGIN OF PROJECT

One of the key objectives of construction research is to develop innovative, economical and efficient method of construction. Initially steel was used as SIP formwork but it was not so popular because of corrosion problems which led to shorter life and high maintenance cost. Recent advances in composite materials for civil engineering have created interesting possibilities for replacing conventional structural forms with components made up of fiber reinforced composite materials. Composite materials offer several advantages over conventional materials such as superior strength/weight ratio, a better stiffness / weight ratio, a high degree of chemical inertness and flexible custom design characteristics.

Durability and structural integrity of concrete structures are adversely affected in aggressive environment through permeability of concrete and corrosion of embedded reinforcing steel. Concrete with formwork made up of FRP can be used as solutions for these problems. As an alternate to conventional reinforced concrete, concrete structures with FRP SIP formwork can increase both durability and strength of the structure.

FRP pre formed shapes in the form of stay in place formwork offer multiple advantages of:

1. Light and effective formwork with superior handling characteristics.
2. Efficient and durable transverse confinement reinforcement with ability to generate high lateral confinement pressure in case of tubular formwork and as tensile reinforcement for resisting positive moments in case of open formwork.
3. Protective shell against corrosion, weathering and chemical attack.
4. The use of FRP formwork will improve the seismic performance of the structure.
5. Though it may have comparatively high initial cost due to high cost of FRPs as compared to conventional materials, yet after considering all its benefits like rapid construction, less labour, durability, low maintenance cost its life cycle cost comes out to be less than conventional materials.

All these advantages will benefit both construction (rapid construction using minimal plant and temporary work) and long term maintenance.

Taking into consideration all the above advantages of FRP SIP formwork this thesis was proposed. This thesis will investigate the use of FRP SIP formwork as reinforcement for concrete slabs. The main aim of this thesis is to find out a way for rapid construction with improved durability using GFRP SIP formwork. Until now all work which has been done on open structural formwork has been done for the development of formwork for bridge panels. No work till now has been done for the development of SIP structural formwork for the concrete flexural members in normal constructions like houses.

Basic aim of this thesis is to start the use of FRP SIP formwork from the grass root level. In this work normally available hand layup GFRP sections have been used. Flat FRP plates are stiffened with FRP channel sections. 1m long FRP panels are tested for both their non structural performance and structural performance. 3m long FRP section in which 1m long FRP panels are combined using connectors are also tested in this research only to test their non-structural performance.

1.3 OBJECTIVES

The primary objective of this study is to assess the performance of GFRP section as stay in place (SIP) structural formwork for concrete flexural members. In this study FRP multiple layered flat sheet sections stiffened with FRP multiple layer channel sections are investigated.

The main topics addressed by this study are

1. Investigating the performance of hand layup GFRP base forms in which flat multiple layer GFRP plates are stiffened by different layer channel sections as stay in place formwork when concrete is in wet state and as reinforcement when concrete has hardened.
2. Investigate if cheap and easily available WRM 450 gsm GFRP sheet can be used as formwork and reinforcement for concrete structures.
3. Investigating different single span slab systems using different GFRP SIP formworks with flat GFRP sheet stiffened with GFRP channels.
4. Assessment of the performance of coarse aggregate adhesive bond mechanism at the concrete FRP interface.
5. Examining the deflection at various points in GFRP SIP formwork caused by wet concrete loading during casting of slabs with different GFRP SIP formworks.
6. Simulating the behaviour of hybrid FRP concrete single span slab systems under flexural loading.
7. Examining various failure modes of the slab.
8. Examining the non structural performance i.e. deflection under the sand or concrete loading of three span FRP SIP specimens.

1.4 SCOPE OF THE WORK

The scope of this study includes experimental investigations and analytical models of the behaviour of flexural concrete members reinforced with GFRP stay-in-place structural open formwork.

The experimental investigation was intended to assess the feasibility of using hand lay-up GFRP sections as stay-in-place structural open forms for concrete slabs. In this research work normally available WRM 450gsm glass fibers are used. Basic aim of this thesis is to investigate the use of GFRP as forms from the grass root level i.e. normal constructions. So least expensive and easily available fibers were chosen for research work.

Two different combinations of base forms and stiffener channels were tested. Firstly double layer base form stiffened with three single layer channel sections was investigated. Wet concrete deflection tests were performed. The effect of transverse channels and aggregates bonded to the base form in this combination was also studied. Then based upon the results of this investigation the section was modified. Now a four layer base form was

stiffened with four, four layered channel sections was investigated. Effect of aggregates bonded to base forms was also studied for this four layered section.

Five 1m x0.5m slabs were tried to be casted using both above mentioned combinations and were tested for wet concrete loading. Out of these only three satisfied the deflection limit and were tested in one point bending test to evaluate their structural performance.

Two 3m x0.5m FRP SIP forms were tested for their non structural performance. Out of these one was double layer stiffened base form and other two were four layer stiffened base forms. The structural performance of these 3m long slabs is beyond the scope of this thesis. In these 3m long FRP sections initially three 1m long sections were prepared and then these three 1m sections were attached using connectors. Basic aim of testing these 3m long sections was to evaluate the performance of the connectors.

1.5 OUTLINE OF THE THESIS

The contents of this thesis are listed below

Chapter 2: In this chapter brief basic about FRPs and FRP SIP formwork is presented.

Chapter 3: A brief review of literature pertaining to the topics studied in this investigation is presented in this chapter.

Chapter 4: In this chapter all steps leading to selection of final design are presented. Analytical work regarding deflection is also presented and equivalent form modelling in ANSYS software is also done to get the idea of deformed shapes.

Chapter 5: In this chapter details about preparing double layer stiffened forms and four layer stiffened forms is presented.

Chapter 6: In this work details about the experimental work done during structural and non structural testing of forms is presented.

Chapter 7: Results obtained from the experimental program are presented in this chapter.

Chapter 8: Conclusions drawn from the research are presented in this chapter

CHAPTER 2

FIBER REINFORCED POLYMER

STAY IN PLACE FORMWORK

2.1 GENERAL

A brief description of different types of commonly used fiber reinforced polymers (FRPs) and their properties is presented in this chapter. Factors affecting properties of FRP and applications of FRPs in construction industries are reviewed. Also a brief introduction about FRP SIP open formwork is presented.

2.2.1 FIBER REINFORCED POLYMERS

Composite materials obtained by reinforcing polymer matrices using fibrous materials like glass, carbon or aramid are known as fiber reinforced polymers (FRP) or Advanced Composite Materials. The reinforcing fibers provides the composite with its structural properties such as high modulus of elasticity and high ultimate strength; whereas the matrix binds the fibers together, protects them from damage and distributes stresses among them. The fillers and additives are used as processor performance aids to impart special properties to the end product. The most common matrices are resinous materials such as vinyl ester, polyesters and epoxies.

2.2.2 PROPERTIES OF FRP COMPOSITES

The most common FRPs in civil engineering applications are glass fiber reinforced polymer (GFRP), carbon fiber reinforced polymer (CFRP) and agamid fiber reinforced polymer (AFRP). The fiber and matrices are combined in such a manner that the resulting composite material shows properties that are superior to those of its individual constituents. These properties mainly depend on the fiber volume, fiber orientation, mechanical properties of the constituents and the procedure used to fabricate the composite. FRP composites are anisotropic (properties vary with the direction). Therefore properties of FRP composite are directional, and typically, the most favourable mechanical properties are in direction of fiber placement.

The functional requirements of fibers in FRP are as follows:

1. They should have high modulus of elasticity to give stiffness to the composite.
2. They should have high ultimate strength.
3. They should have low variation of strength between the individual fibers.
4. They should have stability during handling.
5. They should have a uniform diameter.

The fibers are characterised by very high length to diameter ratios. When embedded in polymers, the fibers will improve the stiffness and strength characteristics of the polymers. A summary of typical fiber properties is presented in table 2.1

Table 2.1 Typical fiber properties (Jaffry; 2001)

Material	Density	Modulus of elasticity	Strength in tension	Strain in tension
	kg/m ³	E MPa	f _t MPa	ε _t %
E-Glass	2500	70000	1500-2500	1.8-3.0
S-Glass	2500	86000	4800	-
High-Modulus Carbon	1950	380000	2000	0.5
High-Strength Carbon	1720	240000	2800	1.0
Carbon	1400	190000	1700	-
Boron	2570	400000	3400	-
Graphite	1400	250000	1700	-
Kevlar49	1450	120000	2700-3500	2.0-2.7
Kevlar	1450	60000-130000	2900	-

The matrix should fulfil certain functions. These are:

- 1) To bind the fibers together and to protect their surface from damage during the service life of the composite
- 2) To transfer stresses to the fibers efficiently by adhesion
- 3) To disperse the fibers and to separate them
- 4) To be chemically and thermally compatible with the fibers

A summary of typical matrix properties is presented in table 2.2

Table 2.2 Typical matrix properties (Jaffry; 2001)

Material	Density	Modulus of elasticity in tension E_t	Strength in tension f_t	Strength in compression f_c	Poisson's Ratio ν	Co-efficient of thermal expansion α
	kg/m ³	MPa	MPa	MPa		10 ⁻⁶ /°C
Polyester	1200-1400	2500-4000	45-90	100-250	0.37-0.40	100-120
Epoxy	1100-1350	3000-5500	40-100	100-250	0.38-0.40	45-65
P.V.C	1400	2800	58	-	-	50
Nylon	1140	2800	70	-	-	100
Polyethylene	960	1200	32	-	-	120

Typical mechanical properties of GFRP and CFRP are given in table 2.3

Table 2.3 Mechanical properties of CFRP and GFRP (Jaffry; 2001)

Material	Fibre content	Density	Modulus of elasticity in tension E_t	Strength in tension f_t
	% by weight	kg/m ³	MPa	MPa
Unidirectional GFRP/Polyester laminate	50-80	1600-2000	20000-50000	400-1250
GFRP/Polyester Randomly Oriented Hand lay-up	25-25	1400-1600	6000-11000	60-180
GFRP/polyester Material Metal Dye	25-50	1400-1600	6000-12000	60-200
GFRP/Polyester Woven Roving Hand Lay-ups	45-62	1500-1800	1200-2400	300-350
Sheet Moulding Compound, Unidirectional Laminate	20-25	1750-1900	9000-13000	60-100
Carbon/Epoxy	70	1930	120000	800
Aramid/Epoxy	50-80	-	70000-80000	1000-1400

2.2.3 ADVANTAGES OF COMPOSITES

The main features of the composite materials are their high fracture energy, ease of fabrication, and chemical inertness. The low cost is particularly true for glass reinforced polymers, which involve low material cost, compared to metal processing. The advantages of the composites over the conventional bulk materials are as follows

1. They can be made with high strength and high specific strength (ratio of strength to specific weight)
2. They can be made with high stiffness and high specific stiffness (ratio of stiffness to specific weight)
3. Their density is generally lower than other conventional construction materials.
4. Their strength can be high at elevated temperature.
5. Their impact and thermal shock resistance are good.
6. Their fatigue strength is good often better than metals
7. Their oxidation and corrosion resistance are particularly good.
8. Their thermal expansion is low and can be controlled.
9. Their stress rupture life is better relative to many metals.
10. Their predetermined properties can be produced to meet individual needs,

FRPs are most commonly found as laminates, which are manufactured by unifying a number of thin layers of fibers and matrix into a desired thickness. Orientation and amount of fibers affect the properties of the laminates. Laminates may be available in unidirectional, two dimensional or three dimensional arrangement of fibers. The properties in any direction will be proportional to amount of fibers in that direction.

2.2.4 APPLICATIONS OF FRP'S

Development of FRPs can be considered as one of the biggest advances in material technology in the 20th century. It has found its applications in many fields for instance medicine, communication engineering and other industries. FRPs are also being introduced in the construction industry. Significant research is being conducted in exploring the various uses of FRP in the field of construction. Considerable progress in application of FRPs in bridge engineering has been achieved. One of the most promising applications of FRP in structural engineering appears to be repair and rehabilitation of different members such as beams and columns. The success of structural rehabilitation measures have led to

development of new lightweight structural concepts utilizing all FRP systems or new FRP/concrete composite system

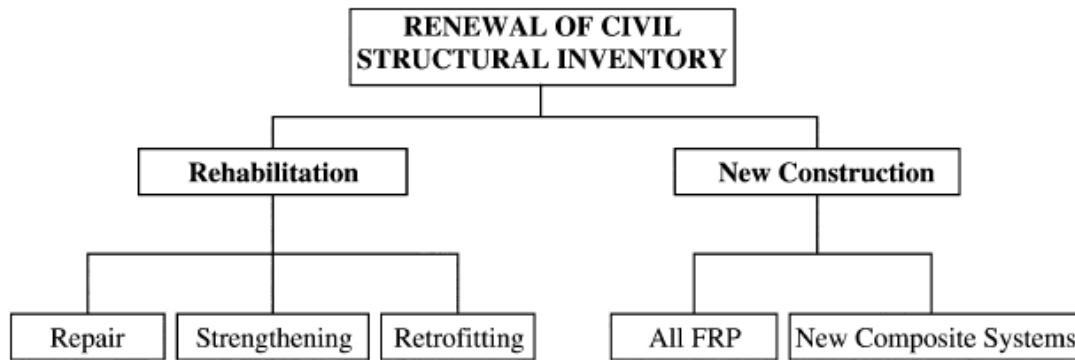


Fig. 2.1. Use of FRP Composite In Civil Engineering (Eindle et al (2003))

2.3.1 STAY IN PLACE FORMWORK SYSTEM

This type of formwork is not removed after the concrete has been cast. With the use of permanent formwork construction speed increases as time for the stripping of the forms is saved. It also results in the saving of labour cost. SIP formwork can be used to improve the constructability and durability of concrete that it encloses. The formwork components are assembled on site, braced and then concrete is poured. After the concrete has gained sufficient strength the bracing is removed and SIP form remains providing exterior shells. It has been found that most of the accidents during construction phase happen while removing the formwork. With the use of SIP formwork these accidents can be prevented. Thus the use of SIP formwork results in fast, economical and safe construction.

Stay in place (SIP) formwork can further be classified into two categories:

1. Structural SIP formwork – These forms part of the structural system that acts compositely with the framing system to resist the in-service live loads as well as wet concrete during casting. In other words they act as reinforcement after the concrete has hardened and as formwork during the plastic stage of concrete.
2. Non structural SIP formwork – These are designed to resist only the loads from the wet concrete and construction live loads until the concrete has hardened.

Structural stay in place are more economical than non structural stay in place forms due to the integration of the formwork with reinforcing system which also reduces the amount of material that needs to be installed

SIP formwork can be made up of:

- 1) Steel
- 2) Reinforced concrete
- 3) Fiber reinforced polymers

2.3.2 OPEN SIP FRP FORMS

The term open form refers to forms that do not completely enclose the concrete within. This type of formwork is essentially a basin into which the concrete is poured. Stay-in-place open structural forms are particularly well suited for applications where positive bending is present. This is because the inherent location of the formwork (at the bottom of the member) allows it to provide tensile reinforcement for resisting positive bending moments. As a result, the majority of research performed on this topic has been related to slabs and beams.

Open formwork can be in the form of open box (Fig.2.2a). This type of formwork is mainly used in girders and beams. It can also be in the form of hollow FRP box with a layer of CFRP at the tension side and concrete at the compression side (Fig. 2.2b). It is mainly used in bridge girders. It can be in the form of flat FRP plate or in the form of FRP plate (Fig.2.3 a) which is pultruded together with I or T shape ribs (Fig.2.2c, 2.3 b, c). When such formworks are used after placing all the plates vertical boundaries are attached at the exterior side and then concrete is poured in. The ribs can be of FRP or any other conventional material. Open FRP forms can also be trapezoidal in shape and can be produced as sheet pile section (Fig. 2.3e). It can be pultruded sheet which is stiffened by hollow FRP boxes (Fig.2.3 d).

Since open forms have excellent stiffness and dimensional stability, the need for scaffolding or shoring is greatly reduced or eliminated completely. In this case, the FRP formwork can simply be rested on supports at either end of the span, and then the concrete can be poured onto the formwork. For successful working of FRP stay in place open formwork both FRP and concrete has to work compositely. FRP resist tension and concrete primarily resist compression.

Till now there has been no widespread use of open formwork. Only few demonstration projects have been done till now with the exception of their use in bridge decks which has gained some popularity and now developed countries like USA and Canada are opting this material for bridge deck construction. This is due to the fact that construction involving FRP SIP formwork is much faster than the construction with conventional formwork. With this traffic delays are avoided and less inconvenience is caused to the public. Life of decks is more when FRP SIP formwork is used and reduces the maintenance cost. Live load carrying capacity is increased with the use of FRP deck panels.

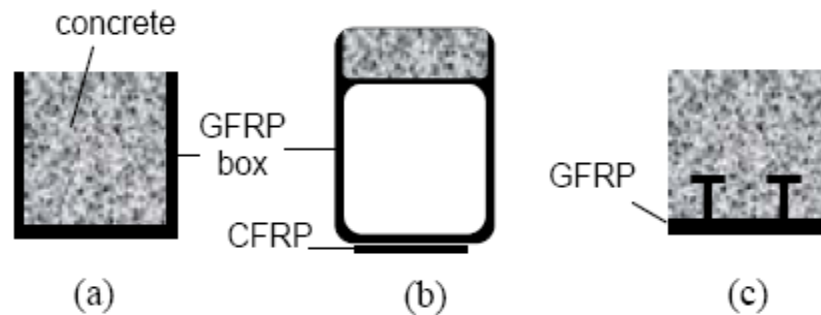


Fig.2.2. Different configurations of FRP structural forms for concrete members
(ACI 440-XR)

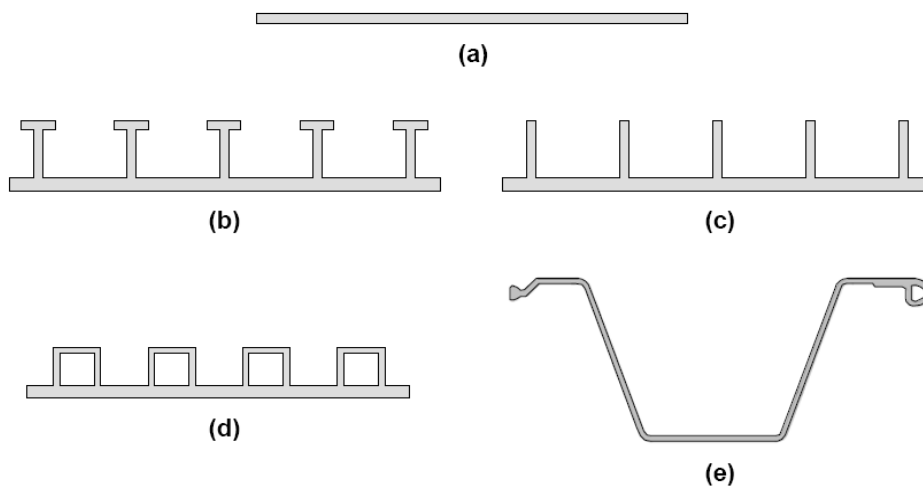


Fig.2.3. Some commonly available FRP sections (Honickman, 2008)

CHAPTER 3

LITERATURE REVIEW ON OPEN FORM SYSTEMS

3.1 GENERAL

This chapter generally reviews research that has been performed on stay-in-place open structural formwork for reinforced concrete flexural members. Firstly, a brief introduction about stay in place formwork is presented. Then a brief introduction about open stay in place formwork is presented. In particular, the chapter addresses FRP profiles that have potential as structural forms, various bond mechanisms, and flexural members that have been developed and studied. It also reviews about the various new techniques by which FRP SIP formwork is used in bridge decks.

3.2 BOND MECHANISMS BETWEEN CONCRETE AND STRUCTURAL FORMS

In order to ensure that stay-in-place open structural forms contribute as tension reinforcement in flexure, it is crucial that an adequate shear connection exists between the concrete and the form. Following studies have been carried out to study the effect of various types of bond mechanisms on the composite action of FRP SIP and concrete.

Hall et al. (1998) worked on a hybrid concrete-FRP section incorporating FRP stay-in-place open structural form. Ribbed FRP sheets produced as floor panels, provided tensile reinforcement, and behaved as permanent stay-in-place open structural formwork for the concrete slab overlay, as shown in Fig.3.1. The resultant concrete-FRP hybrid beams were tested in four-point bending. Initially, it was found that a significant amount of horizontal shear slippage occurred between the concrete and the FRP formwork. This severely limited the flexural capacity of the member since a large strain lag existed between the concrete and FRP.

In an attempt to combat the aforementioned problem, adhesive bonding was used. This was accomplished by applying adhesive (epoxy mortar) directly to the surface of the FRP formwork immediately prior to pouring concrete. This adhesive was specially formulated for bonding to fresh wet concrete. The resultant system behaved monolithically

during positive bending. Plot of mean shear stress versus slip is shown in Fig.3.2. The observed mode of failure was diagonal tension shear cracking in the concrete, which can likely be attributed to the absence of shear reinforcement within the concrete, and the fact that the beams were designed to be over-reinforced. Tension cracking of concrete was severe in the vicinity of the longitudinal stiffening ribs of the FRP sheet. Overall, the concept of applying adhesive to the formwork prior to pouring concrete appears to have yielded positive results. It was an advantageous technique from a fabrication standpoint because it eliminated the need for mechanical shear studs or a bonded coarse aggregate coating on the surface of the formwork, both of which would be far more time consuming to install than an adhesive coating.

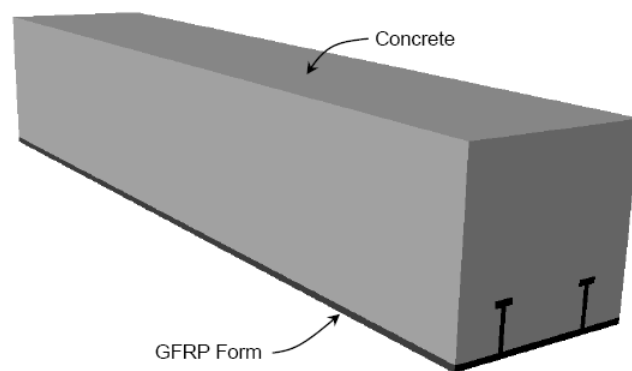


Fig.3.1. Concrete and GFRP ribbed sheet hybrid section (Hall et al., 1998)

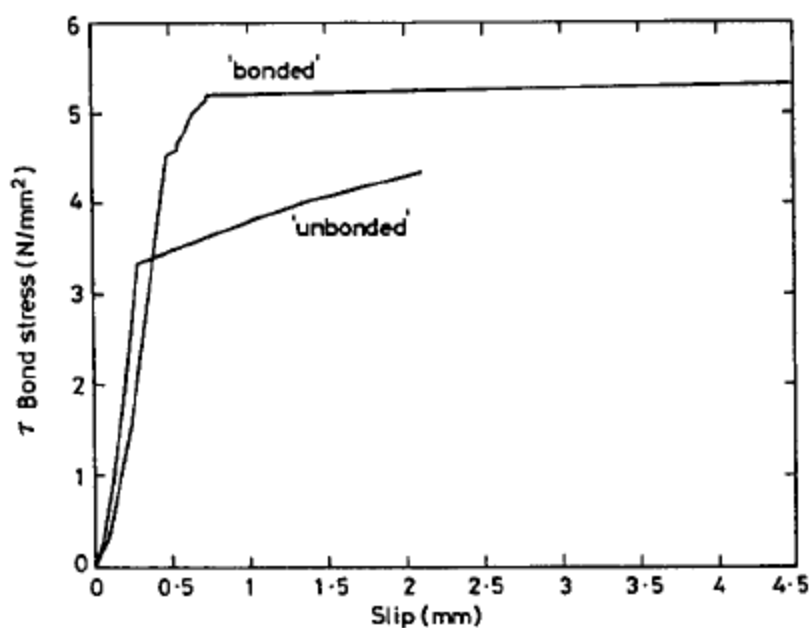


Fig.3.2. Average Bond Stress with Slip (Hall et al., 1998)

Bank et al. (2006) described about the pultruded fiber reinforced polymer (FRP) plank which was used as both the formwork and the tensile reinforcement for a concrete structural member. The study was motivated by the desire to use the FRP plank as a stay-in-place form and reinforcement for a new bridge that was being designed in Wisconsin. For the FRP plank and the concrete to act as a “composite” structural member a satisfactory bond at the interface between the smooth surface of the pultruded plank (Fig.3.3) and the concrete was to be developed. To achieve this interface, stone aggregates of different sizes were bonded to the surface of the pultruded FRP plank. Two kinds of aggregates gravel and sand were bonded to the pultruded FRP plank using a commercially available epoxy system. Concrete beams of different lengths were fabricated using a commercially available pultruded FRP plank. No additional flexural or shear reinforcement was provided in the beams. Two of the beams were used as control specimens. One control beam did not have any aggregate bonded to the FRP plank and the other control had internal steel reinforcing bars instead of the FRP plank. Table 3.1 shows the dimensions of the entire fabricated FRP plank specimen.

The beams were loaded by central patch load to their ultimate capacity. Fig.3.4 shows dimensions of the fabricated beam surface. Depending on the length of the beam, shear or flexural failures occurred, which demonstrated satisfactory bond between the FRP plank and the concrete. Results indicated that coated FRP plank can produce an increase in the initial cracking moment capacity of a concrete beam, which may be a serviceability benefit for a reinforced concrete section, particularly a bridge deck. The beams with the sand coated FRP plank showed higher initial cracking capacity than the specimen with the gravel coated FRP plank indicating that sand coating provided a more even interface than the gravel in the interface region. It was shown that aggregate coating provided a mechanism to distribute the cracks and to transfer bond stresses at the interface between the FRP plank and the concrete.

It was demonstrated that the aggregate coated FRP plank can serve as an effective tensile reinforcement and can distribute flexural cracks in a similar manner to internal steel reinforcements. The aggregate coated FRP plank beams performed as well or better than the steel reinforcement in terms of initial cracking moment capacity, ability to distribute flexural cracks and ultimate load carrying capacity. The use of the FRP plank without the surface treatment as a tensile reinforcement showed the significant slip between concrete and considerably less capacity during test. The ultimate capacity of the aggregate coated FRP plank specimens was higher than that of the control specimens. Fig.3.5 and 3.6 shows the failure mode of all the specimens. This study demonstrated that the FRP plank has the

potential to serve as formwork and as tensile reinforcement for appropriately sized concrete beams.



Fig.3.3. 12 inches wide pultruded FRP plank (Bank et al., 2006)

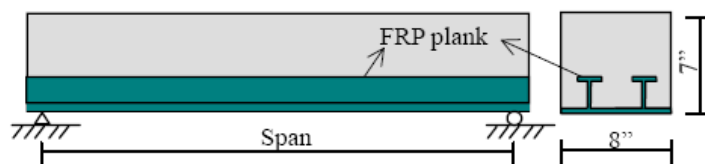


Fig.3.4. Dimension of fabricated FRP plank reinforced beam specimens (Bank et al., 2006)

Table 3.1 Dimension of fabricated FRP plank reinforced beam specimens

(Bank et al., 2006)

Specimen I.D.	Span	Tensile Reinforcement	Compressive Strength(Psi)
1	3'7"	Gravel coated FRP plank	3,740
2	3'7"	Sand coated FRP plank	3,740
3	3'7"	Sand coated FRP plank	3,550
C1	3'7"	FRP plank	3,740
4	6'	Sand coated FRP plank	4,650
5	6'	Sand coated FRP plank	4,860
C2	6'	Sand coated FRP plank	4,775



a) Shear failure of specimen 1



b) Shear failure of specimen 2



c) Shear failure of specimen 3



d) Flexural failure of specimen C1

Fig.3.5. Specimens 1-3 and C1 after test (Bank et al., 2006)



1) Hybrid failure mode of specimen 4



2) Hybrid failure mode of specimen 5



3) Flexural failure of specimen C2

Fig.3.6. Specimens 4-5 and C2 after test (Bank et al., 2006)

Fam et al. (2009) presented a new girder consisting of a trapezoidal pultruded glass fiber-reinforced polymer (GFRP) hat-shaped section which was used in this study as a structural form for concrete. It offered continuity in the transverse direction through a pin-and-eye connection. Five 610 mm x 325 mm and 3,300-mm-long girders were tested in flexure to examine different bond systems, voided and solid concrete cores, and the performance in positive and negative bending. Fig.3.7 shows GFRP profile and concrete fill configurations. Bond systems were wet adhesive bond to freshly cast concrete, adhesively bonded coarse aggregates, and mechanical shear studs (mechanical shear connectors in the form of steel threaded rods anchored to the GFRP flanges). Steel welded wire meshes were installed near the upper surface of the slab of each specimen, mainly for shrinkage crack control.

No slip was observed between concrete and the GFRP section until delaminating failure occurred within a thin layer of cement mortar that remained attached to GFRP. The studs failed by pull out from the concrete flange. In general, 47–75% of the full strengths of concrete and GFRP were reached at ultimate bond failure. Wet adhesive bonding was the simplest and quickest to apply, while resulting in a comparable strength to other systems.

A “moment-curvature” analytical model, incorporating a robust bond failure criterion, was developed, validated, and used in a parametric study. Increasing concrete strength had an insignificant effect on stiffness or the bond failure load. It however, increases flexural strength, when governed by concrete compression failure. Increasing the thickness of the GFRP flanges increased flexural strength and stiffness significantly, but had a negligible effect on the bond failure load.

The voided concrete core in the tension region had an insignificant effect on stiffness. However, because the void extended to the bottom GFRP flange, the reduced bond area resulted in a little reduction, 13%, in strength. Overall, the voided system had a 30% higher strength-to-self weight ratio than the totally filled section. Fig. 3.8 shows the load deflection response of all the specimens. Critical values were found for shear span-to-depth ratio, shear strength of cement mortar, concrete strength, and width of the top GFRP flange, beyond which, the desired flexural failure mode preceded bond failure.

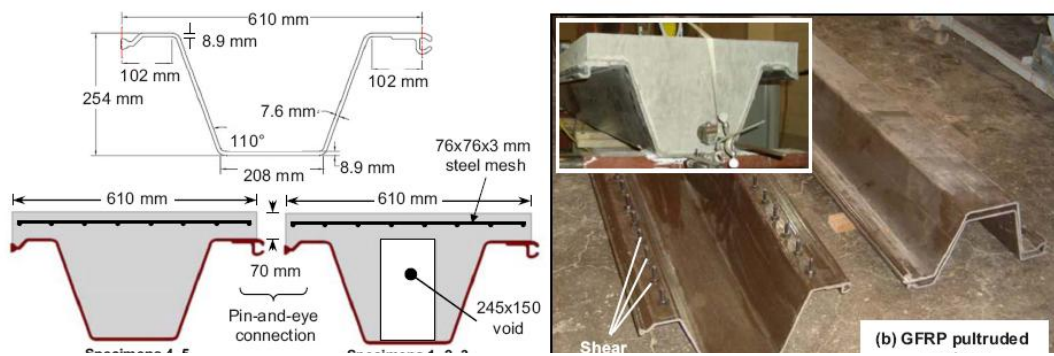


Fig.3.7. GFRP profile and concrete fill configuration (Fam et al., 2009)

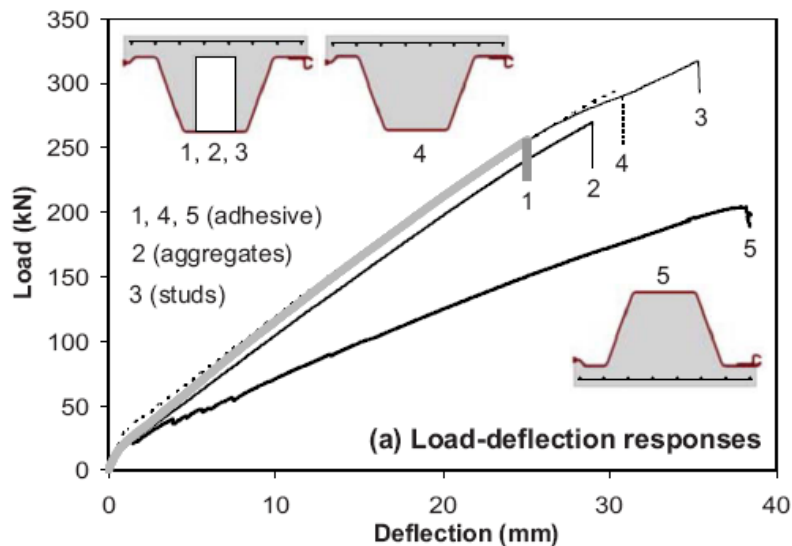


Fig.3.8. Load deflection response (Fam et al., 2009)

Dieter et al. (2002) carried out study on a hybrid concrete-FRP stay-in-place open structural formwork and FRP grid reinforcement for bridge deck applications. A pultruded FRP sheet stiffened by hollow FRP box sections (Fig.3.9) provided tensile reinforcement, and functioned as stay-in-place structural open formwork for the concrete slab overlay. A bi-direction grid composed of pultruded FRP elements provided the upper longitudinal and transverse reinforcement for regions of negative bending moments. In order to generate sufficient shear bond between the FRP stay-in-place form and the concrete slab overlay, the surface of the FRP form was roughened prior to pouring the concrete by coating it with a mixture of epoxy and gravel. Due to the complex geometry of the formwork, this mechanism was only applied to horizontal surfaces. This was found to have a detrimental effect on the

bond performance. In regions where the bond mechanism was absent, severe slippage occurred between the form and the concrete overlay. As a result, the flexural crack pattern in the concrete over unbonded regions was considerably more pronounced than it was in bonded regions.



Fig.3.9. Selection of formwork used (Dieter et al., 2002)

Honickman (2008) investigated glass fiber-reinforced polymer (GFRP) off-the-shelf structural shape as stay-in-place open structural forms for concrete structures, including bridge decks and girders. In this study, eight concrete slabs were constructed using flat pultruded GFRP plates (Fig.3.10), and nine girders were constructed using trapezoidal pultruded GFRP sheet pile sections (Fig.3.11) as stay-in-place structural forms. No tension steel reinforcement was used. All specimens were tested in four-point monotonic uniaxial bending. Table 3.2 and Table 3.4 shows summary of test matrix for slabs and girders respectively.

Bond systems in case of plates included fresh concrete adhesively bonded to the plate, coarse aggregates bonded to the plate prior to casting, and GFRP and steel mechanical shear connectors. The performance of these bond systems was objectively assessed and the failure modes were examined. It was found that the most effective bond system, in terms of structural performance and ease and speed of fabrication, was the wet adhesive bonding of fresh concrete to the GFRP plate. The adhesive bonding methods led to a significantly higher stiffness, than that of the mechanically bonded slabs using shear connectors (Fig.3.12). This was attributed to a complete bond throughout loading in the former, until failure occurred suddenly by debonding; whereas in the latter, progressive slip between the GFRP plate and concrete occurred. He observed that failure was typically due to debonding of the GFRP plate, after flexural or shear cracking in the concrete. The measured low longitudinal strains at mid span suggested that tension failure of the GFRP plate was very unlikely in this system. Compression failure of concrete was imminent in some of the slabs. Table 3.3 gives the summary of test results for slabs.

Four adhesive and mechanical bond mechanisms were explored to accomplish composite action in girders. Mechanism M1 involved a liquid epoxy adhesive applied directly to the surface of the GFRP form immediately prior to pouring the concrete. Mechanism M2 involved applying a rough layer to the surface of the GFRP sections in order to create mechanical interlock between the concrete and the GFRP. This was accomplished by applying a thick mortar-like adhesive to the surface of the GFRP sections, and then applying a layer of 4 to 9mm diameter silica pebble aggregates onto the adhesive. Mechanism M3 utilized shear studs. These studs were created by drilling holes through the upper flat surfaces (flanges) of the GFRP sections, passing threaded steel rods through these holes, and then fastening the rods in place with a nut on either side of the GFRP section. Mechanism M4 was similar to mechanism M3 with the addition of heads on the studs.

It was found that similar to the slabs, girders incorporating either adhesive to wet concrete bond or bonded aggregates systems failed by debonding at the concrete/GFRP interface, within a thin layer of cement paste. A thin layer of mortar remained adhered to the GFRP section after failure. The concrete compressive strain and GFRP tensile strain were well below their ultimate values. The specimen incorporating headed shear studs combined with the adhesive bond system was able to achieve flexural failure by concrete crushing, which occurred at a 45% higher load than that reached by specimens incorporating only the adhesive bond system. The specimen incorporating non-headed studs in addition to the adhesive bond system achieved only a modest increase, 24% in strength, over the specimens incorporating only the adhesive bond system. In this case, failure occurred when the studs pulled out prematurely from the concrete slab. Similar to the slabs, in all adhesively bonded and bonded aggregate girders, excellent monolithic composite action was observed prior to the sudden debonding failure. This was evident by the consistent lack of slip between the concrete and the GFRP throughout the loading history. Summary of test results for girders is presented in Table 3.5.



Fig.3.10. Flat pultruded FRP plates for slabs (Honickman., 2008)



Fig.3.11. Trapezoidal pultruded GFRP section used for girders (Honickman., 2008)

Table 3.2 Summary of test matrix for slabs (Honickman., 2008)

Spec. ID	Length (mm)	Span L (mm)	Shear span a (mm)	Width B (mm)	GFRP plate thickness t (mm)	Total thickness (Rounded) h (mm)	Effective depth d (mm)	a / d	Reinf. ratio ρ (%age)	Bond mechanism
1	1220	1000	375	400	9.5	160	157	2.4	5.7	Concrete cast on wet adhesive
2										Adhesively bonded coarse aggregate
3										GFRP shear connectors
4										Steel shear connectors
5	2440	2200	975			110	106	9.2	8.5	Concrete cast on wet adhesive
6						160	157	6.2	5.7	
7						210	208	4.7	4.3	
8						160	157	6.2	5.7	

Table 3.3 Summary of test results for slabs (Honickman., 2008)

Spec ID	Peak Load	Peak Moment	Strain at peak load		Load at first slip (KN)	Slip at peak load	Failure mode
			Top (Micro)	Bottom (Micro)			
1	149	27.9	-837	1825	149	0	Concrete Shear-bond failure
2	162	30.3	-907	2349	162	0	Concrete Shear-bond failure
3	140	26.2	-4410	2036	43	3.6	shear failure of GFRP studs
4	200	37.5	-2454	3313	66	2.2	Excessive slip of steel studs
5	67	32.5	-2908	3990	67	0	Bond failure
6	87	42.6	-1962	3520	87	0	Bond failure
7	145	70.8	-1585	4693	145	0	Bond failure
8	109	53.2	-2269	4236	109	0	Bond failure

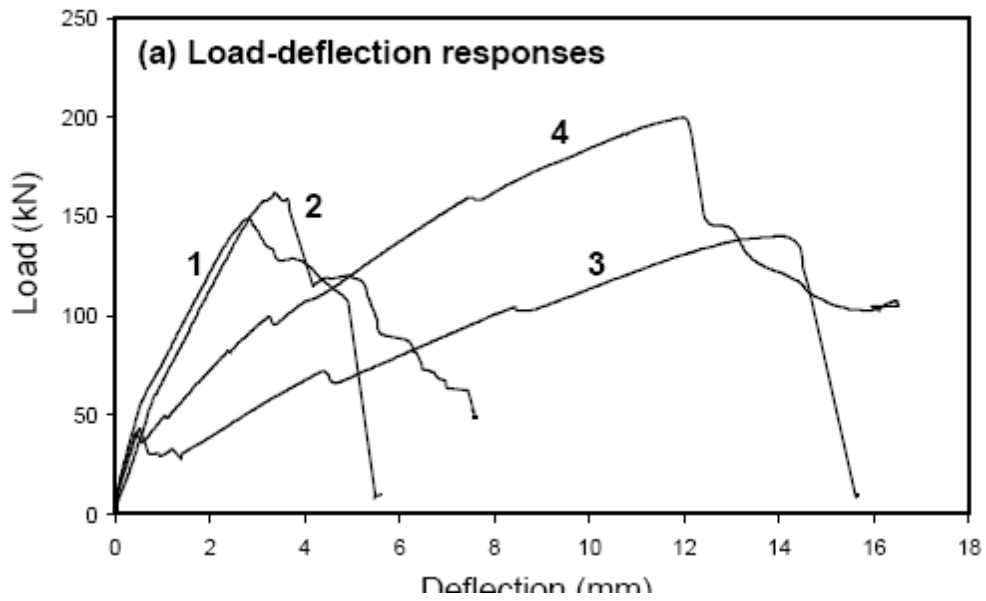


Fig.3.12. Test results of slabs 1 to 4 (Honickman., 2008)

Table 3.4 Summary of test matrix for girders (Honickman., 2008)

	Type	Bond Mechanisms	Concrete fill	Bending orientation
1	1	M1	Voided Concrete	Positive
2	1	M2	Voided Concrete	Positive
3	1	M1 & M3	Voided Concrete	Positive
4	2	M1	Completely Filled	Positive
5	2	M1	Completely Filled	Negative
6	3	M1	Slab on Box Girder	Positive
7	3	M1 & M4	Slab on Box Girder	Positive
8	3	M1 & M4	Slab on Box Girder	Negative
9	3	M3	None	Positive (a) & Negative (b)

Table 3.5 Summary of test results for girders (Honickman., 2008)

Girder	Peak load(KN)	Load at initial bond slip (KN)	Mode of failure
1	250.0	250.0	Bond failure of concrete/GFRP interface
2	269.5	269.5	Bond failure of concrete/GFRP interface
3	317.0	317.0	Vertical pull-out of non headed sheet shear studs
4	294.0	294.0	Bond failure of concrete/GFRP interface
5	204.2	204.2	Lateral opening of GFRP sheet pile section
6	285.0	244.7	Bond failure at concrete/GFRP interface
7	430.0	230.5	Delamination and crushing of concrete slab
8	227.0	47.0	Local buckling and crushing of GFRP section
9a	230.7	NA	Buckling of upper compression flange of GFRP box section

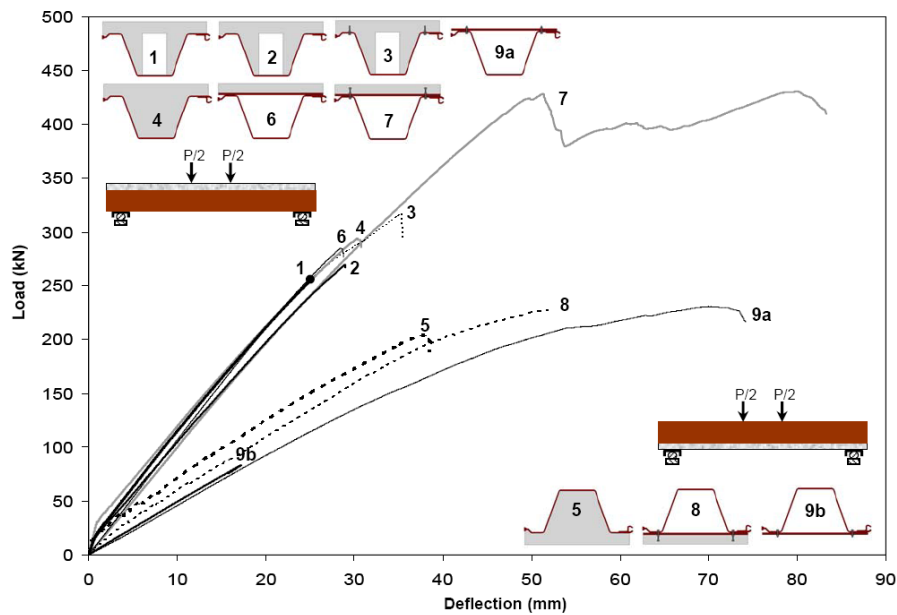


Fig.3.13. Load-deflection responses of girder specimens (Honickman., 2008)

3.3 DIFFERENT STAY-IN-PLACE STRUCTURAL OPEN FORM SYSTEMS

3.3.1 HYBRID FRP-CONCRETE SANDWICH PANELS

Schauman et al. (2008) conducted direct load transmission experiments on hybrid short-span beam specimens for a novel bridge deck. The sandwich construction consists of three layers: a fiber-reinforced polymer composite (FRP) sheet with T-up stands for the bottom skin, lightweight concrete (LC) for the core and the top compression skin of the panel was made from a thin layer of normal density concrete (Fig.3.14). Short-span three-point bending experiments was conducted on eight hybrid FRP-concrete sandwich specimens.

This research provided useful information on the direct load transmission behaviour and the effect of two parameters on the static load-bearing behaviour: the FRP–LC interface (unbonded or epoxy bonded) and the LC composition (low and high density SLWAC (sand light weight aggregate concrete) and ALWAC (all light weight aggregate concrete)). It was shown that specimens with adhesively bonded FRP–LC interfaces showed significantly higher ultimate loads than corresponding unbonded specimens. The ultimate load ratio of bonded to unbonded specimens correlated with the degree of composite action of the unbonded specimens and approached unity for full composite action. The degree of composite action of the unbonded interfaces thereby depended on the LC compressive strength.

Using an ALWAC mixture of high compressive strength provided almost full composite action through pure mechanical interlocking in contrast to a SLWAC mixture of low compressive strength, which lost composite action already after LC cracking. A correlation of the ultimate loads and the LC splitting tensile strengths was found. The cracking load, however, did not exhibit a similar correlation. Combining the splitting tensile strength and the characteristic length, a fracture mechanics property that characterizes material brittleness, led to a good correlation with the cracking loads. Accordingly, the cracking loads of the more ductile SLWAC compositions were significantly higher than those of the brittle ALWAC mixtures, although splitting tensile strength were similar. Ultimate loads or shear resistances of the (SLWAC) were significantly higher (4.4 times on average) than those of the (ALWAC).

The idea of utilising lightweight materials in region of low flexural stresses (near the neutral axis) is quiet attractive because it can significantly reduce the self weight of the

member without an excessive loss of flexural stiffness or strength. However, it is important to recognise that the implementation of such technology could shift the design to one that is limited by its shear strength.

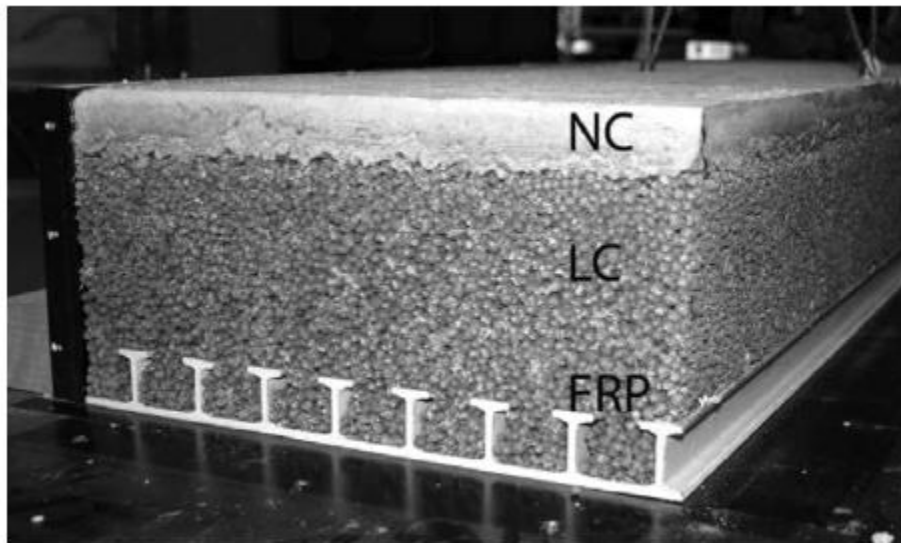


Fig.3.14. Cross-section of hybrid sandwich beams (NC = normal concrete, LC = lightweight concrete, FRP = fiber-reinforced polymer sheet with T up stands).

(Schauman et al., 2008)

3.3.2 STEEL-FREE COMPOSITE SLAB ON GIRDER

Li et al. (2006) investigated a system in which both the steel girder and form were replaced with GFRP sections of comparable dimensions. The system consisted of a pultruded GFRP I-beam (with unidirectional longitudinal fibres) overlaid by pultruded GFRP ribbed sheets (E-shaped sections) oriented horizontally. These ribbed sheets acted as permanent stay-in-place formwork for the concrete slab which was poured on top of the sheets, as shown in Fig.3.15. The ribs on these E-shaped sections were oriented transversely in order to provide adequate stiffness so that these sheets could bear the weight of the wet concrete. This also could potentially aid in providing the completed system with improved flexural strength and stiffness in the transverse direction.

FRP bolts were used to connect the E-shaped sections to the I-beams. These bolts also behaved as shear studs in order to ensure monolithic composite action between the concrete slab and the FRP sections. The resultant composite girders were tested in four-point bending.

Concrete strength and slab thickness were the primary test parameters varied; however, some specimens also included a laminate of carbon-FRP (CFRP) bonded to the bottom flange of the I-beam to improve flexural stiffness and strength. The general mode of failure observed was horizontal shear cracking of the web of the GFRP I-beam. This proved to be a very brittle mode of failure.

The specimens with thicker concrete slabs gave some warning of failure when the bottom of the concrete slab began to crack. This, however, was unrelated to the shear failure mode. It simply illustrated that the neutral axis in this specimen was located within the concrete slab. These cracks served as an indication that large deflections were occurring. The stiffness of the members was largely dictated by the thickness of the concrete slab. A relatively large percentage of deflections were caused by shear deformations occurring within the web of the girder. As a result, the CFRP layers provided very little contribution to stiffness. Also, since the specimens ultimately failed in shear, the addition of the CFRP layers yielded no increase in ultimate strength.

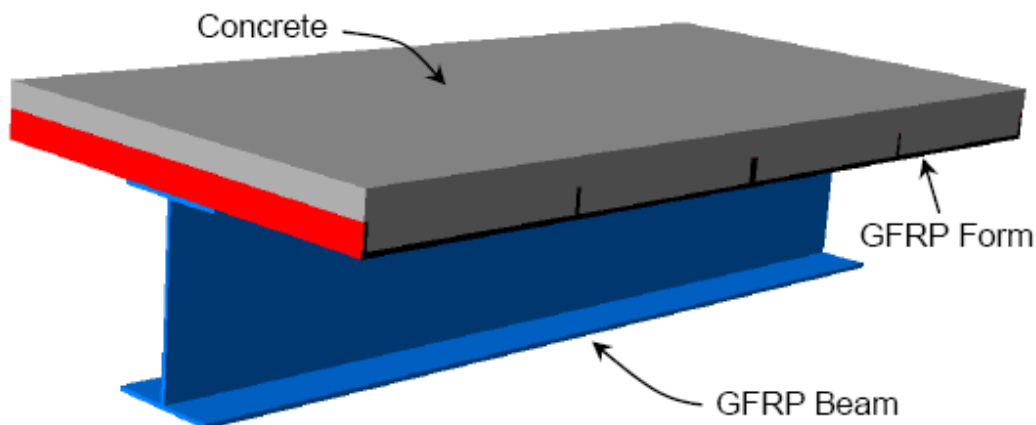


Fig.3.15. Steel-free composite slab-on-girder design (Li et al., 2006)

3.3.3 FRP BOX GIRDER WITH CONCRETE IN THE COMPRESSION ZONE

Deskovic et al. (1995) proposed a novel FRP/concrete hybrid flexural member. The new member was composed of a GFRP rectangular box section that was overlain with a concrete slab (Fig.3.16), and is intended for applications where positive bending is to be resisted. The concrete slab behaved as the compression flange of the member. The upper flange of the GFRP box section behaved as a stay-in-place form for the concrete slab, which

simplifies the construction process considerably. Bond between the concrete and the GFRP section was facilitated by the application of a two-part epoxy adhesive prior to pouring the wet concrete.

The hybrid member also included a CFRP laminate bonded to the bottom surface of the lower (tension) flange of the GFRP box section, to increase flexural stiffness. Also, because CFRP had a lower failure strain than that of GFRP, the CFRP layer would fail prior to the tension flange of the GFRP section, thus providing warning signs of imminent flexural failure (pseudo ductility). This is important since FRP and concrete are both brittle materials that do not provide obvious warning signs prior to failure.

A number of potential failure mechanisms had been studied analytically for this hybrid member. The webs may buckle or fracture, resulting in shear failure; one of the beam's elements could exhibit a flexural failure; the bond between the GFRP section and the concrete slab could fail; and the concrete slab could fail in diagonal shear. The most common mode of failure observed experimentally was debonding between the GFRP section and the concrete slab. Despite this unfortunate premature failure mode, the flexural response of the specimens showed good pseudo ductility as a result of the CFRP laminate tension failure. This study, highlighted the potential of hybrid members composed of hollow GFRP sections overlain with concrete slabs, but it also illustrated that such hybrid systems are highly dependent upon the quality of the shear bond between the concrete and the GFRP section.

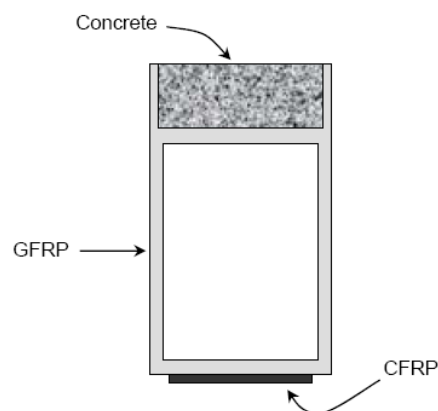


Fig.3.16. Novel FRP/concrete hybrid flexural member (Deskovic et al., 1995)

Honickman (2008) investigated nine girders constructed using trapezoidal pultruded GFRP sheet pile sections as stay-in-place structural forms (ref Fig.3.11). Out of these nine girders one type of specimens were unique in way that they were composed of built up all-

GFRP box sections. These box section girders 6, 7, 8, and 9 were created by bonding flat 9.5mm thick pultruded GFRP sheets, across the upper flanges of the sheet pile sections, resulting in a trapezoidal hollow box section, as shown in Fig.3.17 and Fig.3.18. Girders 6 to 8 incorporated a concrete slab on top of the flat upper sheet of the box section. These slabs were 60mm thick.

He conducted tests on all the specimens. It was found that, the primary difference in behaviour between the slab-on-box sections (6 and 7) and all the other specimens is their lack of a pronounced cracking moment when loaded in positive bending. It was shown that the performance of hollow box sections depended upon the bond mechanism with which FRP plate was connected to box and how concrete is connected to plate. The built-up all-GFRP box section with a concrete slab showed superior performance. When it included headed studs in addition to adhesive bonding, it showed 35% to 70% higher strength than any other specimen. This also occurred in conjunction with a 50% and 65% reduction in weight relative to the voided core and the totally filled specimens, respectively. When the box girder included adhesive bonding only, it showed similar strength to the adhesively bonded totally filled specimen, and 15% higher strength than the adhesively bonded voided core specimen.

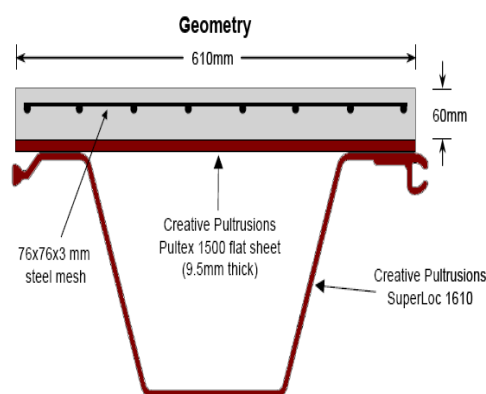


Fig.3.17. Dimensions of girder 6 and 7 (Honickman, 2008)

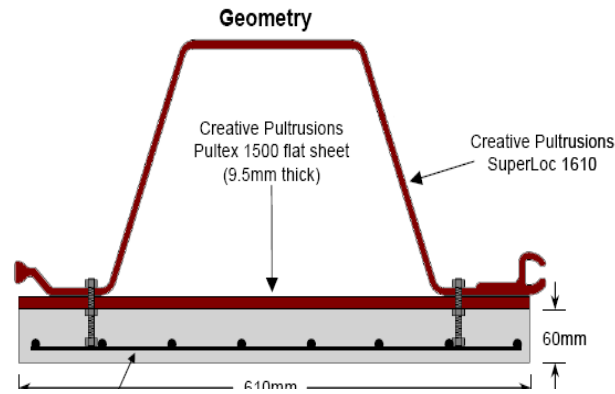


Fig.3.18. Dimensions of girder 8 (Honickman, 2008)

3.4 FLEXURAL BEHAVIOUR

Honickman (2008) in his study of eight slab and nine girders with FRP SIP formwork compared the flexural performance of the hybrid concrete FRP slab and girder system to conventional steel reinforced slabs and girders. He studied the girder systems in both positive and negative bending to simulate continuity.

While flexural stiffness of the slabs increased as their reinforcement ratio was increased, the effect of reinforcement ratio on ultimate moment could not be assessed because of the consistent bond failure, rather than the flexural failure. Conventional steel-reinforced concrete slabs of comparable external dimensions were severely hindered by the requirements to satisfy the limitations of concrete cover. As a result, the concrete-GFRP hybrid system is superior in that the reinforcement is located at the extreme tension fibre. Also, substantial amounts of steel reinforcement are required to match the flexural strength and stiffness of the hybrid sections. It was found that steel-reinforced concrete slabs of comparable flexural strength were considerably stiffer than their concrete-GFRP hybrid counterparts, whereas steel-reinforced concrete slabs of comparable stiffness had considerably lower flexural strength.

The flexural strength of the girders is higher in positive bending than in negative bending by 45% to 90%, depending on cross-sectional configuration. However, since the stiffness is also higher in positive bending by 175% to 225%, the system lends itself to an efficient use in continuous beams, where it can be fully utilized in both positive and negative bending regions. In negative bending, premature failure of the totally filled section occurred by lateral opening of the GFRP sheet pile. In actual applications, however, the sections would be placed side-by-side so that they restrain each other laterally.

In the built-up box sections, the flat plate served as a tie restraining this opening action. In this case, local buckling of the GFRP sheet pile occurred just outside of the grout-filled diaphragm under the load. The analytical model was developed to test theories and concepts pertaining to the complex mechanical behaviour of the aforementioned structural system. The model used cracked section analysis, using a layer-by-layer technique in order to establish the flexural response of the member. It accounts for the non-linearity of the concrete in the section, and adopts conventional empirical tension stiffening theories. As the model synthesized the flexural response of the member, it simultaneously checked various failure criteria such as flexural tension or compression failure, concrete shear failure by diagonal tension, and bond failure at the concrete/GFRP interface.

From the model it was concluded that increasing the compressive strength of concrete increases flexural strength and stiffness slightly, but does not have a significant effect on the load at which bond failure occurs. In most practical applications where shear span-to-depth ratios were far greater than the 4.17 used in this investigation, flexural failure would likely precede bond failure despite the bond strength being limited to 1MPa. Increasing the thickness of the flanges of the sheet pile section had a significant effect on increasing flexural strength and stiffness, as well as improving tension stiffening behaviour (Fig.3.19). However, it had a negligible effect on the debonding failure load. For a given shear span and bond strength, there existed an optimum width of concrete slab that would enable flexural failure to precede bond failure. However, the flexural stiffness per unit width of deck tends to be highest when considerably narrower concrete slabs were used. Fig.3.20 and Fig.3.21 shows the effect of flange thickness and grade of concrete on moment curvature relationship.

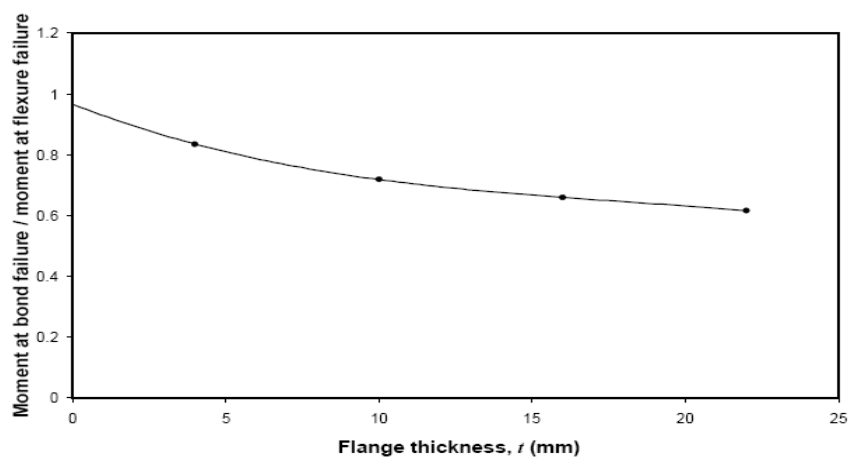


Fig.3.19. Effect of flange thickness (t) (Honickman,2008)

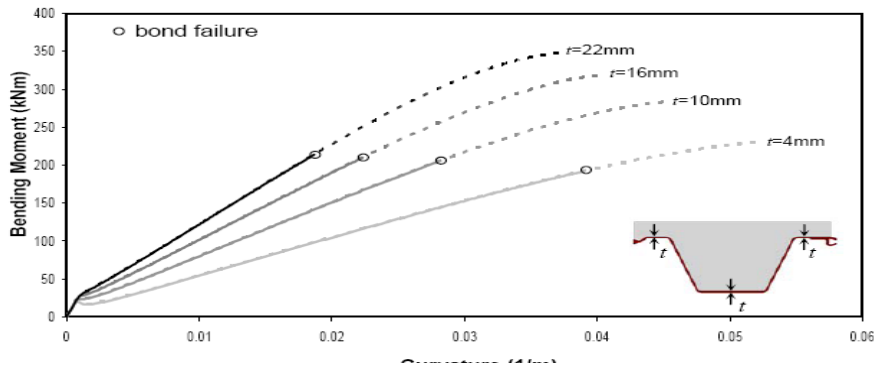


Fig.3.20. Moment curvature relationship (Honickman, 2008)

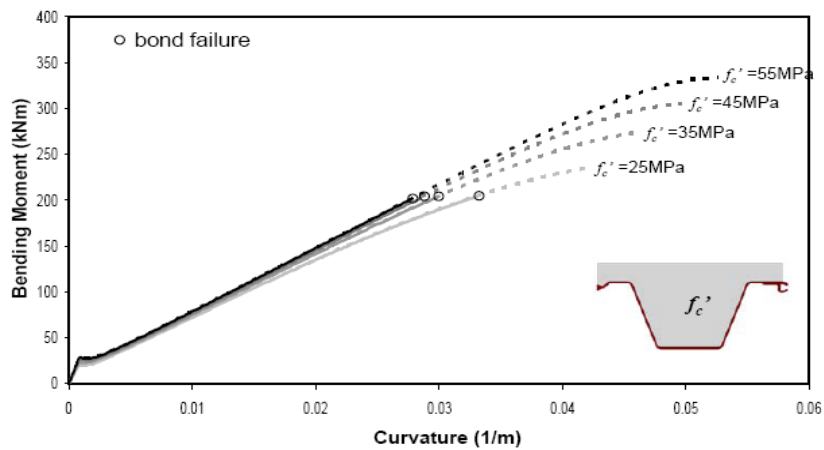


Fig.3.21. Moment curvature relationship (Honickman, 2008)

3.5 FRP SIP FORMWORK IN BRIDGES

There are now the increasing number of field applications of FRP SIP formwork, most of which can be described as demonstration projects. The exception is in area of bridge decks and girders where there has been increasing activity over the last few years driven by the need of lighter weight and more durable system to offset increasing cost of maintenance of conventional structural concrete in areas of harsh climate conditions or where there is need for upgrading of structures to meet new code requirements. The research works done in the field of FRP SIP structural formwork for bridge decks and girders is presented below.

Berg et al. (2005) described the use of FRP materials as reinforcements and formwork for a concrete highway bridge deck. They described the construction process and provided a cost analysis of the project. In this project three forms of FRP reinforcing were combined to reinforce the concrete deck: FRP stay-in-place (SIP) forms, deformed FRP reinforcing bars (rebars), and a special prefabricated pultruded FRP reinforcing grid (Fig.3.20)

The system was developed to reduce the construction labour cost to offset the high initial cost of the FRP materials relative to conventional steel reinforcing. Constructed adjacent to the FRP reinforced deck was a twin structure with temporary formwork and steel reinforcement. The SIP FRP deck panels were 457 mm (1 ft. 6 in.) by 2350 mm (7 ft. 10 in.). Each panel was stiffened by two 76 mm (3 in.) square hollow tubular “cells” spaced 229 mm (9 in.) apart. The deck panels spanned perpendicularly between the prestressed concrete girders and were discontinuous at the girders.

After the concrete was poured, the deck panels served as the bottom tensile reinforcement for the deck in the transverse direction. The FRP bars were used in the deck to provide negative moment continuity for the girders over the centre pier and as temperature and shrinkage reinforcement elsewhere. The FRP bars were finished with a fine sand texture. Prefabricated bi-directional FRP pultruded grid was assembled from 50 mm (2 in.) high T-bars spaced at 100 mm (4 in.) on centre and 13 mm (0.5 in.) diameter three-part cross-rods spaced at 100 mm on centre. The grid served as the top reinforcement of the concrete deck and carried tensile stress over the girders caused by negative bending moments in the transverse direction of the deck. They were joined in the positive moment region of the slab between the girders. A mechanical splice connection (i.e., a pultruded coupler) was used at the ends of the grids to hold them in position during construction

After the concrete girder was placed polystyrene haunches were attached to the edges of the top flange of the concrete girder with an epoxy adhesive. The FRP deck panels were then placed on the foam. The hollow tubular cells at the ends of the panels were filled with expandable polyurethane foam to prevent wet concrete and mix water from flowing into the cavities. The FRP rebars were then placed parallel to the concrete girders and were supported by continuous plastic chairs, which sat on the tubular cells of the deck panels. The FRP grid was then placed on top of the rebars. The T-bars for the grid were laid perpendicularly to the FRP rebars (Fig.3.22). The ends of all FRP materials were sealed prior to the pour with the same epoxy that was used to adhere the aggregate to the horizontal surfaces of the deck panel.

The deck pour was completed in 4 hours. A total of 713 hr. were spent on the decking and placement of reinforcement on the steel reinforced bridge deck compared to 310 hr. on the FRP reinforced bridge deck. The construction of an FRP reinforced concrete bridge deck using conventional construction technology and labour was accomplished with a 57% savings in construction labour over a nominally identical steel rebar reinforced deck. Material costs

for the FRP reinforced deck bridge were 60% higher than that of the steel reinforced deck bridge. Based on the analysis of the short-term material and labour costs it appeared that given the savings in construction time and their potential long-term durability and maintenance benefits, FRP reinforcements for bridge decks were cost-effective, not withstanding their currently high initial costs.

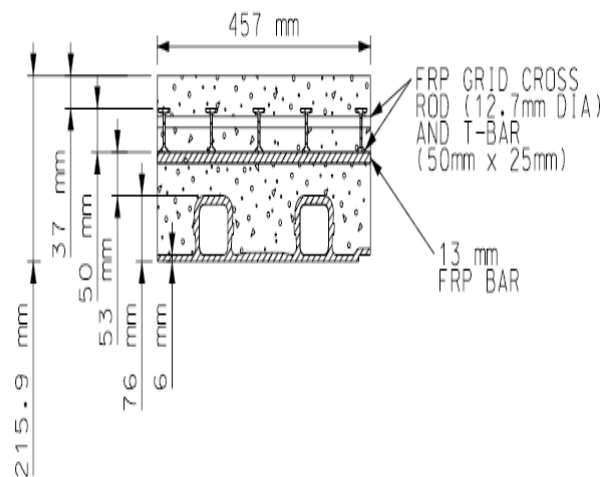


Fig.3.22. FRP reinforcement system (Berg et al., 2005)



Fig.3.23. SIP FRP deck panels, FRP rebars, and bi-directional FRP grid during placement (Berg et al., 2005)

Hanus et al. (2009) investigated a structural fiber-reinforced-polymer (FRP) stay-in-place (SIP) form used to construct and reinforce a deck for a prototype military bridge system. For this application the deck is subjected to combined bending and compressive longitudinal axial load because it also serves as the top chord of the truss for the bridge system. In the bridge the structural FRP SIP form is attached to a deployable truss support system during the construction stage (Fig.3.24). The SIP form is then filled with concrete to form the deck, which also acts as the upper chord of the truss in resisting live loads (Fig.3.25).

Stay-in-place forms for a concrete deck were primarily chosen to reduce the deployment requirements for the bridge system and utilize in-theatre materials, in addition to the accelerated construction benefit. The structural FRP SIP form was chosen for the high strength to weight ratio, which also reduces the deployment requirements of the system, and for the proven composite action development techniques. In this project FRP SIP consisted of a single grid layer having I bars with three part cross rods and 3.18 mm thick pultruded plank was epoxied to it (Fig.3.26).

Ten specimens were constructed and tested in three different configurations (single span, double span, with or without axial load). Several design elements were investigated, including the effect of adding a synthetic short fiber material to the concrete (FRC), and connection details. Maximum allowable deflection limit of $L/180$ was used in this thesis.

The experimental results were analyzed and compared to the equations in the ACI 440 (guide for the design and construction of structural concrete reinforced with FRP bars) design guide. This analysis included a study of the movement of the neutral axis under positive moment loading (compression at the top) through the elastic state to ultimate failure. The downward movement of the neutral axis in FRP reinforced sections was theoretically shown and experimentally demonstrated. This behaviour affects the application of the ACI design guide equations for serviceability and strength limit states. The ACI 440 design guide's flexure equation for over reinforced sections, without longitudinal axial load, was found to accurately predict the capacity for the sections reinforced with the structural FRP SIP form in this study. The ACI 440 design guide is intended for sections reinforced with bars, but appears adequate for the sections reinforced with structural FRP SIP form with respect to over-reinforced flexural failure. It was found that the ACI 440 equations accurately predicted the flexural and flexural-shear capacities under combined loads provided that eccentricity due to the combined loading was accounted for in the calculations.

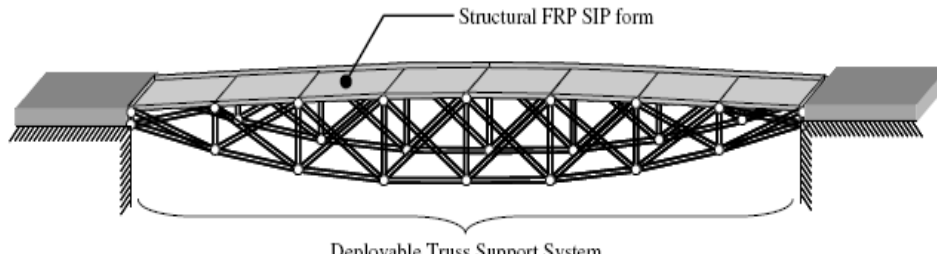


Fig.3.24. Construction stages (Hanus et al.,2009)

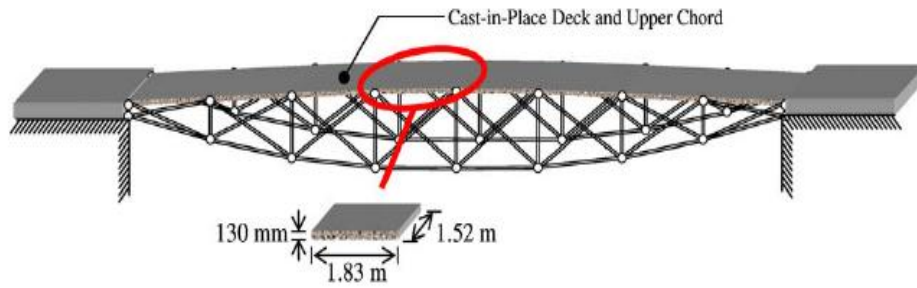


Fig.3.25. Completed stage (Hanus et al.,2009)

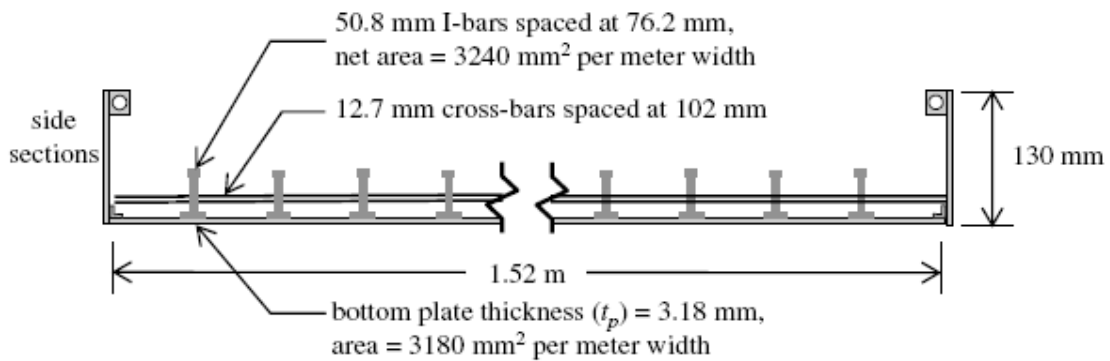


Fig.3.26 Cross-section structural SIP forms for deck component. (Hanus et al., 2009)

Seibal et al. (1998) developed modular FRP bridge based on pultrusion and hand lay-up of a carbon/ glass hybrid material system. The hybrid tube system (HTS) beam-and-slab bridge proposed the use of hollow E-glass /carbon hybrid beams that were connected along their tops with a polypropylene fiber reinforced concrete deck system as shown in Fig.3.27. The girders consisted of pultruded or hand laid-up E-glass /vinyl ester rectangular sections, which were reinforced along the bottom flange with unidirectional carbon fibers. An FRP

panel was snap locked to the pultruded girders providing flexural reinforcement to the concrete slab between girders as well as stay-in-place formwork for the slab. The end hooks of the panel were anchored by filling polymer concrete in the ‘dovetail’ pockets of the top portion of the transverse girder. Prefabricated carbon /vinyl ester snap-in stirrups were also snapped into the grooves to provide horizontal shear transfer between the concrete deck and the girders. A parametric study of a hybrid tube bridge system was performed by evaluating the maximum simply supported span length of the system under a set of allowable design criteria for service and factored loads. The bridge system under consideration consisted of seven transversely spaced HTS girders supporting a 13m wide road surface. The results indicated that the deflection under live load governs the design, which is common for FRP structures.

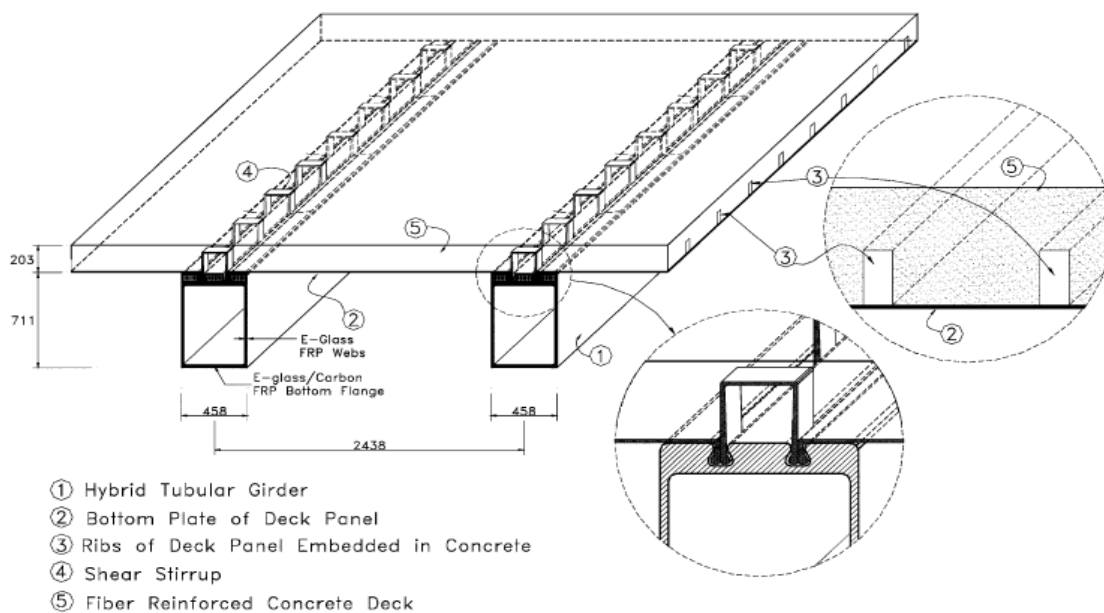


Fig.3.27. Hybrid tube bridge system (Seibal et al., 1998)

Matta et al. (2004) reported about a project in which a prefabricated stay-in-place (SIP) glass fiber reinforced polymer (GFRP) reinforcing system for the accelerated construction of bridge decks was developed and implemented in the reconstruction of Bridge 1482301 in Greene County, Missouri, USA. This project was opted for the replacement of the 70-year old bridge due to the severe corrosion-induced deterioration of the superstructure. A significant joint effort was required for the concept development, design, analysis, detailing, full-scale laboratory validation, development of project special provisions, and construction

planning and execution. Related tasks were completed in coordination between Missouri S&T and the University of Wisconsin- Madison, FRP reinforcement manufacturers, the Greene County Highway Department (owner), the engineer-of-record, and the designated contractor.

Prototype SIP reinforcement panels were prefabricated using off-the-shelf pultruded GFRP profiles arranged in a two-layer grating, where load transfer was achieved by mechanically constraining the core concrete within the three-dimensional grating. The SIP formwork consists of GFRP plates that are epoxy-bonded to the bottom layer of reinforcement. Grid form detailing is shown in Fig. 3.28.

The use of large-size and light-weight (23.7 kg/m^2) panels was aimed at allowing easy and rapid installation with single picks of a crane, thereby eliminating time-consuming and labour-intensive setting and removal of plywood forms and tying of bars on-site. The steel-free deck system was complemented by a newly designed open-post concrete railing reinforced with light-weight; prefabricated cages made of pultruded GFRP bars.

The design of post-deck connection and deck were validated through laboratory testing of full scale overhang subassemblies and deck panel specimens. The results substantiated the design outcomes, and confirmed significant safety margins at failure with respect to applicable code mandated strength requirements. The series of ultimate capacity tests performed on the deck slab specimens illustrated that punching shear was the critical failure mode. Accelerated fatigue cyclic performance upon a slab specimen had not revealed any apparent adverse fatigue effect on the ultimate strength and overall performance of the FRP reinforced bridge deck after 2,000,000 load cycles.

Construction was planned with the contractor to minimize time. The job was completed in five days, instead of the typical 2-3 weeks for similar steel reinforced concrete bridges built by the same contractor. A total of 18 panels were installed by six workers in six hours during the first day, covering the total length of 44 m of the slab-on-girder bridge. The second day was dedicated to mounting the railing post cages into the deck panels, preparing the formwork for expansion joints, chamfers and drip edges, and setting the finishing machine. The deck was cast and finished in the third work day. In the morning of the fourth and fifth days, the railing beam cages were mounted on top of the post cages prior to forming and casting. The project demonstrated a technology that combines the superior durability of internal FRP reinforcement for concrete, and the substantial constructability advantages that

derive from the use of light-weight advanced composite systems engineered in an innovative, integrated stay-in place form.

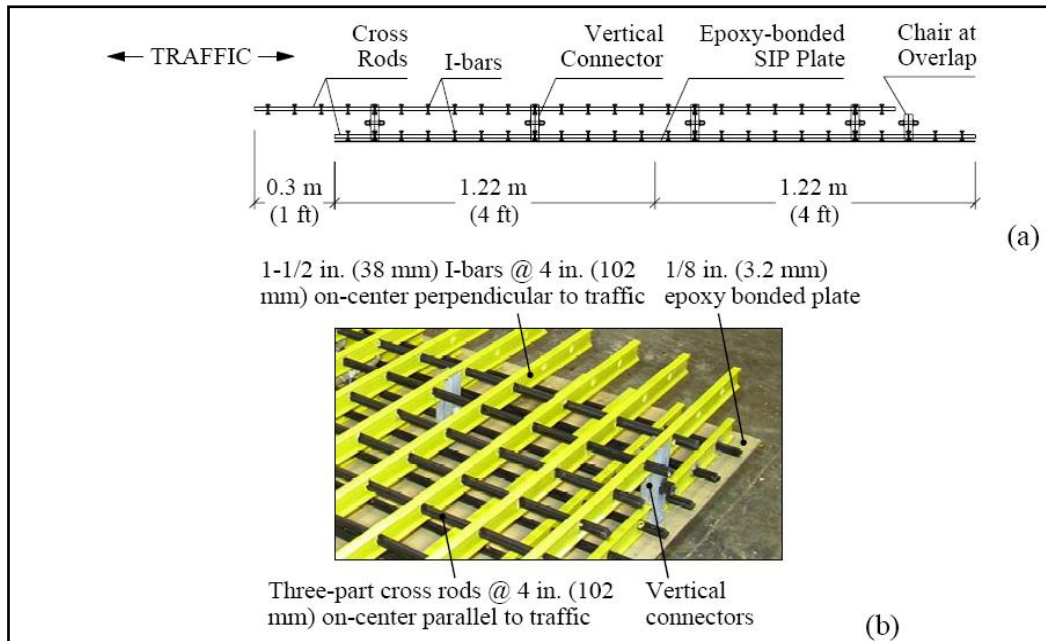


Fig.3.28. Gridform reinforcement panels: longitudinal section (a) and close-up (b)

(Matta et al., 2004)

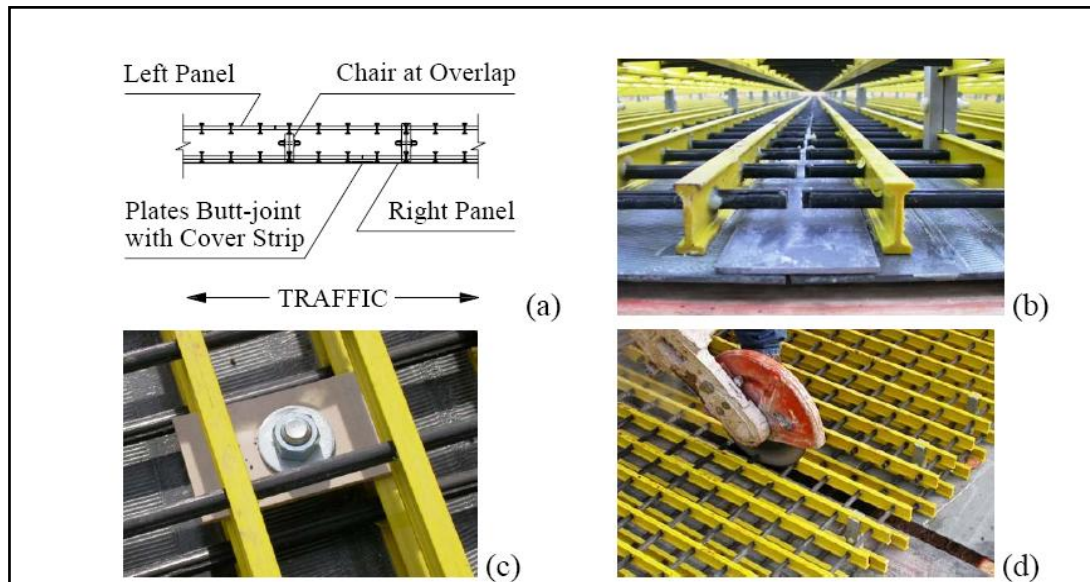


Fig.3.29. Gridform detailing: panel-to-panel overlap connection (a, b); anchoring to girder (c); and cutting of end panels at expansion joint (d). (Matta et al., 2004)

Bank et al. (2006) has described the research on the evolution of a cost-effective, structural stay-in-place (SIP) formwork bridge deck system with an integrated modular three dimensional fiber-reinforced polymer (FRP) reinforcement cage. A cost-effective structural FRP stay-in-place formwork system that was integrated with the reinforcing for concrete highway bridge decks has been developed and tested at the University of Wisconsin–Madison. In this research three types of bridge decks were tested: 1) CDS system -SIP forms separated from top layer of reinforce grating (Fig.3.30.). 2) SafPlank –it consist of panels integrated with one layer of grating and separated from top layer of grating (Fig.3.31.). 3) Grid form-it consists of panel separated with two layers of grating (Fig.3.32.).

All these systems have been shown to be able to provide safe support of the design loads for highway bridges. Fig.3.33. shows load deflection behaviour of all three types of formwork. The most promising option is currently the Gridform system, because of the material cost and the potential for rapid construction. Laboratory testing of full-scale panel and beam specimens has shown that the Gridform system meets the strength and deflection code requirements; the strength is over five times that required and the stiffness over four times the recommended stiffness. Benefits of the Gridform over conventional steel reinforcement are the corrosion resistance and the potential for accelerated construction because of the modular nature of the system. The Gridform solution has been successfully implemented in the superstructure replacement of a slab-on-girder bridge in Greene County, Missouri, where the duration of deck construction was 3 days.



Fig.3.30. Installation of CDS deck panels

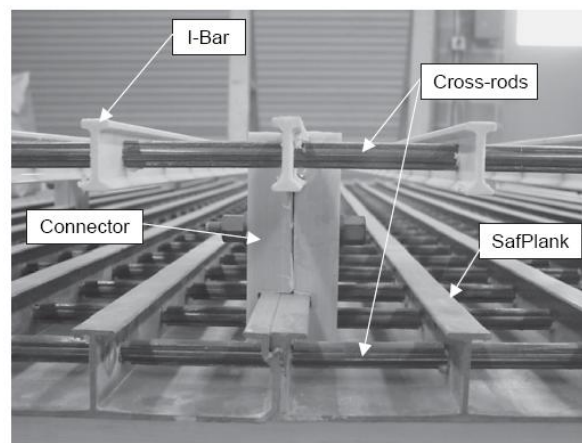


Fig.3.31. SafPlank panel

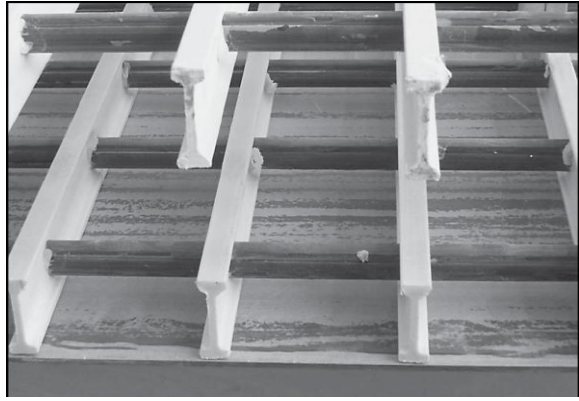


Fig.3.32. Gridform reinforcement detail (*Bank et al., 2006*)

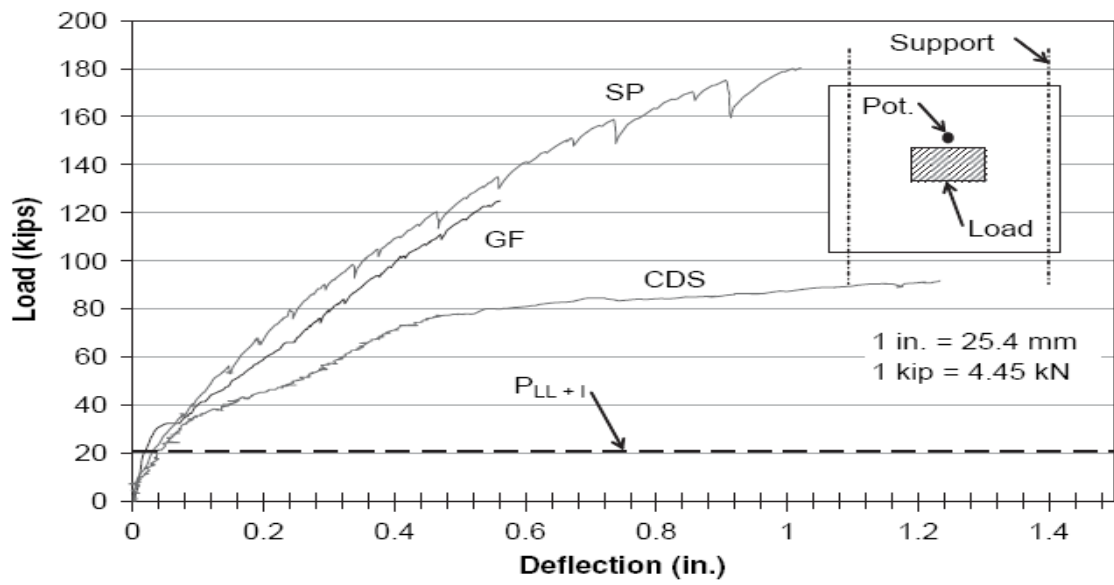


Fig.3.33 Load and deflection behaviour for panel specimens. (*Bank et al., 2006*)

Chapter 4

STEPS OF INVESTIGATION

4.1 INTRODUCTION

The objective of the test program was to investigate the behaviour and capacity of fiber reinforced concrete slabs in which GFRP plates stiffened with GFRP channels serve the dual purpose of stay in place formwork and reinforcement. In this chapter step by step approach for selection of the formwork used in casting slabs is discussed. Analytical work regarding the deflection of the form work is also presented in this chapter.

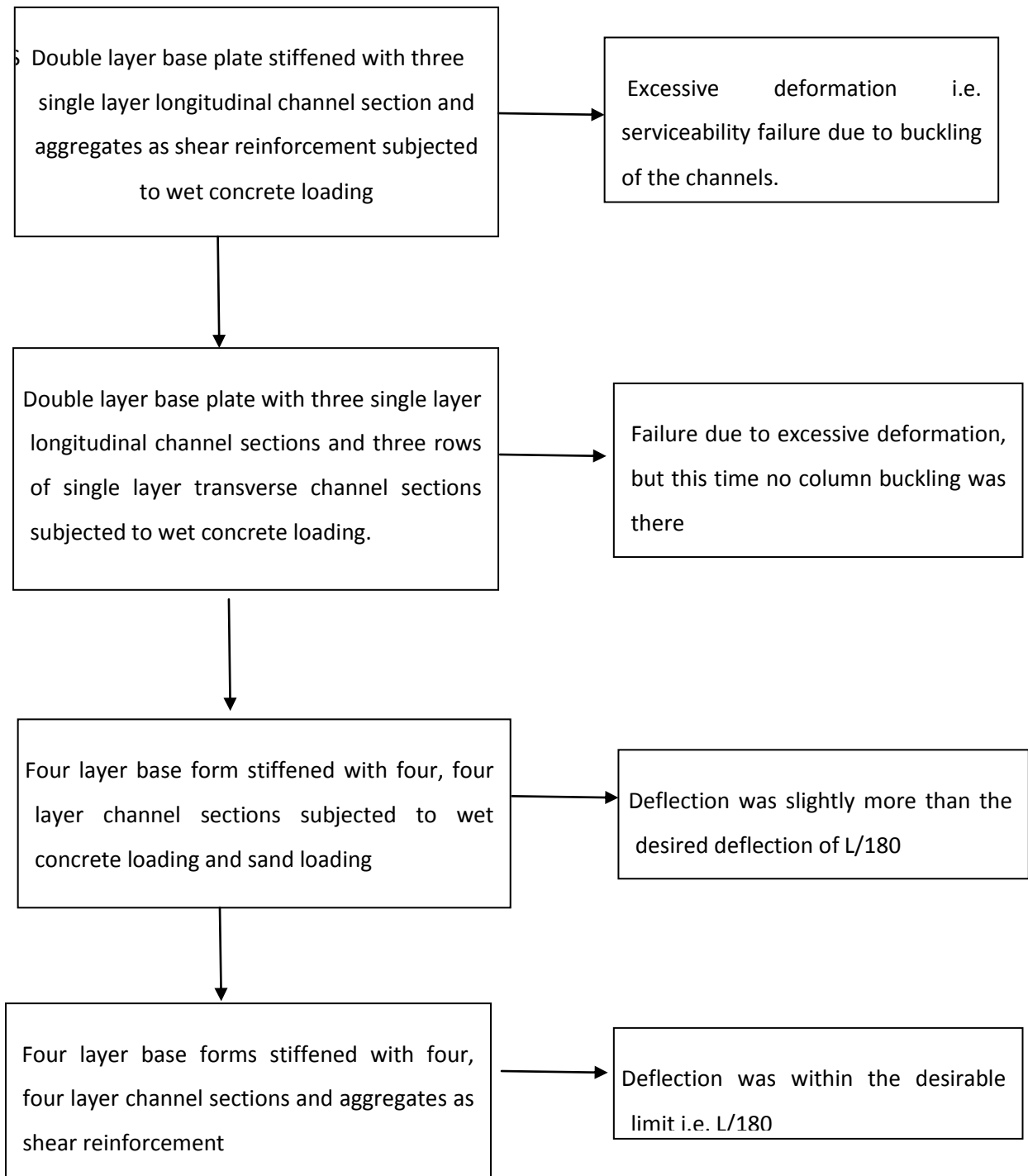
4.2 MATERIAL SELECTION CRITERIA

In this program it was decided to use normally available WRM 450 gsm mat with 50-50 orientation of the fibers as it is the most commonly used glass fiber and its availability is not a problem and more over the objective of the test program is to start the use of fibers as SIP from the grass root level i.e. to use it as base forms in normal constructions like houses, so the most easily available option was selected. Also cost of 450 gsm mat is less than the other fiber mats.

Firstly double layer base forms stiffened with three single layer channel sections were tested and based on their performance section was modified to four layer base form stiffened with four, four layer channels. Structural (formwork and reinforcement) and non structural (only formwork) performance for 1m single span forms was tested and only non structural performance of 3m three span forms was tested in this research.

Sand loading test and wet concrete loading tests were performed initially and the slabs casted on base forms which satisfied the deflection limit for SIP forms ($L/180$) were further tested for the role of GFRP as reinforcement. Concrete was removed from the base forms which were not able to satisfy the deflection criteria and the failure mode was examined and on that basis modifications were made.

Step by step approach



After this work the slabs casted in step 3 and 4 were cured for 7 days and were tested in loading.

4.3 ANALYTICAL WORK

4.3.1 DOUBLE LAYER BASE FORM STIFFENED WITH SINGLE LAYER CHANNEL SECTIONS

Initially when this research program was started, then the only information provided by the manufacturer was that the sheets they will use in preparing base forms is WRM 450 and it is 50-50 orientation sheet. Then from the literature review, value of young's modulus for the fiber resin matrix was assumed to be 20GPa. Size of the slab to be casted was 1m x0.5m x0.2m. It was noted from the GFRP forms that each layer of fiber along with resin is approximately 1mm in thickness. From the load deflection formula (eq.1), deflections under wet concrete loading were calculated.

$$\Delta = 5Wl^4/384EI \quad \text{----- (1)}$$

Where W=wet concrete load in casting (1m x0.5m x0.2m) slab 2500N.

L= span 0.9m While casting the slab supports were provided at the distance of 50mm from both ends.

E= young's modulus of form 20 GPa

I=moment of inertia of the section with 2mm base plate stiffened with three 1mm thick channel sections.

This gives,

$$\Delta=4.5\text{mm}$$

Safe deflection limit for SIP formwork =L/180

For 900mm slab

$$\Delta_{\text{safe}} = 900/180$$

$$=5\text{mm}$$

Thus from initial analytical calculations it appeared that double layer base form stiffened with three single layer channels will be safe form from deflection point of view.

From literature survey it was decided to put aggregates on the form to act as shear reinforcement.

Experimentally it was observed that double layer base forms stiffened with three single layer channel sections failed because of high deflection. Even after introducing transverse channels deflection was very high. From this it was concluded that double layer base form stiffened with three single layer channels is not a right cross section to act as formwork.

4.3.2 FOUR LAYER BASE FORM WITH FOUR NO., FOUR LAYER CHANNELS

After the failure of double layer base form stiffened with three single layer channel sections, back calculation was done to get the value of E using formula (1). Experimentally it was observed that the deflection with this formwork was around 25mm at load of 2000N. Putting the values in the formula we get

$$0.020 = (5 \cdot 2000 \cdot 0.9^4) / (384 \cdot E \cdot 247266 \cdot 10^{-12})$$

$$E = 3.5 \text{ GPa}$$

Now for deflection of 5mm in casting 250 mm thick slab

$$5 = (5 \cdot 2500 \cdot 0.9^4) / (384 \cdot 3.5 \cdot 10^9 \cdot I)$$

$$I_{\text{req}} = 1240424.107 \text{ mm}^4$$

Value of I for different sections with different number of layers in base forms and channels and different number of channels were calculated and finally GFRP form with four layer base form stiffened with four, four layer channel section was selected with I value 1237173 mm^4

When wet concrete testing and sand testing was done on this formwork then deflection observed was 5.44mm which was slightly more than the permissible deflection of 5mm.

Then in the next slab casting to control this deflection aggregates were attached to the base form of formwork with four layered base form stiffened with four, four layered channel

sections. Experimental deflection in this case was 3.96mm which was within the permissible deflection limit.

The results obtained from above analytical discussion were verified through ANSYS modelling. The details about ANSYS modelling are presented in appendix A. Tensile testing of FRP matrix is presented in appendix B. Also analysis of form as reinforcement is presented in appendix C

In the next chapter all the details about the forms used and the experimental tests are presented.

Chapter 5

PREPARATION OF BASE FORM

5.1 INTRODUCTION

In this chapter base forms used in this research work has been discussed. Details about the different types of forms used in the research and details about manufacturing process used for preparing forms is presented in this chapter.

5.2 GFRP SIP FORMWORK

In this investigation base forms used are prepared using contact molding (hand lay-up) process. The hand layup process is the simplest method used for the fabrication of small to large size FRP composite products without any infrastructure and sophisticated machinery. The base forms used were prepared in the industry where large glass platform was available for fabrication of base sheets.

Materials used in the fabrication of formwork are:

- 1) GFRP mat- In this investigation 450 gsm WRM (woven roving mat) with 50-50 orientation of fibers in both longitudinal and transverse direction was used. Fig.5.1 shows the picture of mat used in this research.



Fig.5.1. WRM 450 gsm GFRP used for making forms

2) Resin- Normally available iso-resin was used in this research. This iso-resin was mixed with small amount of hardener before applying to the fiber sheet.

In this investigation forms used consisted of two parts which were bonded together to serve the desired function of formwork and reinforcement. These two parts are:

1. Base forms
2. Channels

Two types of base forms were used in this project:

1. Double layer stiffened base form
2. Four layer stiffened base forms

5.3 CHANNELS

In this research work two types of channel sections were used

1. Single layer channel section
2. Four layer channel section

Channels were prepared using a mould (Fig.5.3). For preparing single layer channels initially a gel coating was done on the mould (Fig.5.4). Then after gel coating a layer of resin was spread and then first fiber sheet was placed (Fig.5.5). Then again resin was spread (Fig.5.6). After curing for about 12 hours it was removed from mould and was trimmed from the sides.

For preparing four layer channel section, after gel and resin coating, four alternate layers of fibers and resin each were spread on the mould and were then allowed to cure. Then it was removed from the mould and was trimmed. Fig.5.2 shows the dimensions of the single layer and four later channel sections

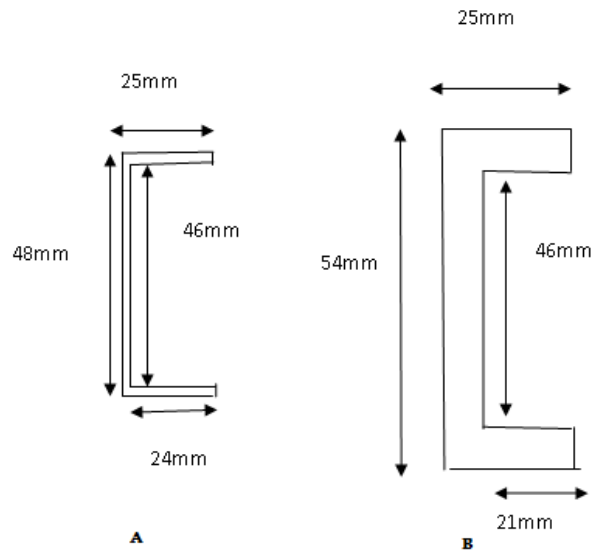


Fig.5.2 (A) single layer channel (B) four layer channel



Fig.5.3 Mould for making channel



Fig.5.4. Applying gel coat on mould

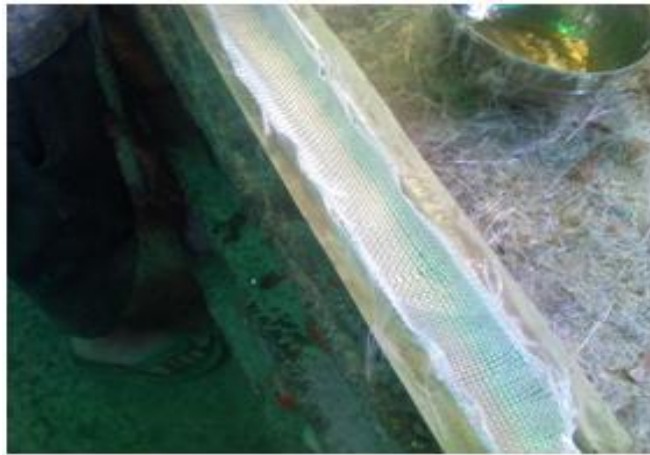


Fig.5.5. Applying fiber sheet on mould



Fig.5.6. Applying resin coating on fiber sheet

5.4 BASE FORMS

5.4.1 DOUBLE LAYER STIFFENED BASE FORM

5.4.1.1 Single span form

In double layer base form initially a single fiber layer base form was prepared and then channels were attached to it with resin. Then second fiber layer was placed on it. It was not a continuous layer. Point of discontinuity was at the webs of the channels. Fig.5.7a shows points of discontinuity of second layer and Fig.5.7b shows dimensions of various parts of the form. Thickness of double layer base form was 2mm.

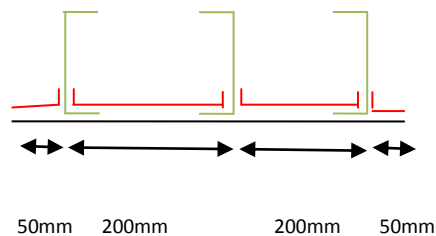


Fig.5.7a Connection of channels with the base form
(not on scale)

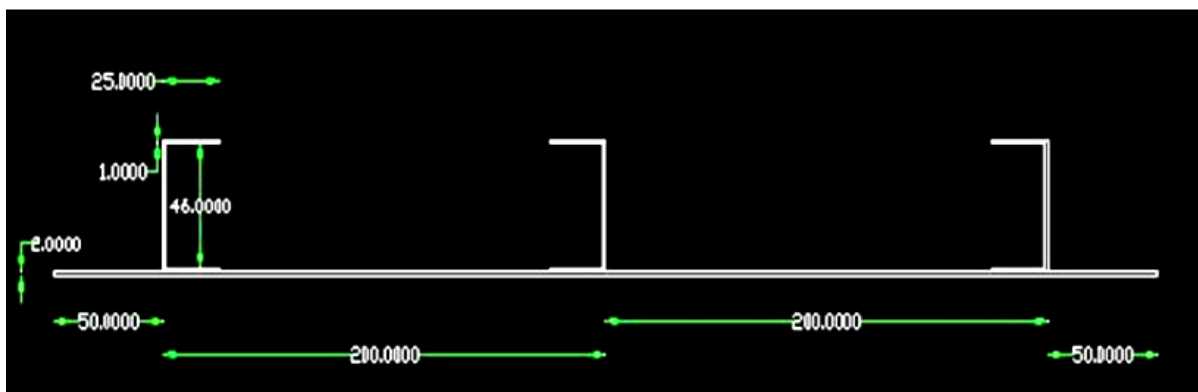


Fig.5.7b. Detailed dimensions in mm of the double layered form

In addition to length of 1m and width of 0.5m additional provision of about 25mm was provided for placing wooden side forms (Fig.5.8).

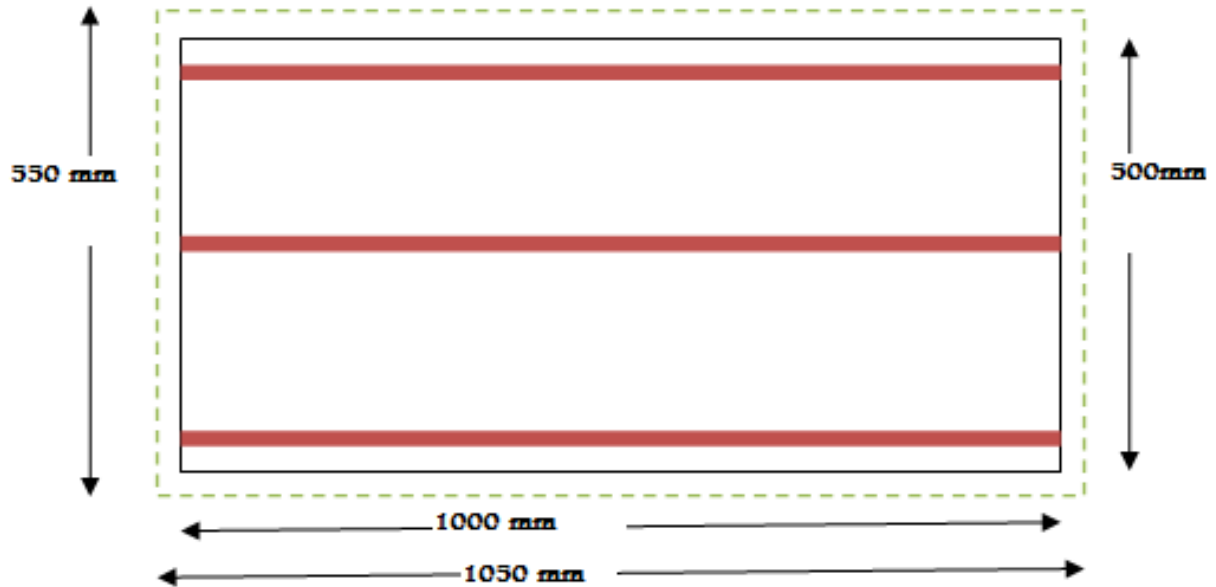


Fig.5.8 Provision for wooden side forms

For preparing a single layer base form firstly a resin coating was applied on the glass platform (Fig.5.9). After it has dried again a resin layer was applied and then immediately fiber sheet was spread on that resin layer. Now again a resin layer was spread on that fiber sheet and pressed down with brush (Fig.5.10). It was then allowed to cure for about 12 hours. Then this single layer of fiber sheet was removed from the glass platform and lines were marked where the channels were to be attached. Then resin was spread on the base of the channels and then channels were attached to the single layer fiber sheet. After it has dried second layer of fibers was spread. Fig.5.11 shows single layer sheet when it is removed from glass platform and Fig.5.12 shows final prepared double layer stiffened form.



Fig.5.9. Applying initial resin layer on glass platform

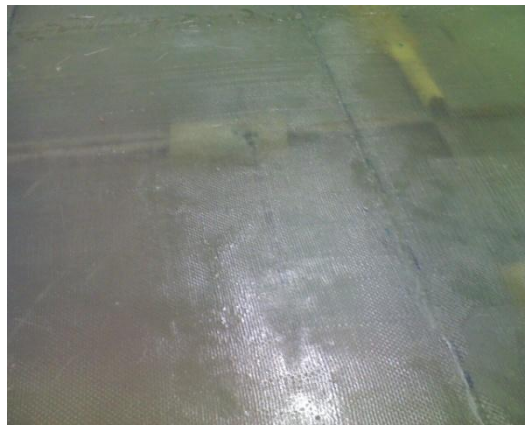


Fig.5.10. Glass fiber single layer and resin coating on glass platform



Fig.5.11. Removing single layer sheet from glass platform



Fig.5.12. Prepared double layer base form with stiffener channels

5.4.1.2 Three span forms

By using the above described method single span 1m forms were prepared. For preparing 3m, three span forms, firstly 3 single span forms were prepared (Fig.5.13). Then they were connected together to form 3 span form using connectors (Fig.5.14). Connectors consisted of fiber sheets 200mm long with 100mm overlap on each adjacent form. In first layer of connectors sheet was spread only on the base forms. This was a discontinuous sheet with discontinuity at the webs (Fig.5.15). In second layer a sheet was spread covering the webs also with points of discontinuity at the end of the top flange (Fig.5.16).



Fig.5.13. Three 1m span forms placed adjacent to each other before connection

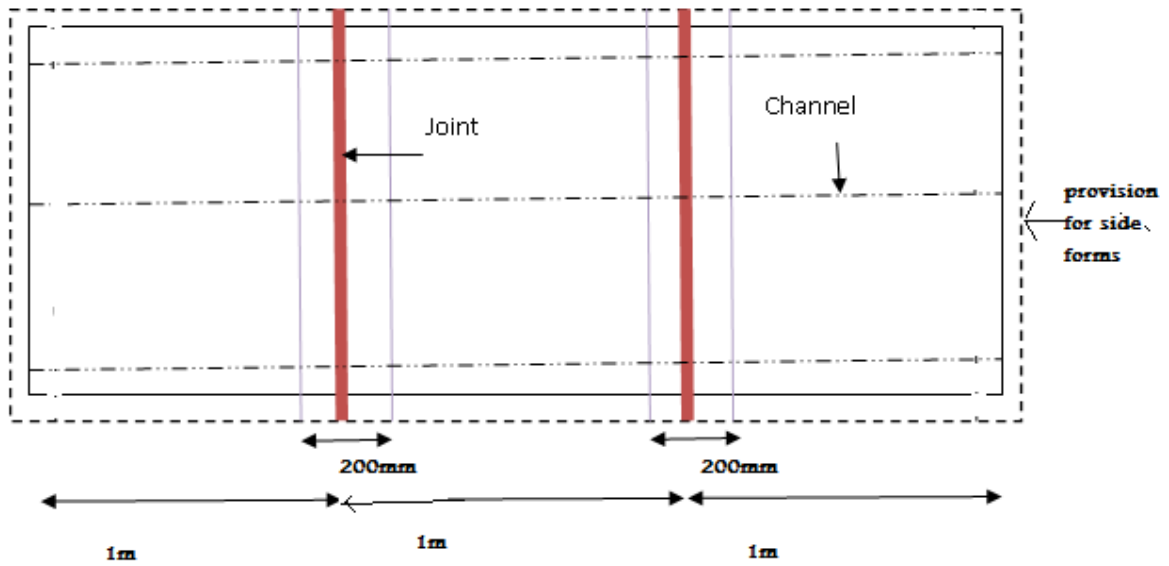


Fig5.14. Position of joints in three span double layered base form



Fig.5.15. Forms after first connection layer

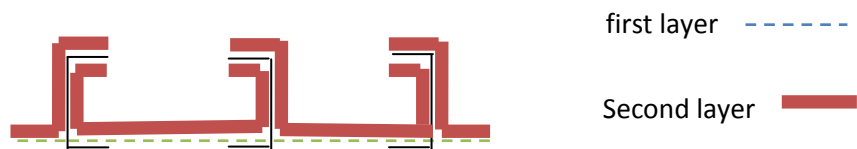


Fig.5.16 Layout of two connecting layers

5.4.1.3 Form with transverse stiffener

For preparing two layer base form with both transverse and longitudinal stiffeners (Fig.5.12) initially a form was prepared having only longitudinal channels and then three columns of single layer channel sections were introduced. Connection was done with fiber layers. Firstly, a fiber sheet was spread covering bottom flange of transverse channels and 100mm of base form. Then layer of fiber sheet along with resin was spread covering angle shaped interaction of webs of longitudinal and transverse channels.



Fig.5.17. Double layer base form with both longitudinal and transverse stiffeners

5.4.2 FOUR LAYER BASE FORM

5.4.2.1 Single span form

In this type of forms four layer base forms were stiffened with four no., four layer channels. In this firstly a three layer base form was prepared and then channels were attached at the required positions. Then fourth layer was spread and it was not a continuous layer (Fig.5.18). Provision for side forms was also provided as in double layer forms.

For preparing a three layer base form, firstly a single layer base form was prepared on the glass platform and then after removing this single layer from the glass platform two other layers of alternate fiber sheet and resin each was spread on it. Then it was allowed to cure for 12 hours. Then channels were attached and fourth layer was spread. Weigh of one base form was 4.2 kg. Fig.5.19 shows final prepared four layered stiffened base form.

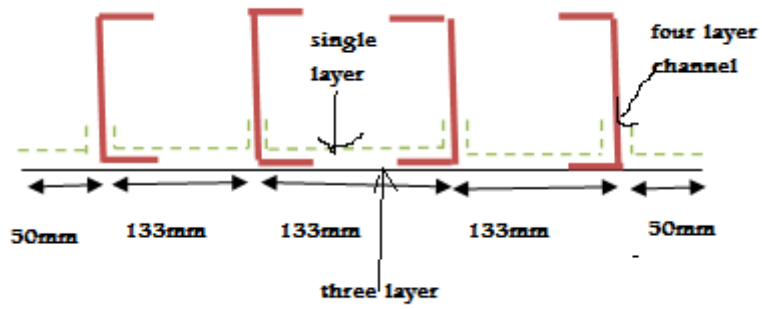


Fig.5.18a. Description of four layer base forms

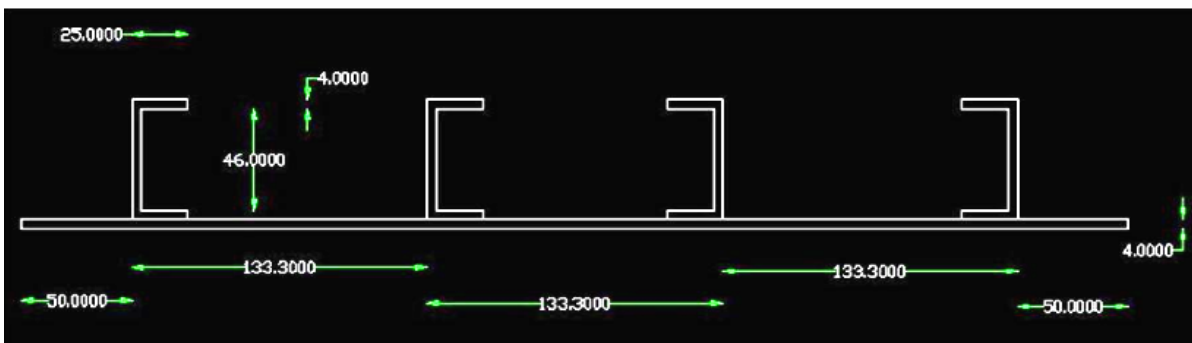


Fig.5.18b. Dimensions in mm of four layered form



Fig.5.19. Four layer base form stiffened with channels

5.4.2.2 Three span forms

In 1m span forms additional margin of 2.5cm on each side was there for wooden forms. For preparing 3m span forms firstly three 1m span forms were prepared. Out of these two were having margin for wooden formwork on two longitudinal sides and one transverse side. Third one had margin only on the longitudinal side. Then these were placed side by side such that channels of three sheets touch each other and were in same straight line. Then layers of fiber sheets 200mm broad was used to connect two 1m span forms covering 100mm of each form. Position of joints is shown in Fig.5.20

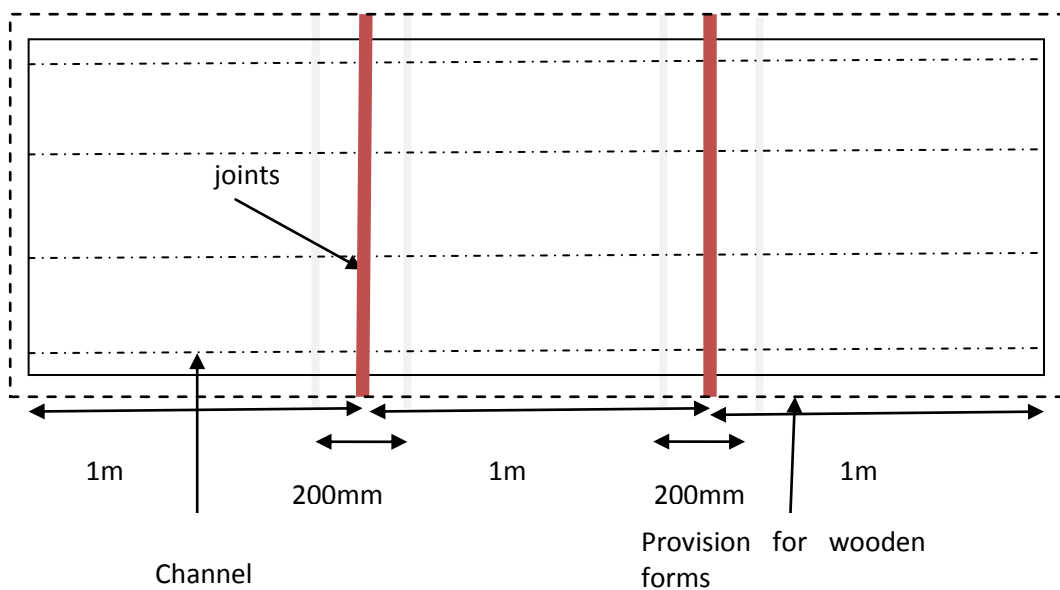


Fig.5.20. Position of joints

5.4.2.2.1 Double layer connectors

In double layer connectors, for connecting two 1m formed two fiber sheets with width 200mm to cover 100mm of each form was used. The layer arrangement is shown in Fig.5.21



Fig.5.21. Connection arrangement using two layers

Chapter 6

EXPERIMENTAL PROGRAM

6.1 INTRODUCTION

This chapter provides experimental investigation into the behaviour of one way concrete slabs casted on GFRP formwork used simultaneously as formwork and tensile reinforcement. In this investigation double layer base form stiffened with three single layer channel sections and four layer base forms stiffened with four, four layer channel sections were investigated. This chapter details the design of experimental program, measuring deflection of the forms due to wet concrete loading, test set up, instrumentation and one point loading test. Basic aim of this research is to find out suitable GFRP cross section having combination of GFRP base forms and channels so that it can satisfy strength and serviceability limits. Bond system in which coarse aggregates were bonded to formwork prior to casting was also tested. The performance of slabs casted on base forms with and without aggregates was assessed and the failure modes were examined.

6.2 MATERIALS USED

In this research following materials were used:

1) Concrete

M-25 grade of concrete was used for casting. The IS codal provisions were followed for designing the mix. The final mix proportions are 1:1.19:2.49 with w/c ratio of 0.5. Ordinary Portland cement (grade 43) is used for preparing concrete. Aggregates used were of maximum size 10mm and had specific gravity 2.66. Sand used was having specific gravity of 2.6 and it belonged to zone 3.

2) Base forms

In this research broadly two main types of base forms were used. These were the double layer base forms stiffened with three single layer channel sections and four layer base forms stiffened with four no., four layer channel sections. Details about these forms are presented in chapter 5.

Tests were conducted on base forms 1m (single span) and 3m (three span) long. 1m base forms were tested for their structural and non structural behaviour and 3m base forms

were tested only for their structural behaviour. One more objective of this research is to find out if the bond mechanism between the forms and concrete can be improved by using coarse aggregates which are bonded to forms using resin. After the aggregates are bonded to form, it is allowed to dry completely (min 12 hours) so that it can form a good bond with the base forms.

Table 6.1 provides details about the forms used in this work.

Table 6.1 Details about the forms used

Base form number	No. of spans	Fiber layers in base forms	Fiber layer in channels	Number of channels longitudinal	Number of channels transverse	Agg. Bonded	Tested for(*)
D11	1	2	1	3	0	Yes	NS
D21	1	2	1	3	3	No	NS
D123	3	2	1	3	0	Yes	NS
F11	1	4	4	4	0	No	S&NS
F21	1	4	4	4	0	Yes	S&NS
F31	1	4	4	3	0	No	S&NS
F223	3	4	4	4	0	Yes	NS

*S-structural performance NS-non structural performance

3) **Wooden side forms**

In this research two wooden side forms were used. These wooden side forms were of interior dimensions 1m x0.5m x0.250m and 3m x0.5m x0.3 m. These wooden side forms were placed on the sides of the base forms to retain concrete and sand which was poured on base forms while testing.

6.3 LAB EQUIPMENTS USED

In this research following lab instruments were used:

1) **Concrete Mixer**

Concrete mixer was used for mixing concrete ingredients.

2) Dial gages

Dial gages were used to measure deflection during wet concrete and sand testing. Deflections were also measured during ultimate load carrying capacity test. Dial gauges used were of capacity of measuring deflections upto 25mm.

3) Needle vibrator

Needle vibrator was used for providing vibrations to the concrete during slab casting.

4) Hydraulic jack

Hydraulic jack of capacity 50 t was used for measuring ultimate load carrying capacity of the slabs prepared during the research.

6.4 NON-STRUCTURAL TESTING OF SINGLE SPAN FORMS

Basic aim of this research is to find out whether the GFRP forms made from WRM 450gsm mat can serve the purpose of base form or not. Suitability of a material as a form depends upon how much deflection is caused when concrete is poured on the form during casting stage. The formwork should be such that it takes the concrete load when it is in the plastic stage while satisfying the deflection limits.

In non structural testing, before actual pouring of concrete, sand testing was carried out. This was so because with this it could easily be find out if the form is suitable for concrete casting or not. With this, wastage of concrete could be avoided.

In the following sections details about the tests carried out on the single span forms is mentioned in detail. All the single span forms were of length 1m and width 0.5m. In addition to this length and width all forms were having provision for side forms (about 1 inch on each side). Test set up was same for all the forms and is mentioned in detail in section 6.4.1

6.4.1 DOUBLE LAYER BASE FORM D11

In D11 form double layer base forms were stiffened with three single layer channel sections and aggregates were bonded on the base form (Fig.6.1). Slab to be casted on this form was of dimension 1m x0.5m x0.2m (Fig.6.2). During casting of slab wet concrete

loading test was done. In it was only tested for wet concrete loading and not sand loading (as after the results of this test need for sand loading was realised).

In non structural test (concrete loading test) deflections at mid span and quarter span were noted after every 20Kg load increment during casting of 200mm thick slab.



Fig.6.1. Form D11 coated with aggregates

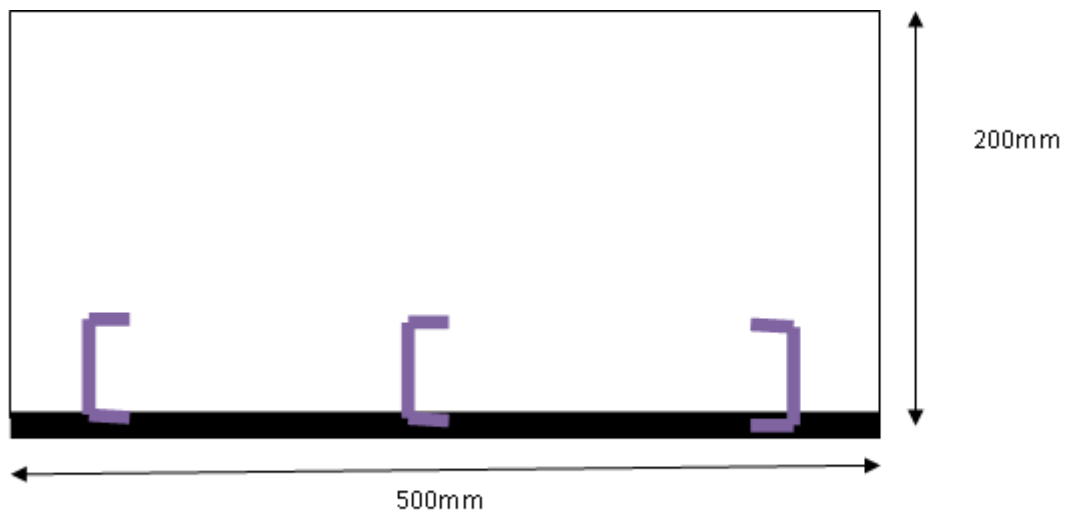


Fig.6.2. Cross sectional area of slab to be casted

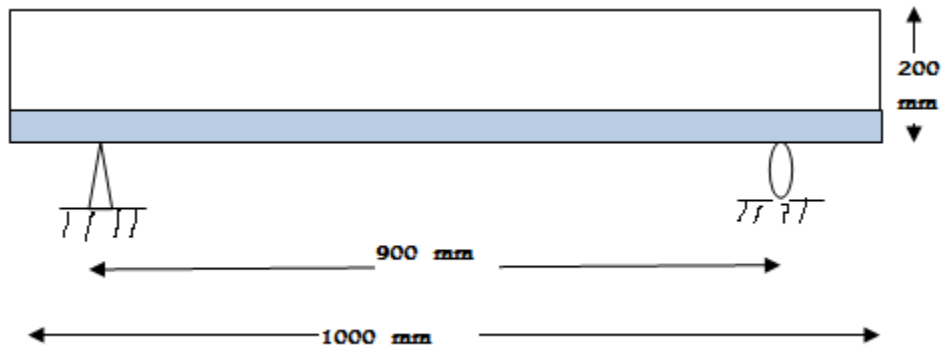


Fig.6.3. Test set up for form D11

In test set up firstly concrete blocks were placed on the floor to raise the loading platform (Fig.6.4). Three cubes were placed under each corner of the form. Provisions were provided for hinge type and roller type support by placing roller section and angle sections on the two transverse sides. Distance between these two supports was 900mm (Fig6.3). Then D11 form was placed on the supports with 50mm in addition to provision for side forms as overhang on both transverse sides.

Six dial gages were placed, three at the central portion and three at the quarter portion to measure the deflection (Fig.6.5). Then wet concrete loading was done with 20Kg concrete load steps. Deflections at all six points were noted at each load step.



Fig.6.4. Test set up for form D11

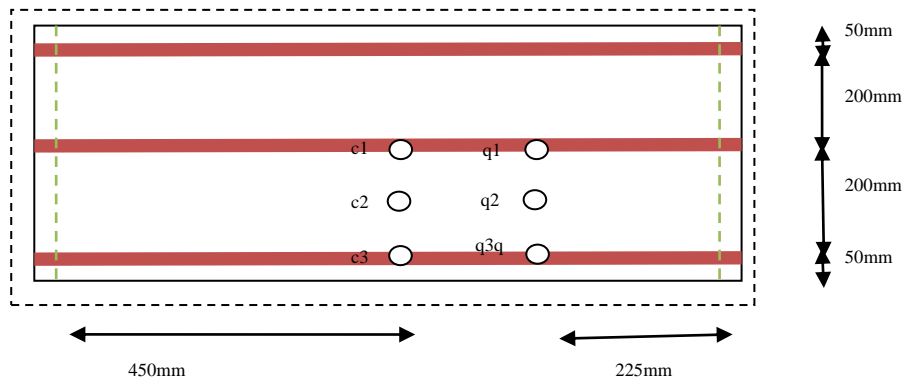


Fig 6.5 Location of points where deflection was measured

Results of the test carried out on D11 are presented in section 7.2.

6.4.2 DOUBLE LAYER STIFFENED D21 FORM

In D21 form additional transverse channels were also present to prevent buckling of the channels (Fig.6.7). On this form both sand loading and wet concrete loading test was done. Test set up was almost same as D11 form with the only difference in the position of the dial gages (Fig.6.6). Slab of dimension 1m x 0.5m x 0.2m was tried to be casted on this form.

After setting up the loading platform firstly sand loading test was done. In this test deflections were measured after every 20 Kg of sand was added (Fig.6.8). Then after sand loading test, sand was removed and again on that form wet concrete loading was done. Both sand loading and concrete loading was done at an increment of 20kg per loading.

It was taken care of that while applying the load (concrete or sand), it was uniformly spread throughout the form and there was no impact loading. Reading was taken 20Kg load was properly spread.

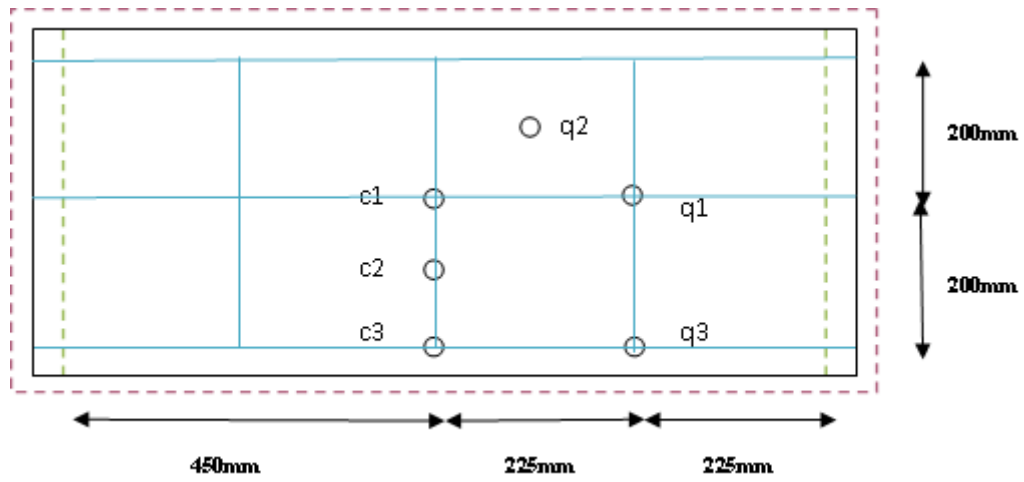


Fig.6.6 Position of dial gages on form D21



Fig6.7.a) Front view of the test set up b)Top view showing form within side forms



Fig.6.8. Sand loading test being done on form D21

Results on tests carried out on form D21 are mentioned in section 7.22

6.4.3 FOUR LAYER STIFFENED FORM F11

In this form four layered base forms were stiffened with four no., four layered channel sections. Same test set up as for D11 was used except for the position of dial gages (Fig.6.9a). Dial gages were arranged at central and quarter sections as shown in fig.

In this case both sand and wet concrete loading was done. Sand loading was done up to 260 Kg with load increment of 20 Kg at each step (Fig.6.9b). At each load step 20 Kg sand was uniformly spread throughout the form. Dial gage readings were noted after each load step.

After the last load step, readings were taken and then sand was removed. Then at the same load set up wet concrete loading was done at the increment of 20 Kg and dial gage readings were noted down. Needle vibrator was used after loading of 200Kg and 260 Kg. At load level of 260 kg concrete depth on the form was 200mm (Fig.6.10). At that time final deflection during casting stage was noted down.

To get the idea about creep deflection readings were noted for four days. Side form height was 250mm and the concrete depth in it was 200mm. Remaining space was filled with

water for water curing after 24hr. Side forms were removed after four days and after that slab was cured with the help of wet mats for seven days.

After seven days side form boundaries on the form were cut because it was difficult to pick up the slab having boundaries.

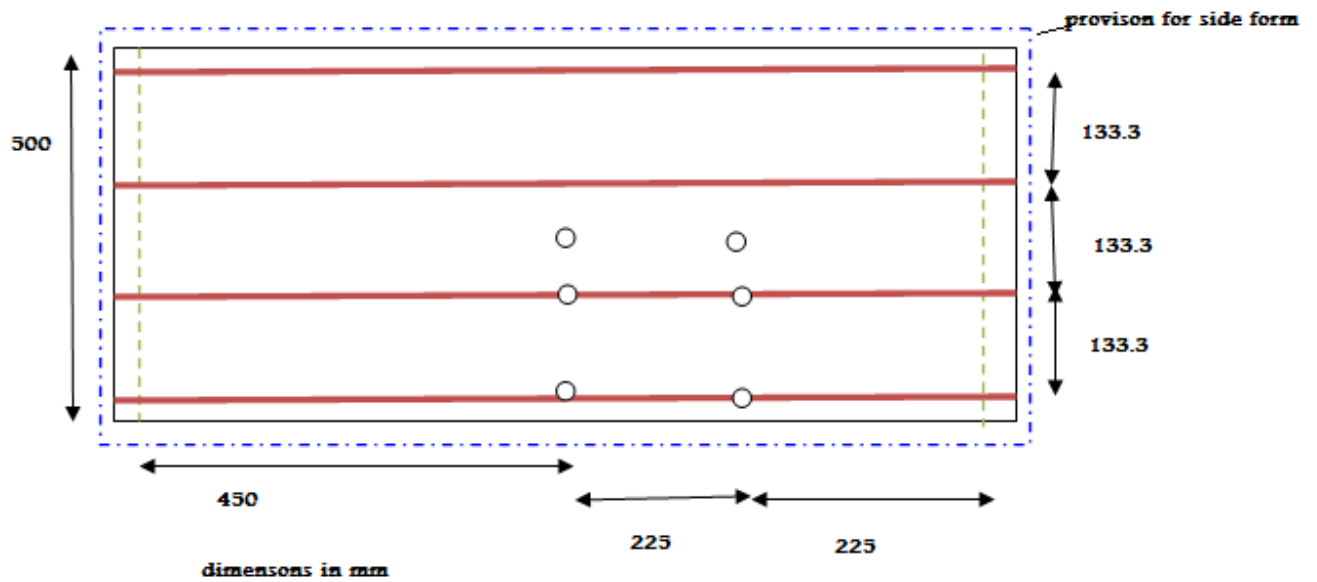


Fig.6.9a. Position of dial gages in form F11



Fig 6.9b. Sand loading test on form F11



Fig.6.10. Slab casted on form F11

Results of the sand loading and wet concrete loading tests carried out on form F11 are presented in section 7.23.

6.4.4 FOUR LAYER STIFFENED FORM F21

Form F21 was same in size and dimensions to form F11 with only difference that it aggregates were bonded to this form before it was subjected to loading (Fig.6.11). Aggregates were bonded to the form with the help of resin and were allowed to properly get cured before loading. Everything including test set up, way of testing, position of dial gages was same as for F11. Dial gage readings were taken after every 20 kg load step during wet concrete loading and sand loading.

Readings were also taken after slab casting to measure creep deflection.



Fig.6.11. Aggregates bonded to form F21

Results of sand and wet concrete loading tests carried out on form F21 are presented in section 7.2.4.

6.4.5 FOUR LAYERED STIFFENED FORM F31

This was the first form to start the research with. It was also considered as trial form. Set up for this form was same as for form F11 with the only difference on the position of dial gages (Fig.6.12). On this form only wet concrete loading was done and readings were taken on the basis of volume filled. Deflections were measured after 35%, 70% and 100% volume was filled. Slab casted was having depth of 200mm (Fig.6.15).

Readings were taken for four days to measure the creep effect.

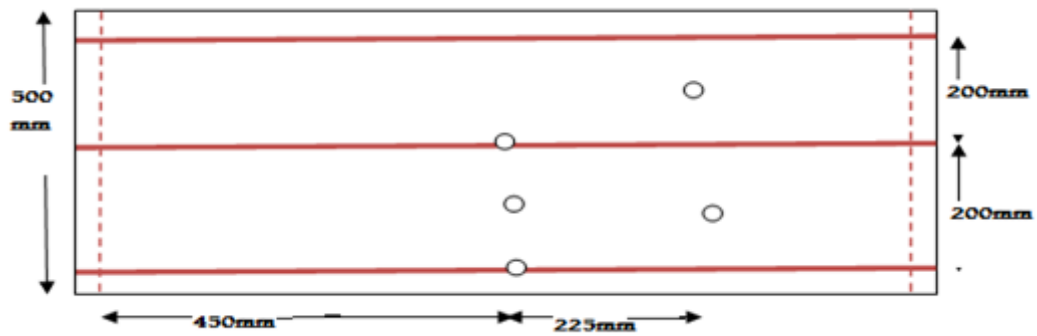


Fig 6.12. Position of dial gages in form F31

There was one difference between this form and all other forms that in this there was no provision for side forms (Fig.6.13). Side forms were placed around the form and not on the form.



Fig.6.13. Side forms around the base form



Fig.6.14. Use of needle vibrator

Fig.6.14 shows how needle vibrator was used to give vibrations to the concrete. Fig.5.15 shows the casted slab.



Fig.6.15. Slab casted on form F31

Results of tests carried out on form F31 are presented in section 7.2.5.

6.5 NON-STRUCTURAL TESTING OF THREE SPAN FORMS

In the three span forms three one meter long forms were connected to form three meter form. Three, three span forms were tested in this research. Test set up was same for all the forms. Details about the tests carried out on three span forms is presented in this section

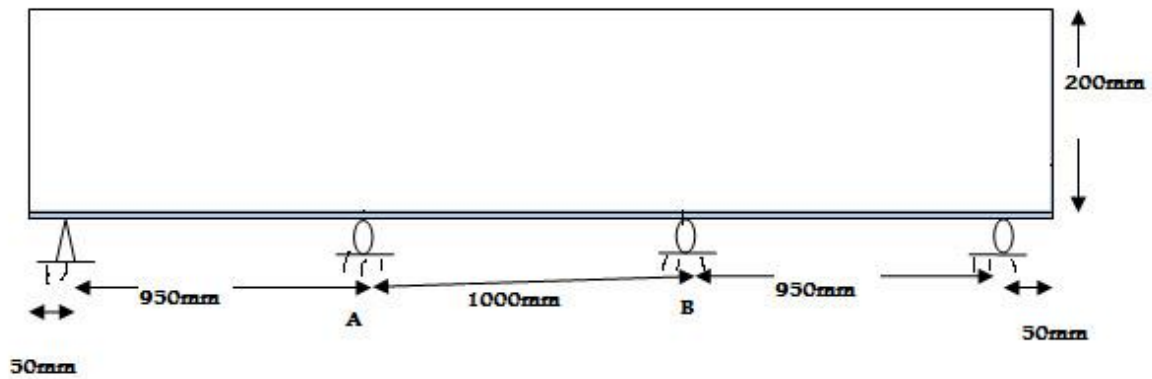


Fig.6.16. Test set up for three span beams

6.5.1 DOUBLE LAYER STIFFENED THREE SPAN FORM D13

Form D13 was subjected to sand loading only. Two supports were provided at distance 50mm away from the corners and two at the joints of the 1m forms. Side forms were put on the provision provided for the side forms. Nine dial gages were installed to measure the deflection (Fig.6.17). With load step of 60 Kg total 780 Kg of sand load was put in the form. Deflections were measured after every load step. Fig.6.18 shows the view of sand loading test.

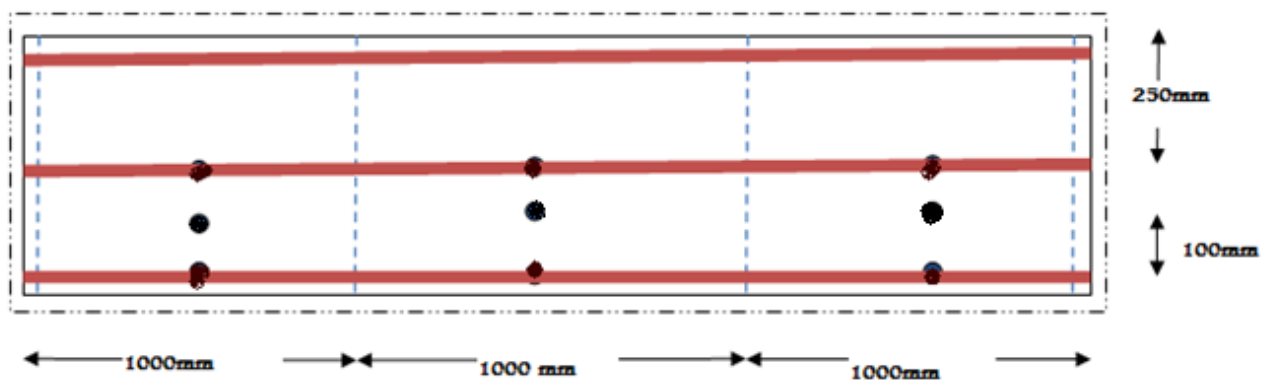


Fig.6.17 Position of dial gages on form D13



Fig.6.18. Sand test being carried out on form D13

Results of tests carried out on form D13 are presented in section 7.3.1.

6.5.2 FOUR LAYER STIFFENED THREE SPAN FORM F23

In this firstly four layer stiffened three span forms was prepared as described in 5.4.2.2.1. In test set up for this form loading platform was raised with the help of cubes and car jacks as shown in fig. Four car jacks were used beneath the intermediate supports. The purpose of using car jacks was to measure the deflection when intermediate supports were removed after hardening of concrete. With the help of jacks supports could be easily removed.

For this form only wet concrete loading was done. Load step was 60 Kg with total load of 780 Kg. Total eight dial gages were provided to measure the deflection (Fig.6.20). Deflection was noted down after every load increment. After the slab was casted upto height of 200mm concrete was allowed to dry down and then after one day it was moist cured for seven days. Dial gage readings were taken for 12 hr after concrete casting.

After two days when the concrete was properly hardened, car jacks were removed and then again deflection was measured for about 10hrs. This time position of dial gages was changed (Fig.6.22). Deflection measurement was done at points near the joints and at the centre of each span.



Fig.6.19. Use of car jacks during testing of form F23

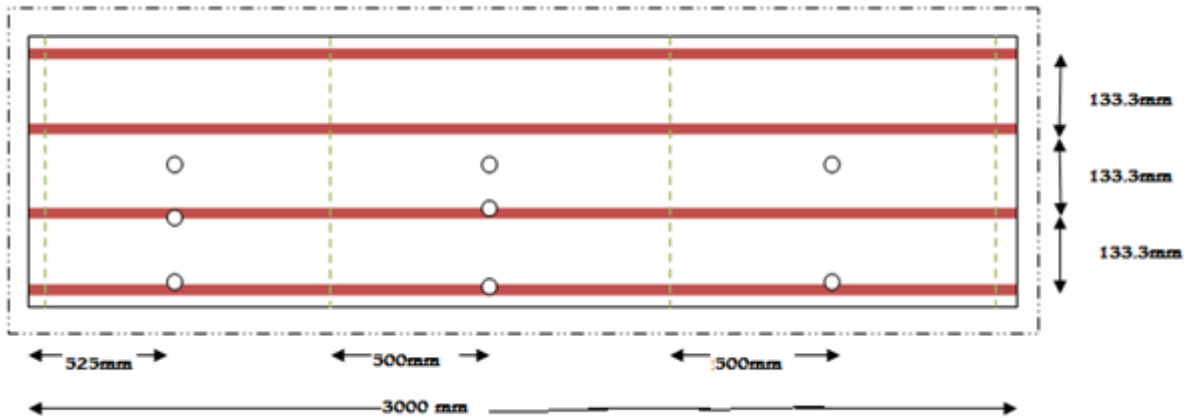


Fig.6.20. Position of dial gages if form F23



Fig.6.21. 200mm slab casted on form F23

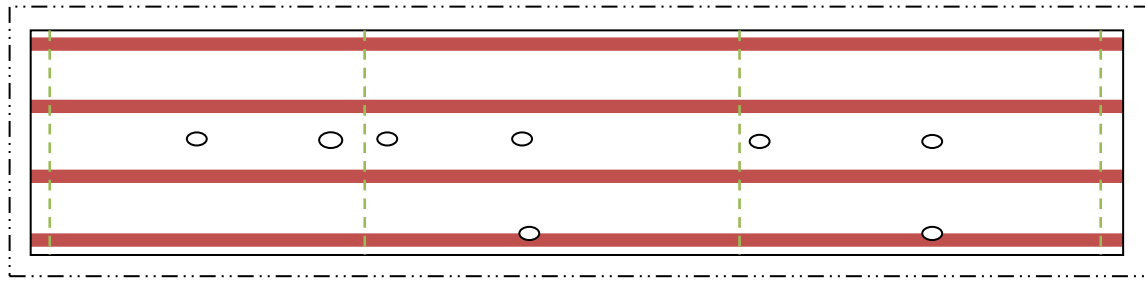


Fig.6.22 Position of dial gages during jack removal

6.6 STRUCTURAL TESTING

Structural testing was performed on 1m slabs in which deflection during the stage of casting was near to limit $L/180$. Three slabs casted on forms F11, F21, F31 satisfied the deflection criteria and were subjected to structural testing. Details about the structural testing are described in the following sections.

6.6.1 F11 Slab

Slab casted on form F11 was subjected to structural testing to evaluate forms performance as reinforcement. Hydraulic jack was used in the structural testing. Slab specimen (1m) was kept on the iron channels (rollers were fixed on the channels so that simply supported condition can be created) spaced 900mm apart. Dial gages were fixed at three positions –centre and quarter sections. Steel plate measuring 450mm x250 mm was kept at top of slab. Plate was kept at the central position. Load was applied on plate through jack and deflections were measured.

Loading test was performed to access the structural performance. To carry out the test channels were stiffened with the help of rods and the test was performed.

Fig.6.23 Structural testing of slab on form F11 with unstiffened supports



Fig.6.24 Test set up with stiffened supports

6.6.2 F21 SLAB

Structural testing of form F21 was done in same way as that of form F11. Slab casted on form F21 was supported on stiffened channels and steel plate was kept on its top. Dial gages were fixed at its central and quarter sections and load was applied on plate through jack. Deflections were measured at different load levels till wide cracks were developed and then dial gages were removed and load was applied till the ultimate failure.

6.6.3 F31 SLAB

Structural testing of form F31 was also done in the same way as form F11 and F21. Slab casted on form F31 was subjected to loading through hydraulic jack. Steel plate and channels were used in the same way and dial gages were installed at centre and quarter sections. Deflections were noted at different load levels. Load was applied till the ultimate failure.

Chapter 7

RESULTS AND DISCUSSION

7.1 INTRODUCTION

In this chapter, results obtained during the experimental investigation about the performance of 450 gsm, hand layup GFRP sections as stay in place formwork has been discussed. Results obtained during the structural and non structural performance tests of double layer base forms stiffened with single layer channel sections and four layer base forms stiffened with four no., four layer channel sections have been have been mentioned. Single span forms were tested for both structural and non structural performance and three span forms were tested only for their non-structural performance.

7.2 SINGLE SPAN FORMS

Results of tests carried out on forms of length 1m are presented in the following sections.

7.2.1 D11 STIFFENED DOUBLE LAYER BASE FORM COATED WITH AGGREGATES

The results of the wet concrete loading during slab preparation are presented in Table 7.1. Fig 7.1 shows the points where deflection was measured in form D11. Fig 7.2 shows the load deflection plot at these points. It was observed that at load level of 180Kg, all dial gages had to be removed as very high deflection occurred at that load level. After that continuous deflection was occurring without increasing the load level. Fig 7.3 shows the deformed shape at failure point. From this it was concluded that this is not a suitable GFRP profile to act as a formwork. To check about the failure mode, concrete poured on this form was removed. It was observed that the failure mode was due to buckling of the channels. It was noted that there was no debonding between base form and stiffener channels. Fig 7.4 shows the buckled channels after concrete was removed.

From this test it was concluded that D11 base forms were not suitable as forms due to buckling of channels. To avoid buckling of channels it was decided to provide transverse channels. Then three columns of channels were arranged in the transverse direction to avoid buckling of longitudinal channels.

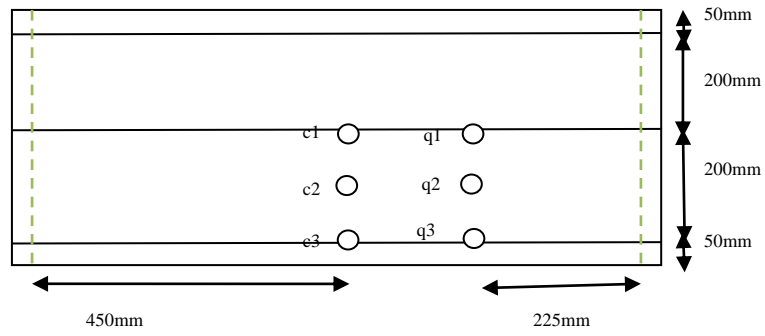


Fig 7.1 Location of points where deflection was measured

Table 7.1: Deflection at various points during wet concrete loading in D11

Concrete load	Deflection in (mm)					
	c1	q1	c2	q2	c3	q3
Load(x9.8N)						
0	0.00	0.00	0.00	0.00	0.00	0.00
20	3.50	2.75	4.15	4.74	3.00	0.00
40	4.50	3.62	7.07	5.09	3.50	0.13
60	7.00	5.11	8.08	7.54	4.50	1.68
80	10.50	6.18	9.51	8.73	5.50	2.49
100	12.50	7.47	11.91	9.23	6.00	2.51
120	13.00	8.39	13.41	10.29	7.50	3.52
140	14.50	9.49	15.07	11.39	10.00	4.77
160	16.50	10.31	17.83	12.49	11.00	5.75
170	18.50	11.68	19.13	14.07	13.00	6.28
180	21.00	12.90	21.51	15.75	15.00	8.80

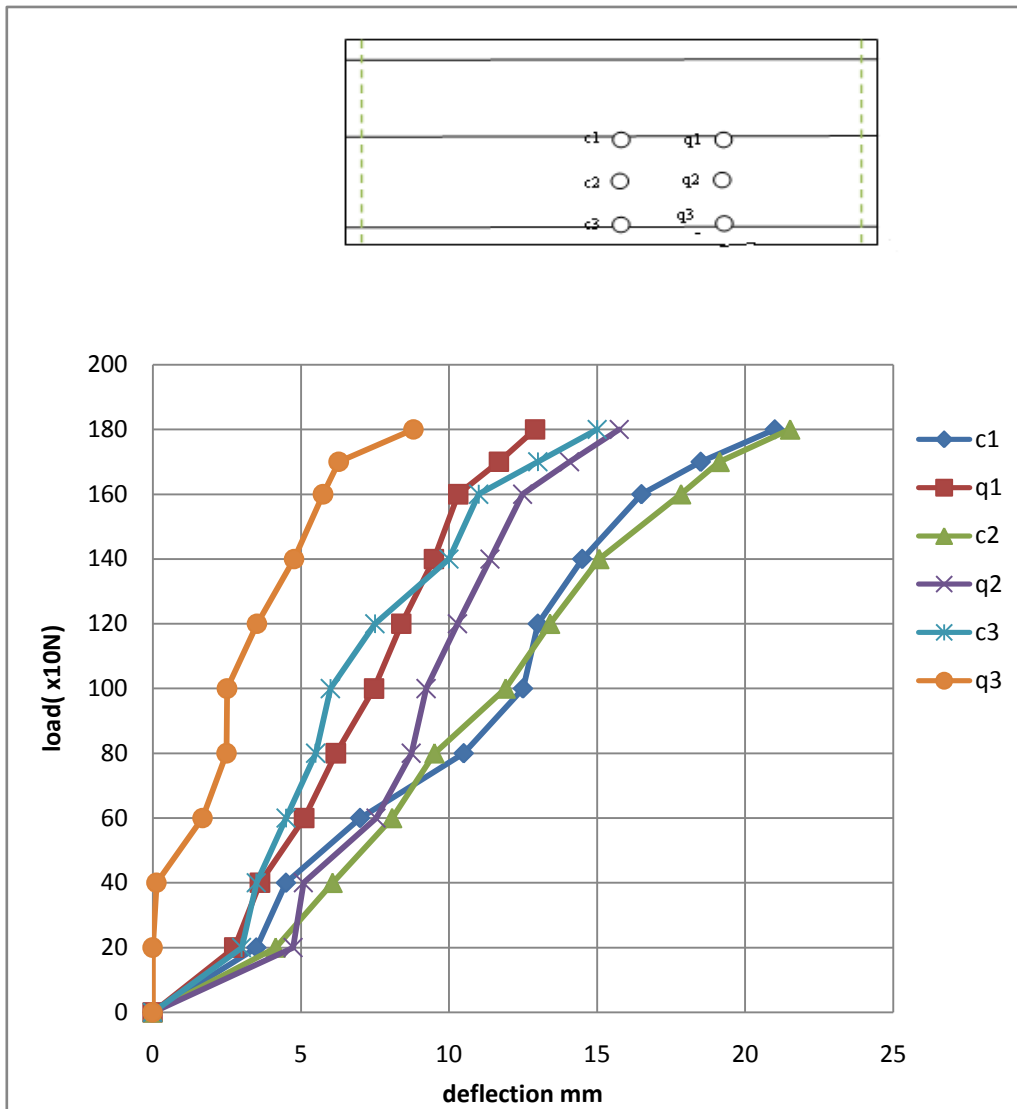


Fig 7.2 Load deflection plot at various points in form D11



Fig 7.3 Excessive deflection during slab casting on form D11



Fig 7.4 Buckling of channels in form D11

7.2.2 D21 DOUBLE LAYER BASE FORMS STIFFENED WITH LONGITUDINAL AND TRANSVERSE CHANNELS

After failure of D11 forms due to buckling of channels, it was decided to use transverse channels for buckling control. In D21 forms there were both longitudinal and transverse channels. Firstly sand test was carried out on this formwork. Capacity of side forms was to retain only 160 Kg of sand. A deflection at different loads during sand testing is shown in Table 7.2. Fig 7.5 shows the points where deflection was measured in form D21. Fig 7.6 shows the load deflection plot at these points. It was observed that the maximum

deflection was at point q2 which was not on any channel section. Although the deflections were higher in this case also, the casting was done in order to find out the actual behaviour of the form for the full 250 kg load.

During wet concrete loading there was failure due to excessive deformation. Form D21 has also sagged during loading due to excessive deflection but sagging was less as compared to form D11. Table 7.3 shows deflection at various load levels during wet concrete loading. Fig 7.7 shows the load deflection plot at various points in form D21. From this test it was clear that this was also not a suitable form for construction purposes. Concrete poured was removed to observe the failure mode. After removing it was observed that sheet was in its original state. It was in its elastic stage throughout the test. This time no channel buckling was there. Fig 7.8 shows deflected shape at the time of concrete removal.

From tests done on forms D11 and D21 it was clear that double layer base forms stiffened with single layer channel sections were not suitable for the role of forms. Flexural rigidity of these forms is less than that required for forms. Back calculations were done to get the value of E for the fiber and resin matrix. Then based on the back calculations four layer stiffened base forms were designed.

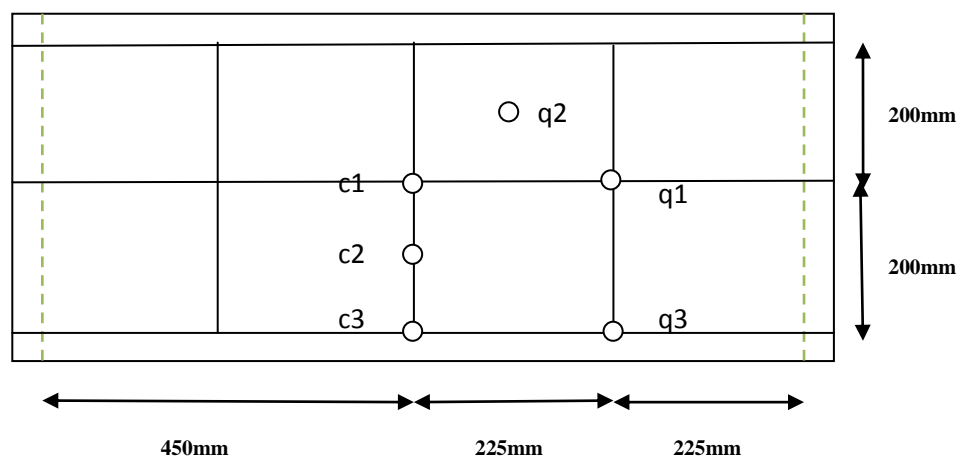


Fig 7.5 Location of deflection measurement points in form D21

Table 7.2 Deflection of form D21 during sand loading

Sand load	Deflection at points (mm)					
Load(x9.8N)	C1	Q1	C2	Q2	C3	Q3
0	0.00	0.00	0.00	0.00	0.00	0.00
20	2.22	0.833	1.15	1.83	1.53	1.15
40	3.56	1.61	2.28	3.62	2.84	2.17
60	4.34	2.40	4.00	4.36	4.00	2.98
80	5.26	3.23	4.53	5.50	4.86	3.59
100	5.95	4.06	5.73	6.63	5.90	4.33
120	8.25	5.00	6.90	7.83	7.05	5.00
140	9.44	5.91	8.33	8.85	8.56	5.93
160	11.42	7.36	10.80	12.06	9.93	6.80

Table 7.3 Deflection of form D21 during wet concrete loading

concrete load	Deflection at points (mm):					
Load(x9.8N)	c1	q1	c2	q2	c3	q3
0	0.00	0.00	0.00	0.00	0.00	0.00
20	1.30	1.00	1.10	2.22	0.40	0.95
40	2.52	1.80	2.40	2.45	1.51	1.75
60	3.80	2.80	3.72	3.85	3.70	2.60
80	5.18	3.80	5.22	6.35	4.80	3.39
100	6.78	4.99	6.80	7.77	6.21	4.33
120	8.62	6.25	9.80	9.70	7.70	5.35
140	10.52	7.65	11.00	12.75	9.10	6.27
160	12.35	9.10	14.41	14.20	9.55	6.55
180	14.20	11.10	18.60	18.05	10.12	6.86
200	19.60	13.25	23.20	22.15	10.80	7.22
220	20.94	14.95			11.20	7.37
240	21.90	15.23			11.95	7.59
260	23.72	15.94			13.00	7.85

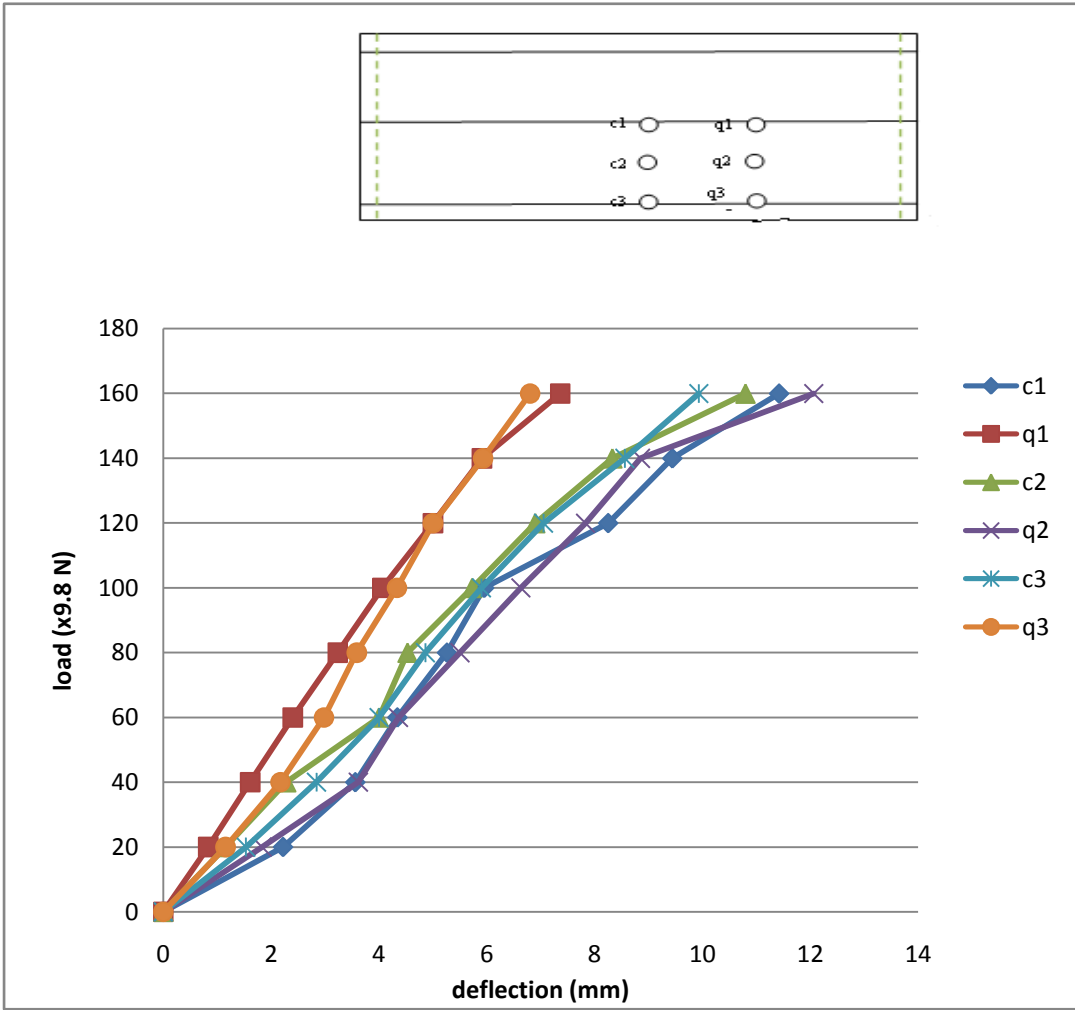


Fig 7.6 Deflection at various points during sand loading (D12)

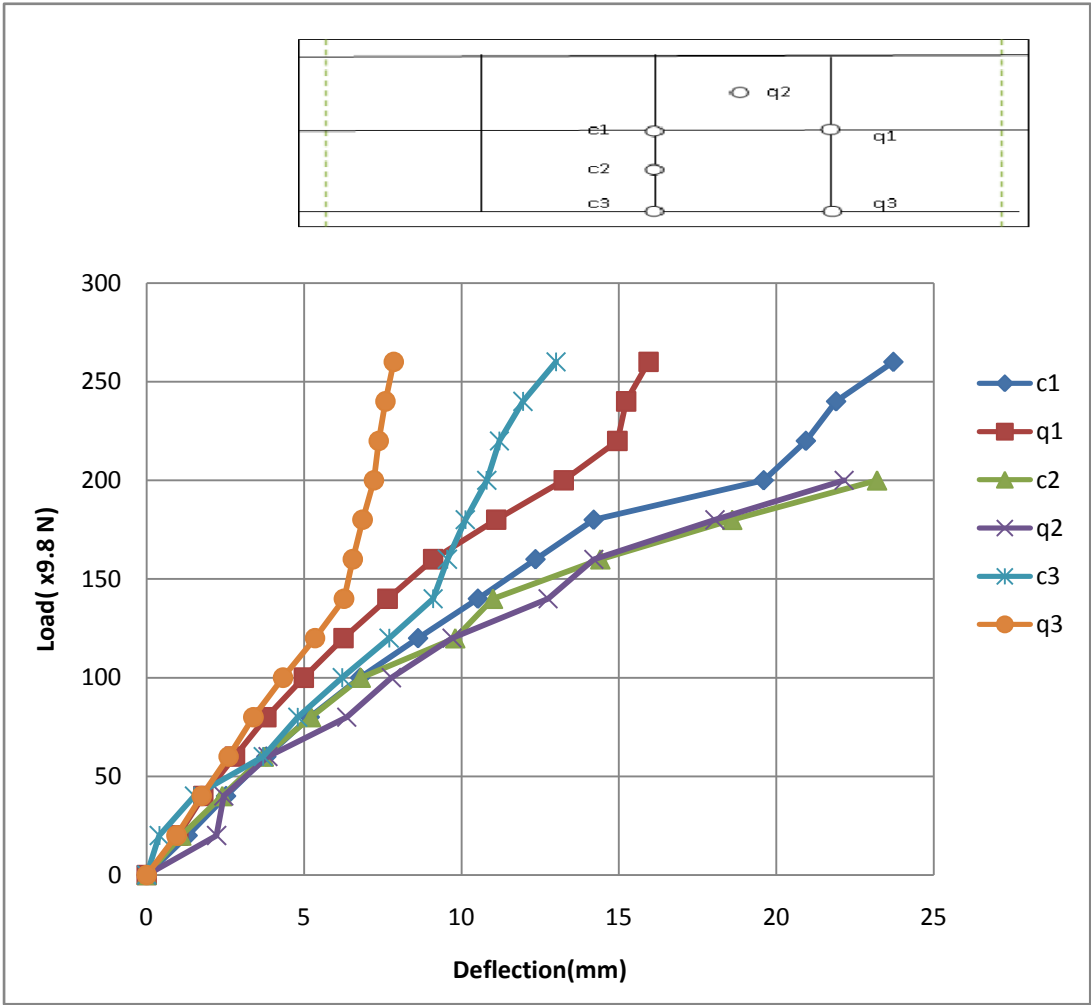


Fig.7.7 Load deflection plot of form D21 during wet concrete loading (D21)



Fig7.8. Excessive deflection of form D21

7.2.3 Four layer forms stiffened with four layer channel sections (F11)

In form F11 there was no aggregate coating. Sand testing and wet concrete testing was done on this form. During sand testing maximum deflection of 4.27mm was observed which was below the limiting value ($L/180=5\text{ mm}$). So, from sand testing it seemed that it is a suitable profile to act as a formwork. Fig 7.9 shows the points where deflection was measured in form F11. Table 7.4 shows the deflections at various load levels during sand testing. Fig 7.11 shows the load deflection plot at these points.

When concrete loading was done, it was observed that at the end of the last load step max deflection observed was 4.81mm which was below the limiting value. So the concrete poured was not removed and the concrete was allowed to dry. Table 7.5 shows the deflections at various load levels during wet concrete testing. Fig 7.12 shows the load deflection plot during wet concrete loading.

Deflections were taken at regular time intervals to get the idea about creep deflections. It was observed that final deflection was about 5.44mm which was slightly above then the limiting value (5mm). Maximum deflection was found to be at the centre. Table 7.6 Shows creep deflection of form F11. It was also observed that deflection at all points was more in wet concrete loading than in the sand loading. This was because sand loading was done first and then after its removal concrete loading was done so hysteresis effect was there.

As the difference between the limiting value and the observed value was very small, so slight change was required so that desired deflection level could be obtained. So in the next test aggregates were bonded to the forms.

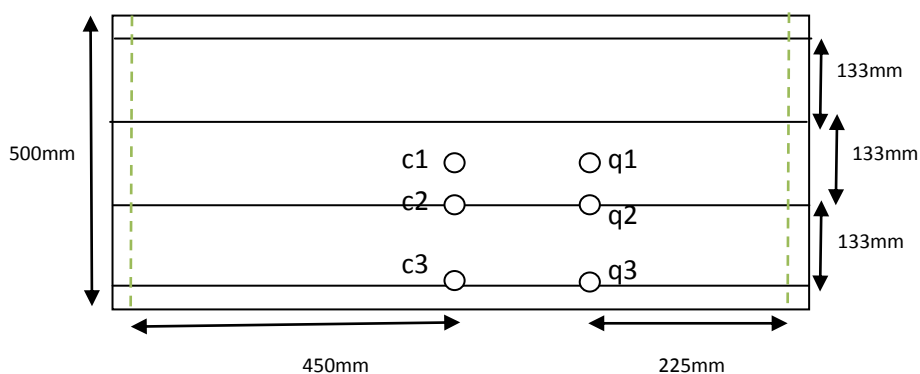


Fig 7.9 Points where deflection was measured in form F11

Table 7.4 Deflection of F11 during sand testing

LOAD	Deflection (mm) at points					
Load(x9.8N)	c1	q1	c2	q2	c3	q3
0	0.00	0.00	0.00	0.00	0.00	0.00
20	0.57	0.40	0.24	0.41	0.27	0.22
40	0.99	0.66	0.54	0.60	0.50	0.41
60	1.23	0.90	0.85	0.83	0.71	0.55
80	151.00	1.10	1.06	1.04	0.91	0.74
100	1.73	1.31	1.26	1.22	1.11	0.86
120	2.02	1.48	1.47	1.40	1.28	0.97
140	2.32	1.69	1.68	1.59	1.48	1.12
160	2.64	1.90	1.92	1.80	1.66	1.24
180	2.97	2.15	2.15	2.03	1.79	1.36
200	3.36	2.43	2.41	2.25	1.95	1.48
220	3.70	2.65	2.70	2.46	2.12	1.61
240	3.96	2.83	2.92	2.62	2.44	1.70
260	4.27	3.06	3.17	2.81	2.50	1.82

Table 7.5 Deflection of F11 due to wet concrete loading

LOAD	Deflection (mm) at points					
Load(x9.8N)	c1	q1	c2	q2	c3	q3
0	0.00	0.00	0.00	0.00	0.00	0.00
20	0.43	0.40	0.29	0.20	0.39	0.19
40	0.86	0.64	0.54	0.47	0.62	0.35
60	1.22	0.91	0.85	0.66	0.74	0.49
80	1.54	1.15	1.15	0.87	0.91	0.60
100	1.86	1.36	1.40	1.08	1.14	0.77
120	2.23	1.61	1.70	1.30	1.36	0.91
140	2.53	1.87	2.00	1.53	1.58	1.70
160	2.88	2.20	2.29	1.73	1.76	1.19
180	3.27	2.37	2.54	1.95	2.02	1.39
200	3.61	2.60	2.80	2.20	2.24	1.54
220	4.14	2.94	3.14	2.53	2.39	1.64
240	4.48	3.20	3.44	2.75	2.55	1.76
260	4.81	3.43	3.68	2.96	2.79	1.93

Table 7.6 Creep deflection of form FF1

Day	Deflection at					
	c1	q1	c2	q2	c3	q3
Casting day 1:30	4.91	3.50	3.76	3.07	2.88	1.97
Casting day 3:30	5.12	3.80	4.10	3.29	3.03	2.10
Casting day 5:30	5.37	3.83	4.20	3.36	3.07	2.14
Casting day 8:00	5.44	3.86	4.25	3.39	3.13	2.18
Casting day 10:00	5.46	3.88	4.26	3.41	3.15	2.21
Second day	5.48	3.89	4.27	3.41	3.15	2.21
Third day	5.47	3.88	4.27	3.42	3.15	2.21
Fourth day	5.47	3.89	4.26	3.43	3.15	2.21



Fig 7.10 Prepared slab on form F11

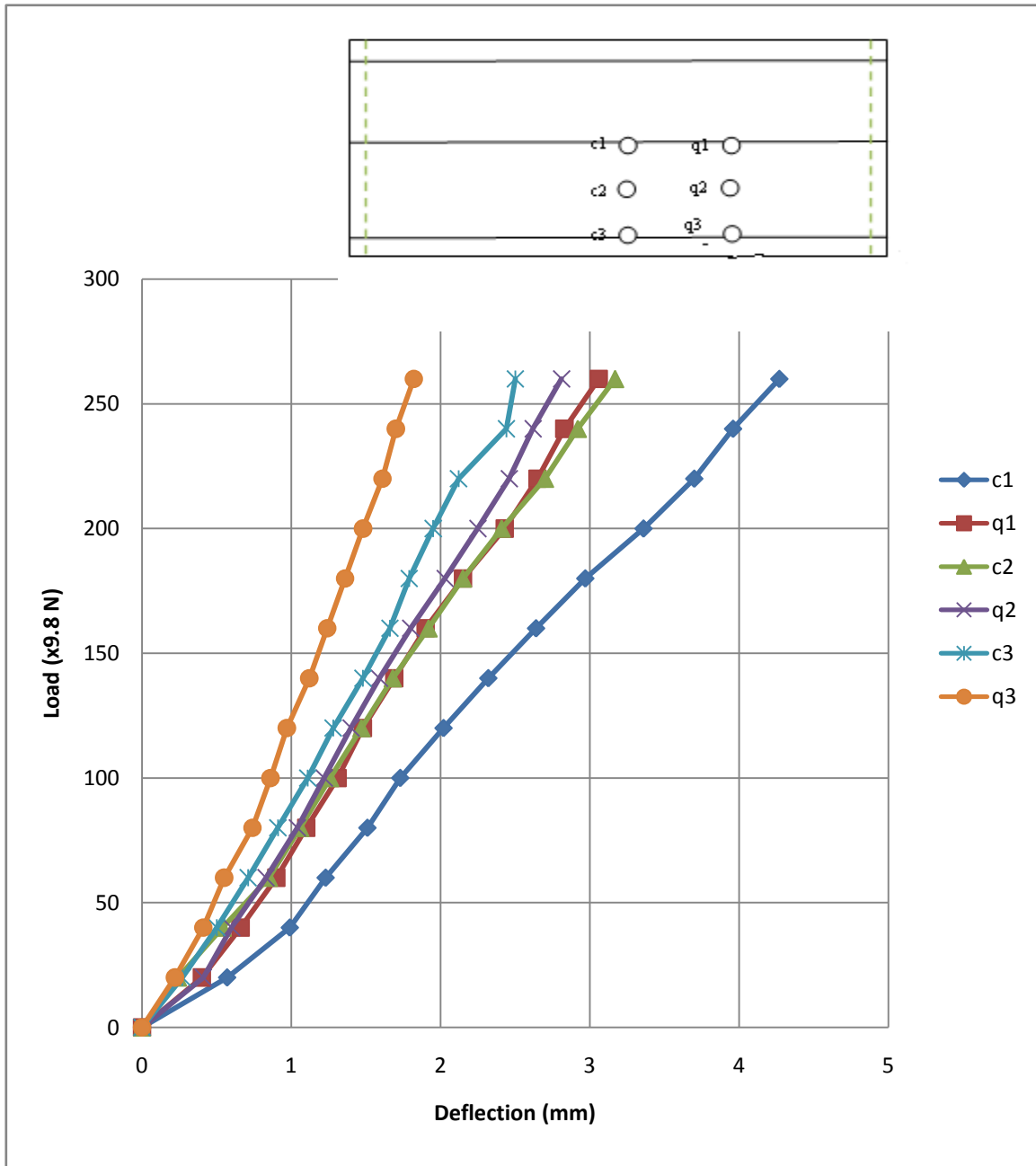


Fig 7.11 Load deflection plot at various points for form F11 during sand testing

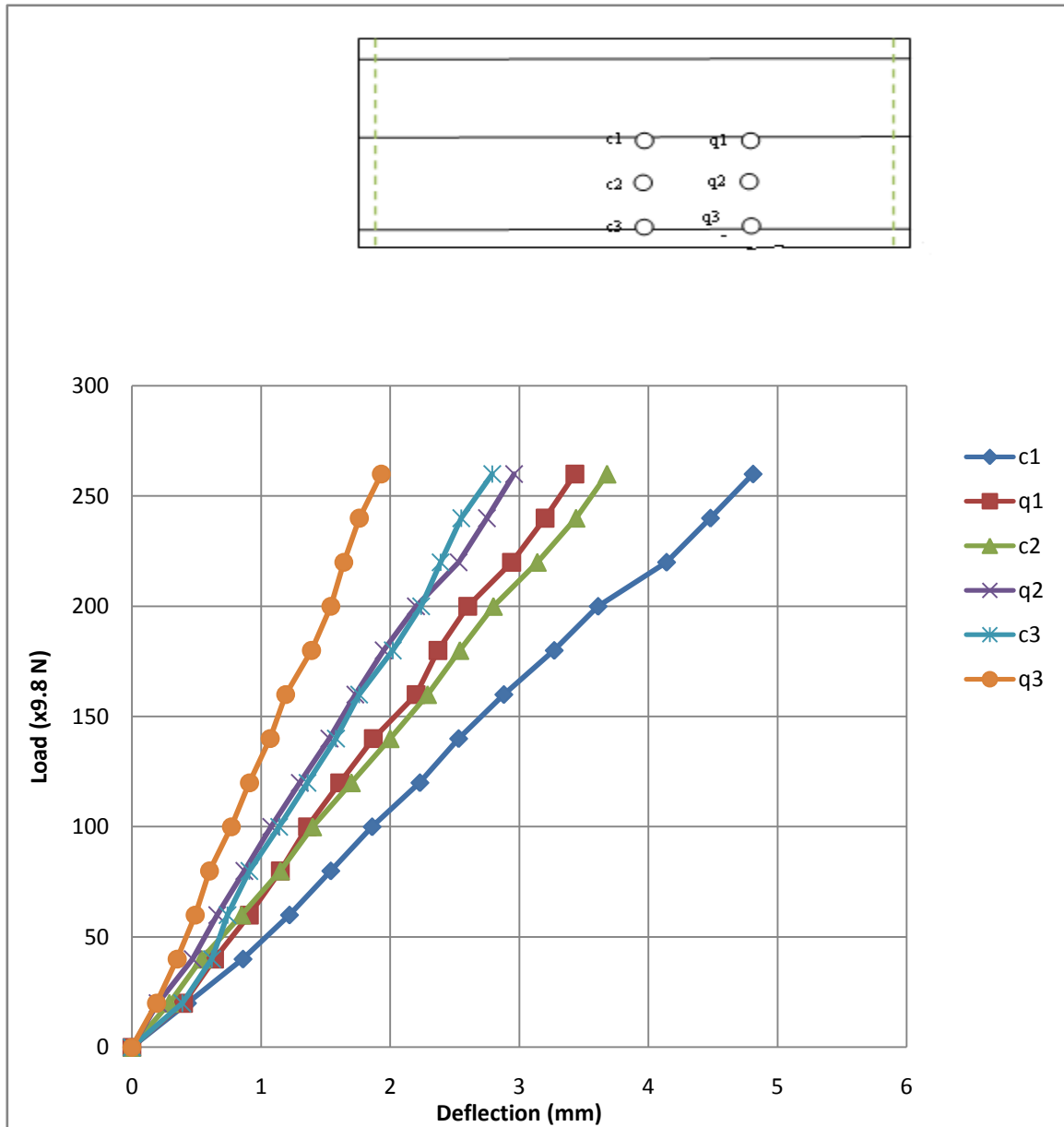


Fig 7.12 Load deflection plot for various points in form F11 during wet concrete loading

7.2.4 STIFFENED FOUR LAYER BASE FORM WITH AGGREGATES (F21)

In F12 four layer base form was stiffened with four, four layer channels. Load deflection tests carried out on this form were successful. Initially sand testing was carried out and it was observed that the maximum deflection obtained was 3.14mm which was within the permissible limit. Maximum deflection obtained was at the centre. Fig 7.13 shows the points

where deflection was measured in form F21. Fig 7.14 shows the load deflection plot at these points during sand testing. Table 7.7 shows the results of sand loading on form F21.

After sand testing, wet concrete testing was carried out. Maximum deflection was 3.65mm, which was within permissible limit. Table 7.8 shows the results of wet concrete testing. Final deflection after creep was 4.21mm which was also within permissible limits. Table 7.9 shows the final deflection after creep. Maximum deflection obtained was at point c3 as it was supported from only one side (channel stiffeners acting as support). Deflection at quarter sections was also within permissible limits. Fig 7.15 shows the load deflection plot at these points during sand testing.

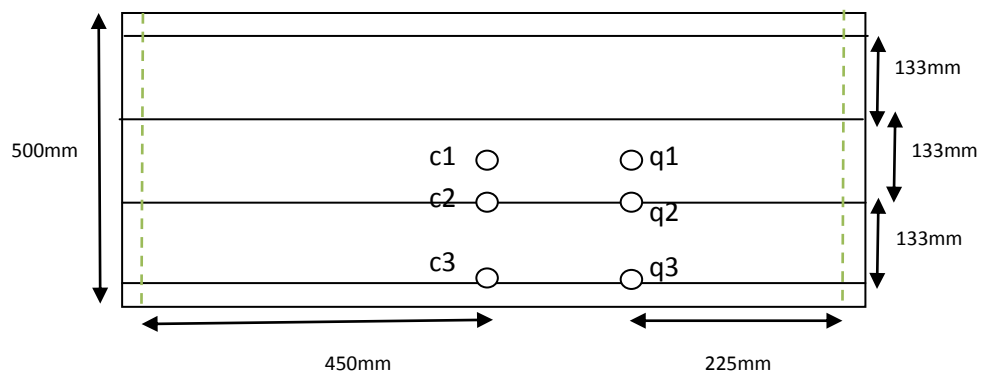


Fig 7.13 Points where deflection was measured in form F21

Table 7.7 Deflection of form F21 during sand testing

Sand load	Deflection at points					
Load(x9.8N)	C1	Q1	C2	Q2	C3	Q3
0	0.00	0.00	0.00	0.00	0.00	0.00
20	0.41	0.30	0.46	0.66	0.21	0.06
40	0.65	0.48	0.68	0.74	0.48	0.11
60	0.90	0.68	0.87	0.92	0.75	0.31
80	1.15	0.85	1.00	1.14	0.99	0.48
100	1.35	1.02	1.30	1.26	1.19	0.60
120	1.55	1.19	1.50	1.40	1.40	0.74
140	1.75	1.35	1.71	1.54	1.60	0.85
160	2.00	1.51	1.92	1.69	1.76	1.00
180	2.19	1.66	2.10	1.82	1.98	1.13
200	2.42	1.87	2.38	2.04	2.18	1.28
220	2.61	2.02	2.54	2.18	2.36	1.43
240	2.90	2.20	2.77	2.34	2.58	1.50
260	3.14	2.40	3.01	2.48	2.76	1.64

Table 7.8 Deflection of form F21 during wet concrete loading

Concrete	Deflection at various points (mm)					
Load(x9.8N)	c1	q1	c2	q2	c3	q3
0	0.00	0.00	0.00	0.00	0.00	0.00
20	0.54	0.30	0.52	0.57	0.35	0.20
40	0.79	0.55	0.81	0.76	0.60	0.43
60	1.14	0.75	1.02	0.99	0.88	0.59
80	1.40	0.92	1.21	1.15	1.15	0.75
100	1.56	1.10	1.48	1.34	1.45	0.90
120	1.84	1.41	1.72	1.52	1.95	1.07
140	2.06	1.51	1.92	1.69	2.00	1.21
160	2.33	1.71	2.21	1.87	2.29	1.41
180	2.55	1.90	2.42	2.01	2.50	1.56
200	2.82	2.05	2.64	2.19	2.75	1.69
220	2.99	2.25	2.86	2.35	3.04	1.82
240	3.26	2.45	3.11	2.58	3.30	2.00
260	3.64	2.60	3.28	2.67	3.65	2.13

Table 7.9 Deflection of form F21 taking into account creep effects

Day	Deflection on					
	c1	q1	c2	q2	c3	q3
Casting	3.68	2.65	3.41	2.76	3.90	2.33
First	3.96	2.95	3.81	3.06	4.18	2.56
Second	3.97	2.97	3.82	3.07	4.20	2.56
Third	3.96	2.99	3.82	3.07	4.21	2.56

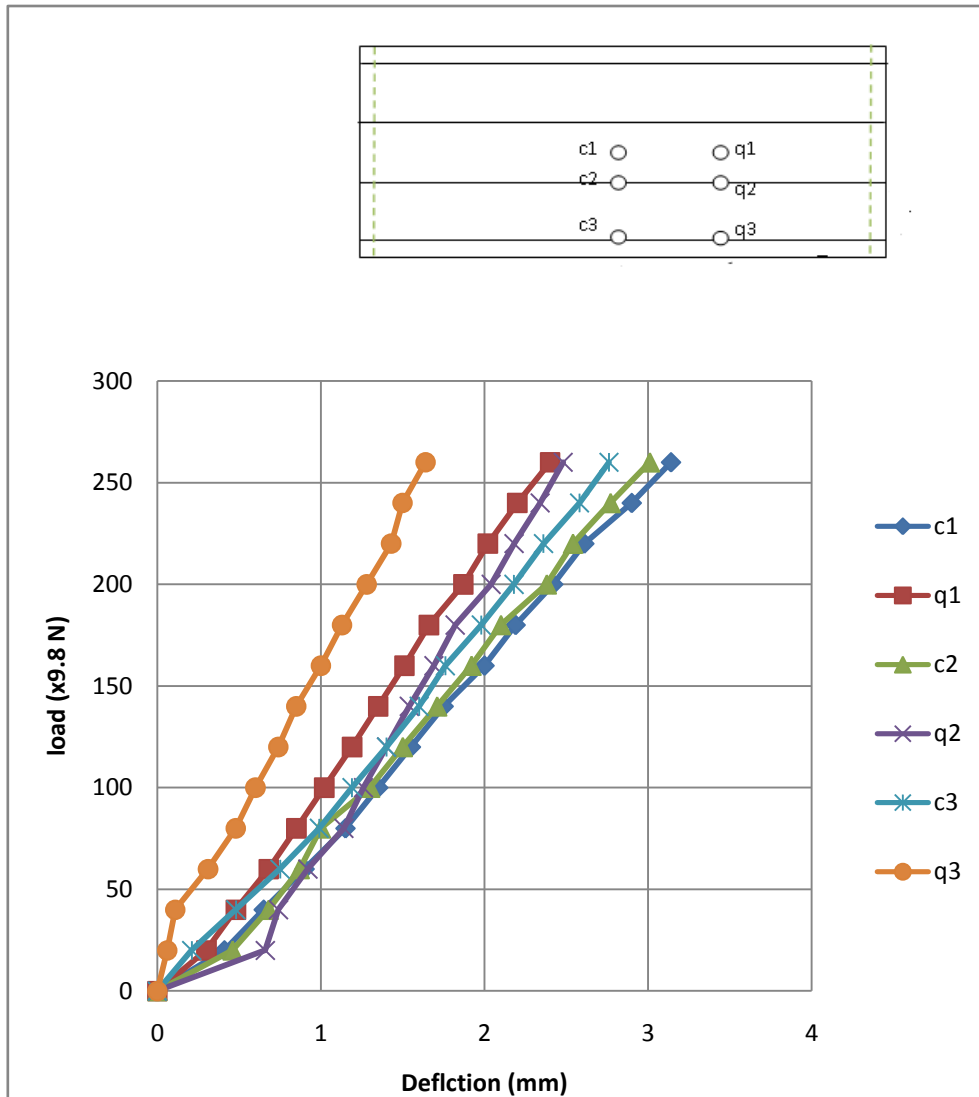


Fig 7.14 Load deflection plot at various points in form F21 due to sand loading

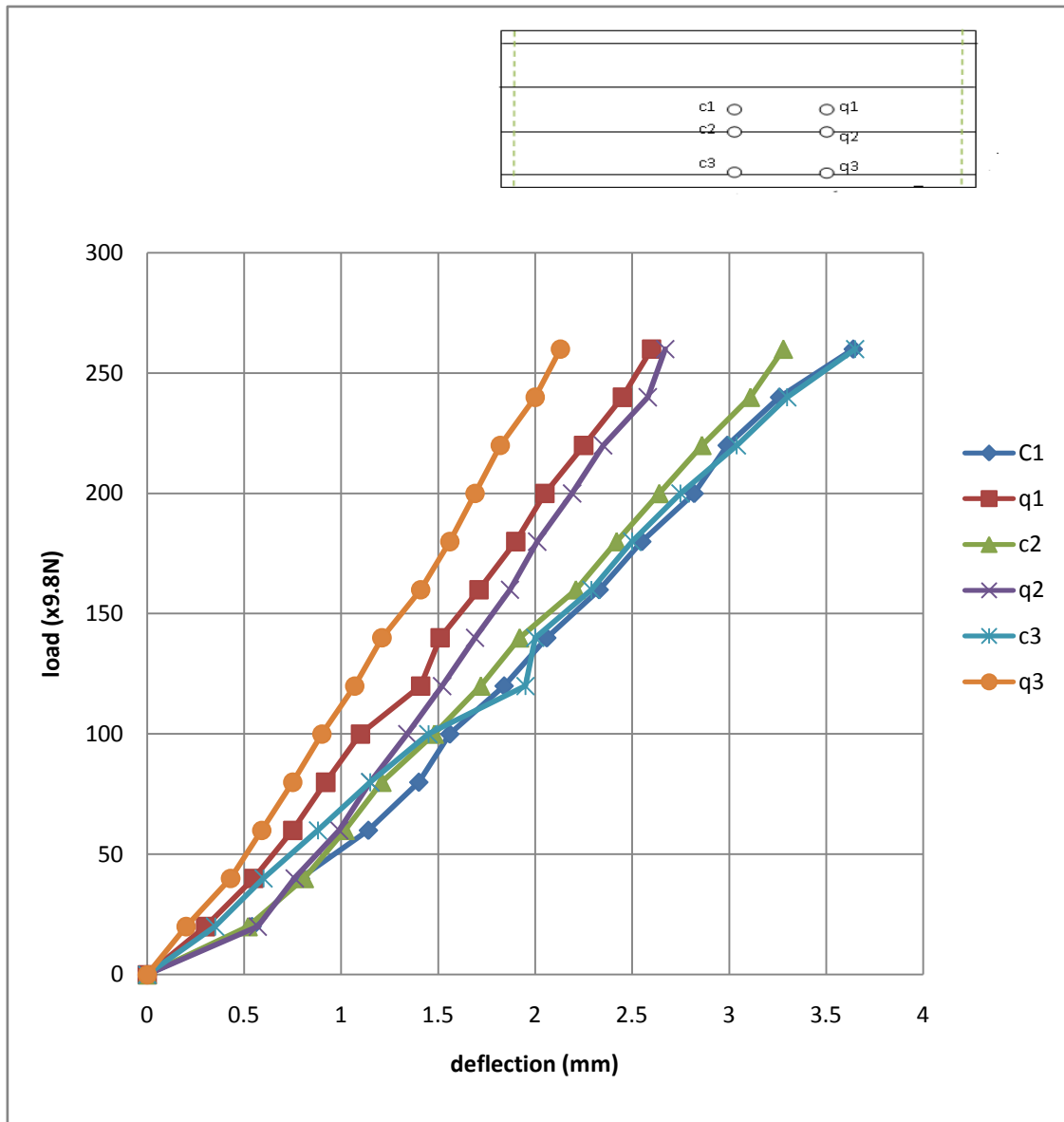


Fig.7.15. Load deflection plot at various points for form F21 due to wet concrete loading

7.2.5 FOUR LAYER STIFFENED CHANNEL F31

In this form four layer base form was stiffened with three channel sections. This was the first form which was tested. About this form incorrect information was provided by the manufacturer that this was a two layer form but later on through weight and thickness of samples provided, it was concluded that it was a four layer form. Information provided about channels is also doubtful that those were single layer channels. From thickness and weight these appeared to be four layered. Fig 7.16 shows the points where deflection was measured

in form F31. Fig 7.17 shows the load deflection plot at these points. Table 7.10 shows the results of wet concrete loading on this form.

In this test deflection was obtained taking into consideration volume filled. Only wet concrete loading test was done on this form. Maximum deflection 5.85mm was at centre of form. Final deflection taking into account creep factors was 6.25mm which was above the permissible limit but concrete poured was not removed and the slab prepared was kept for curing.

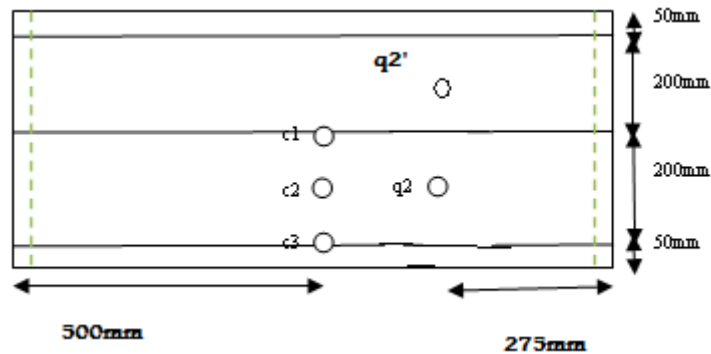


Fig7.16 location of deflection measurement points in form F31

Table 7.10 Deflection at various points in form F31

Deflection on	Deflection(mm) at points				
	c1	c2	c3	q2	q2'
Date(vol. Filled)					
23/3 (0%)	0.00	0.00	0.00	0.00	0.00
23/3 (35%)	2.70	2.61	2.00	2.57	0.89
23/3 (70%)	4.10	3.58	3.10	3.77	3.85
23/3 (100%)	5.85	5.55	4.40	5.35	4.25
24/3	6.30	6.05	5.50	5.75	4.30
25/3	6.30	6.06	5.63	5.72	4.41
26/3	6.25	6.00	5.60	5.65	4.03
27/3	6.25	6.00	5.60	5.65	4.03

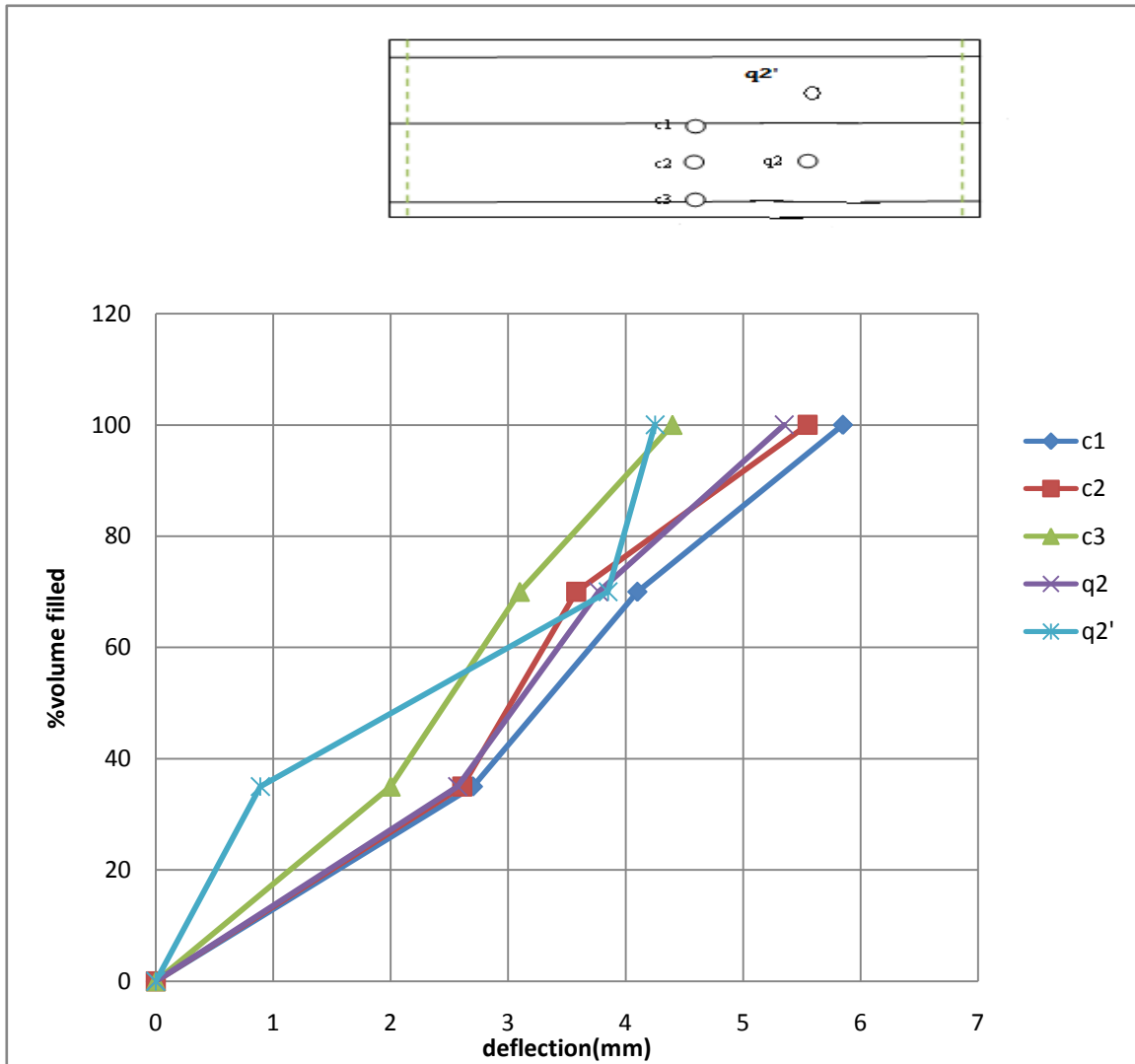


Fig. 7.17. Load deflection plots for form F31

7.3 THREE SPAN FORMS

Results of tests carried out on three span forms are presented in this section.

7.3.1 THREE SPAN STIFFENED DOUBLE LAYER FORMS D13

During testing of stiffened double layer forms it was observed that these forms failed prior to ultimate load level of 260Kg. It is known that deflection is much more in single span beam than in three span beam. So it was decided to perform sand loading test on three span forms with double layer base form stiffened with three single layer channel sections and to find out if these satisfy the permissible limits for deflection. Fig 7.18 shows the points where

deflection was measured in form D13. Fig 7.19.21 shows the load deflection plot at these points.

It was observed that deflection in mid span section was about 7.34mm which was very less than that in case of single span sections (21mm at load of 180 Kg). Deflection at one of the side spans was about 16.61mm and at other side form it was 21.07mm. Also there was delaminating of fiber strip connecting channels.

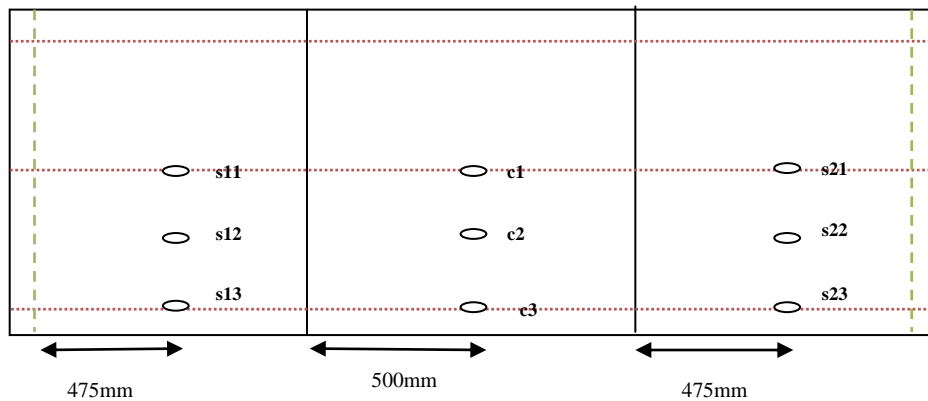


Fig 7.18 Points of deflection measurement in form D13

Table 7.11 Deflections at various load levels in form D13

Load(x9.8N)	Deflection at								
Sand	c1	c2	c3	S11	S12	S13	S21	S22	S23
0	0.00	0.00	0.00	0.00	0.00	0.00	0.00	0.00	0.00
60	1.09	2.15	0.70	2.18	1.37	1.20	1.93	2.35	2.32
120	1.39	2.95	0.05	2.43	2.65	2.30	2.52	4.15	2.86
180	2.39	3.30	0.55	4.86	3.89	3.29	3.72	3.29	3.05
240	3.11	3.62	0.83	6.31	5.02	5.00	4.72	7.22	3.55
300	3.73	4.15	1.25	7.36	5.92	5.74	5.87	8.22	4.37
360	4.01	4.42	1.45	9.16	7.37	6.79	7.12	8.47	5.30
420	4.60	4.88	1.85	10.06	8.24	7.54	8.32	9.65	6.33
480	5.29	5.78	2.27	11.16	9.22	8.34	10.07	11.29	7.77
540	5.89	7.10	2.25	14.46	12.80	10.17	15.93	16.70	12.45
600	6.07	-	2.40	14.56	12.92	11.24	16.07	16.89	12.65
660	6.49	-	2.75	15.86	13.28	11.54	16.71	17.49	13.32
720	6.84	-	3.14	16.16	13.47	12.14	17.78	18.57	14.47
780	7.34	-	3.50	16.61	13.92	12.59	20.21	21.07	17.07

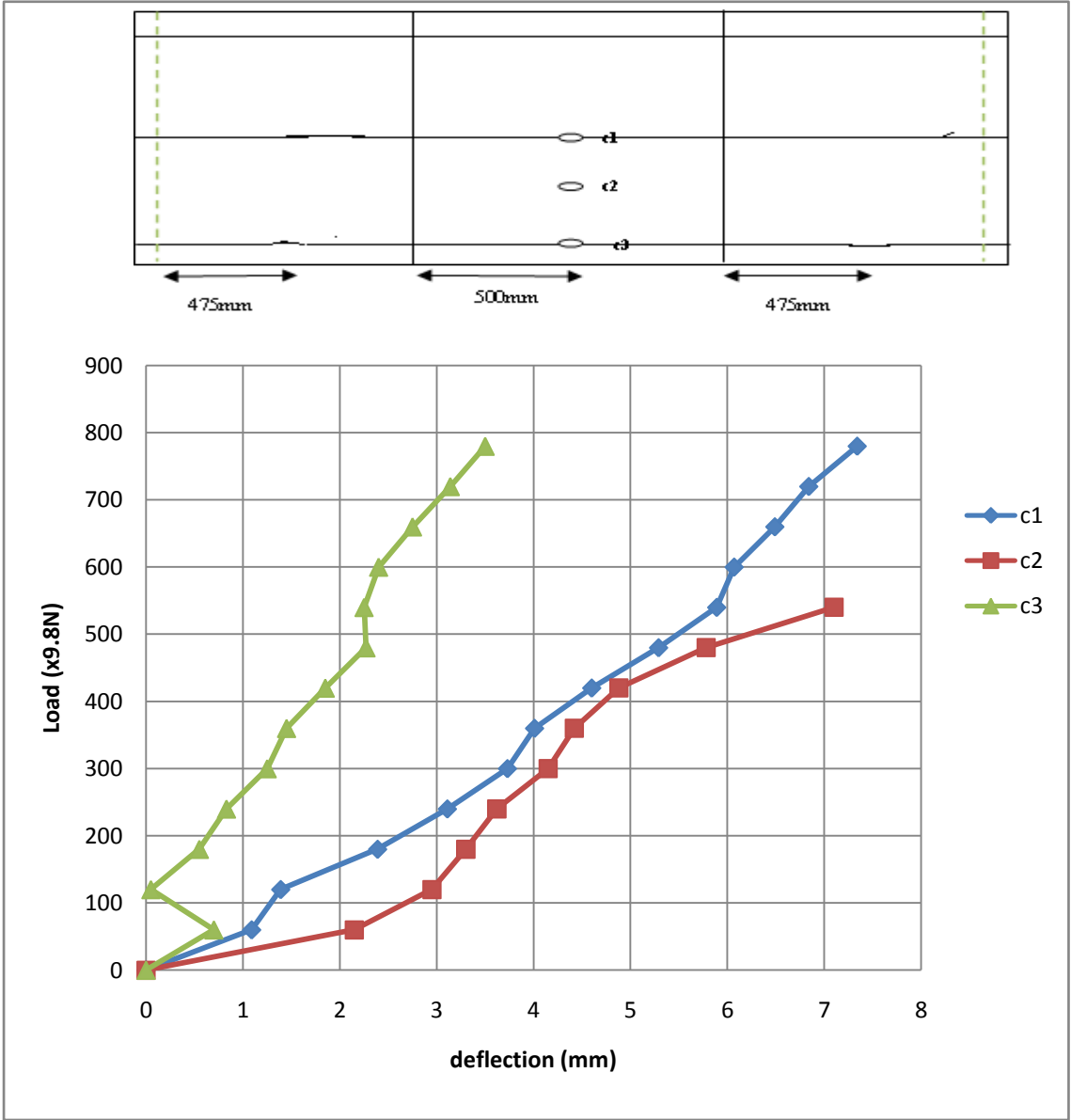


Fig. 7.19 Load deflection curve for points on central pan during sand testing

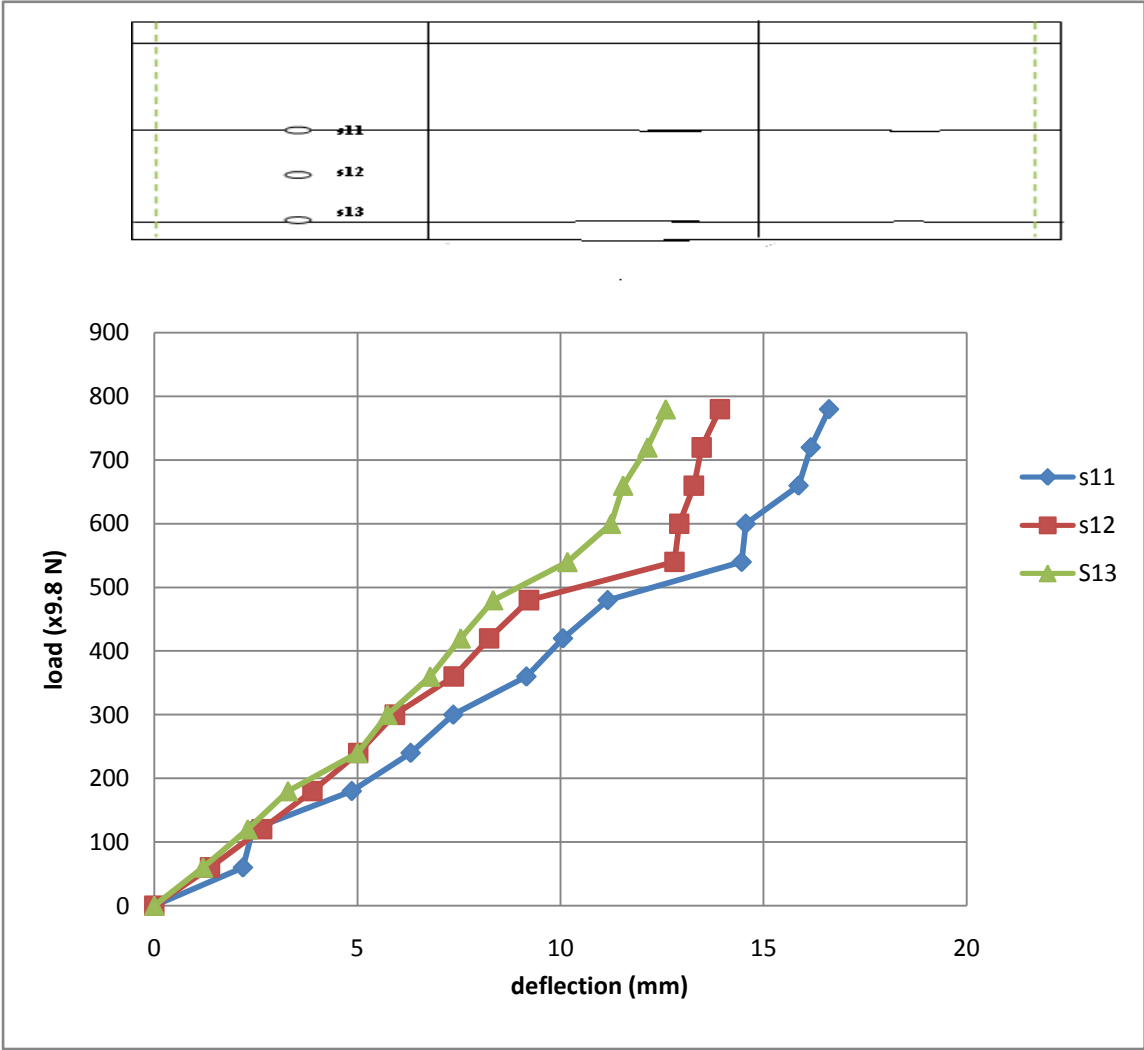


Fig 7.20.Load deflection curve for points on side span during sand testing on form D13

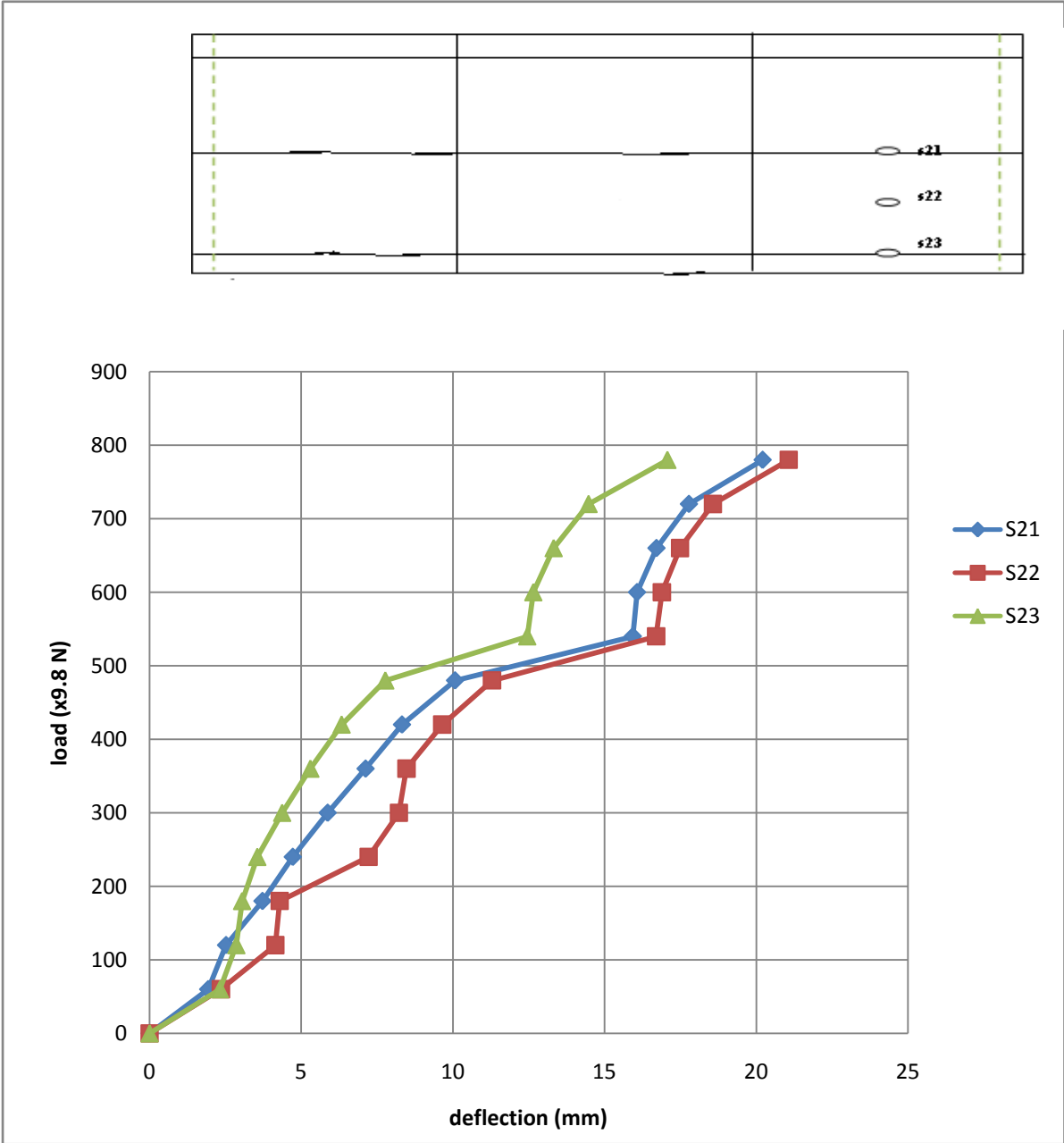


Fig 7.21 Load deflection plot for points on side span during sand load test on form D13

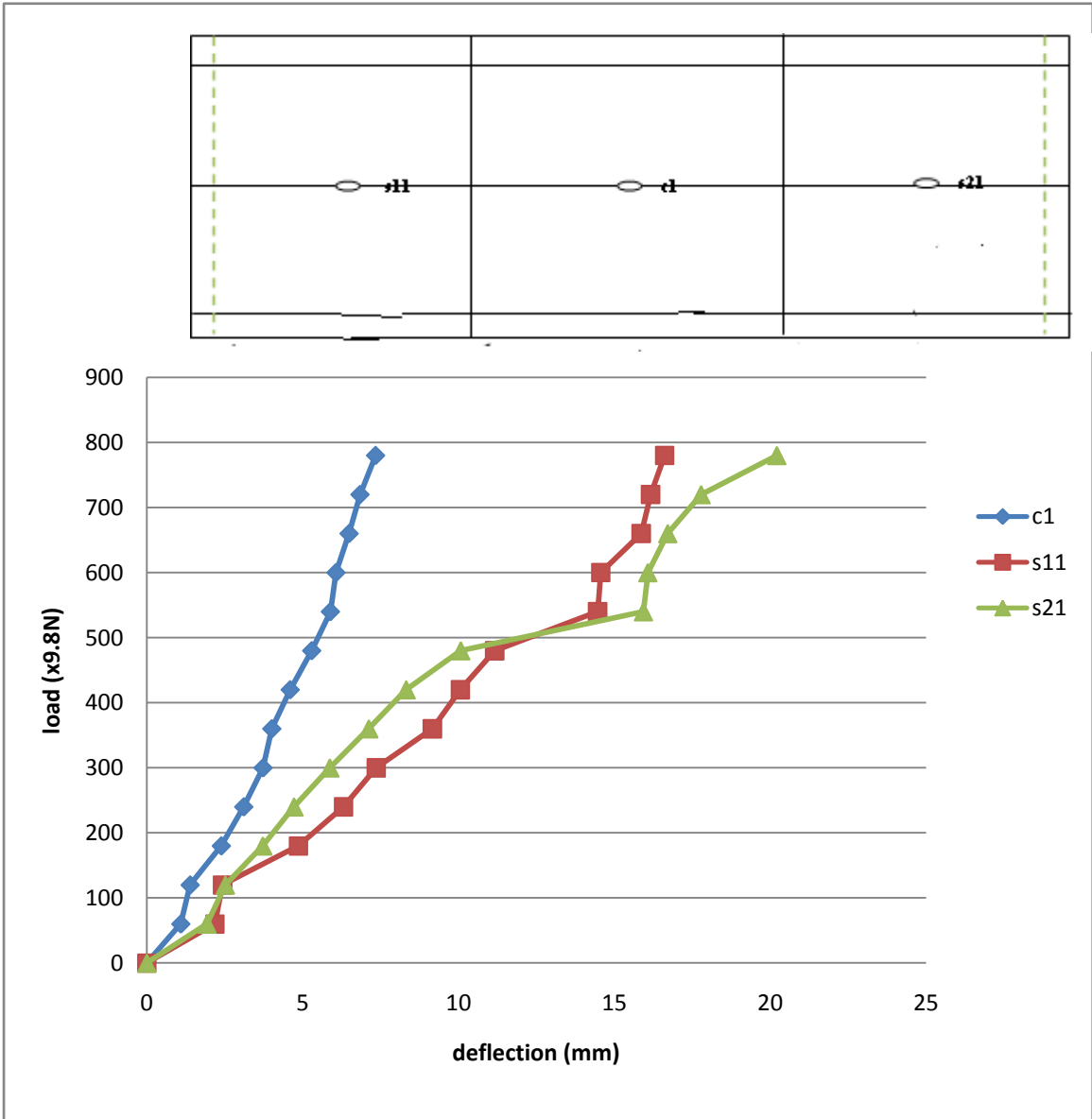


Fig 7.22 Comparison between deflection at central form and side forms



Fig 7.23 Delamination of the second connector layer

7.3.2 THREE SPAN FOUR LAYERED STIFFENED BASE FORM (F23)

In this three span form, four layered base form was stiffened with four no., four layered channel sections. Table 7.11 shows deflection at various points at different load levels. Fig 7.24 shows points where measurement is taken. Fig 7.25-7.28 shows load deflection plots. Fig 7.28 shows the comparison between the centre line deflection of centre form and side forms.

In this test four car jacks were used while casting 3m three span slab. These jacks were used at interior support points so that after concrete has properly hardened these supports could be easily removed so that effect of removing internal supports could be easily studied. Table 7.14 shows effect of removing supports at points shown in Fig. 7.29.

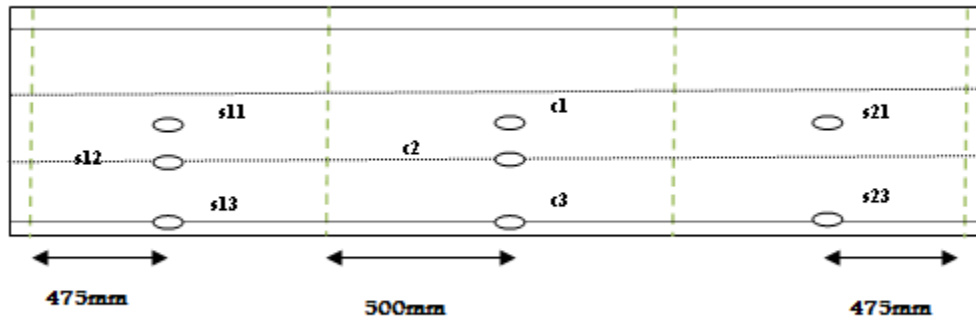


Fig 7.24 points where deflection measurement was taken for form F23

Table 7.12 Deflection at various points on form F23 during wet concrete loading

Load(x9.8N) concrete	Deflection at							
	c1	c2	c3	s11	s12	s13	s21	s23
0	0.00	0.00	0.00	0.00	0.00	0.00	0.00	0.00
60	0.91	0.6	0.22	1.70	0.89	1.06	1.05	0.86
120	1.40	1.05	0.55	2.21	1.23	1.54	1.45	1.28
180	1.87	1.41	0.89	2.88	1.83	2.12	1.85	2.30
240	2.30	1.70	1.13	3.43	2.42	2.70	2.27	3.33
300	2.73	2.10	1.43	4.18	2.92	3.88	2.80	3.90
360	3.25	2.55	1.73	4.41	3.18	3.99	3.05	5.36
420	3.63	2.89	1.98	4.85	3.60	4.25	3.31	5.65
480	3.96	3.20	2.28	5.28	4.08	4.59	3.61	5.92
540	4.33	3.54	2.52	5.62	4.46	4.86	4.01	6.35
600	4.70	3.90	2.93	5.88	4.70	5.25	4.38	6.85
660	5.13	4.33	3.38	6.20	5.05	5.67	4.65	7.20
720	5.36	4.60	3.78	6.50	5.45	6.33	5.01	7.63
780	5.76	5.01	4.28	6.96	5.93	6.95	5.37	8.38

Table 7.13 Creep deflection at various points in form F23

Time	Deflection at							
	C1	C2	C3	S11	S12	S13	S21	S23
Casting	5.76	5.01	4.25	6.96	5.93	6.95	5.37	8.28
2hr	6.27	5.45	4.98	7.35	6.29	7.22	5.91	8.87
5hr	6.50	5.70	5.13	7.50	6.47	7.39	6.11	9.10
12hr	6.45	5.57	5.05	7.42	6.38	7.30	6.07	9.00

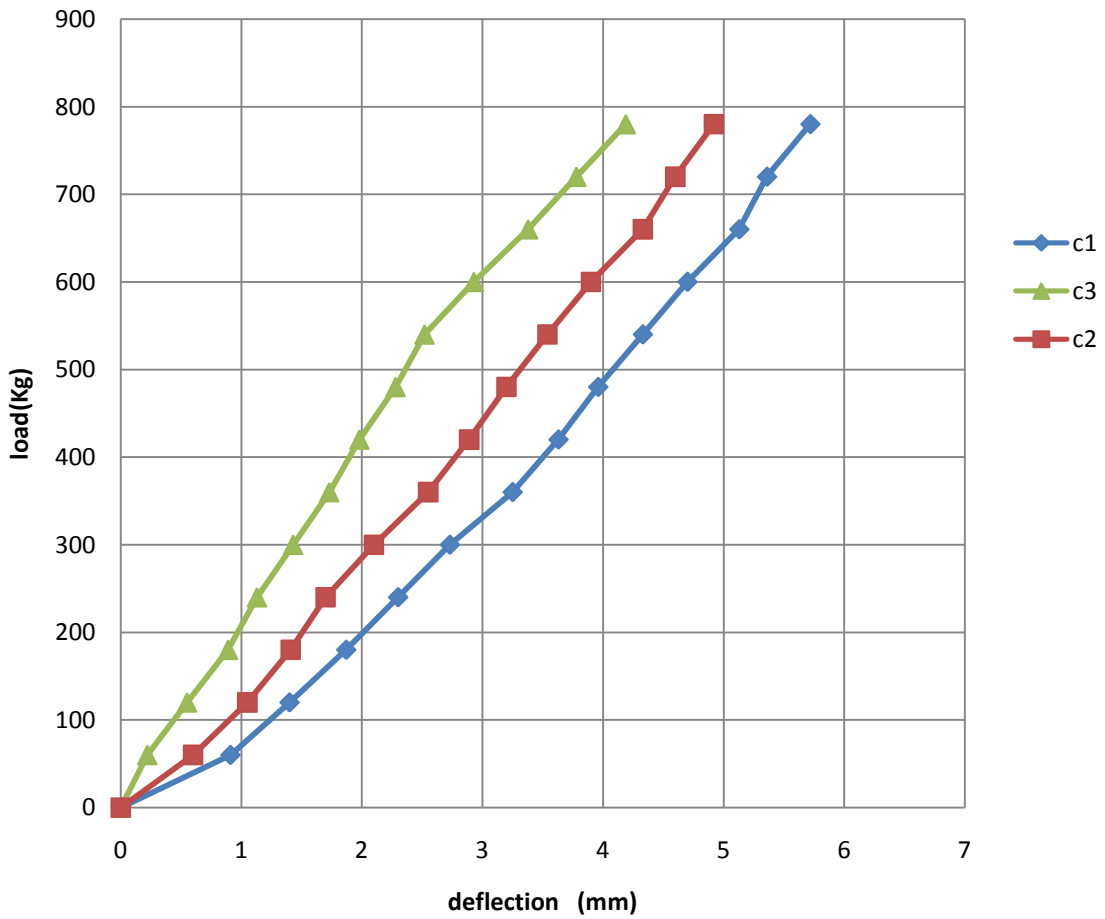
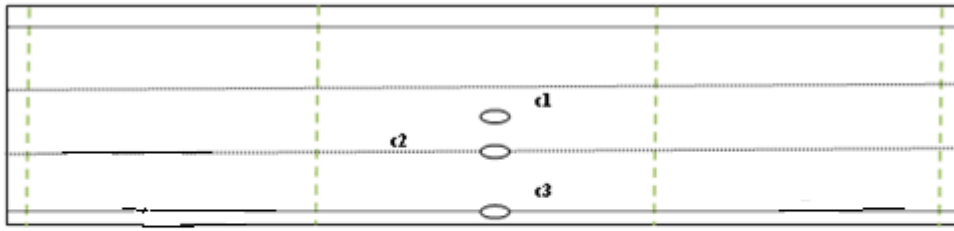


Fig 7.25 Deflections at various load levels on the central span form

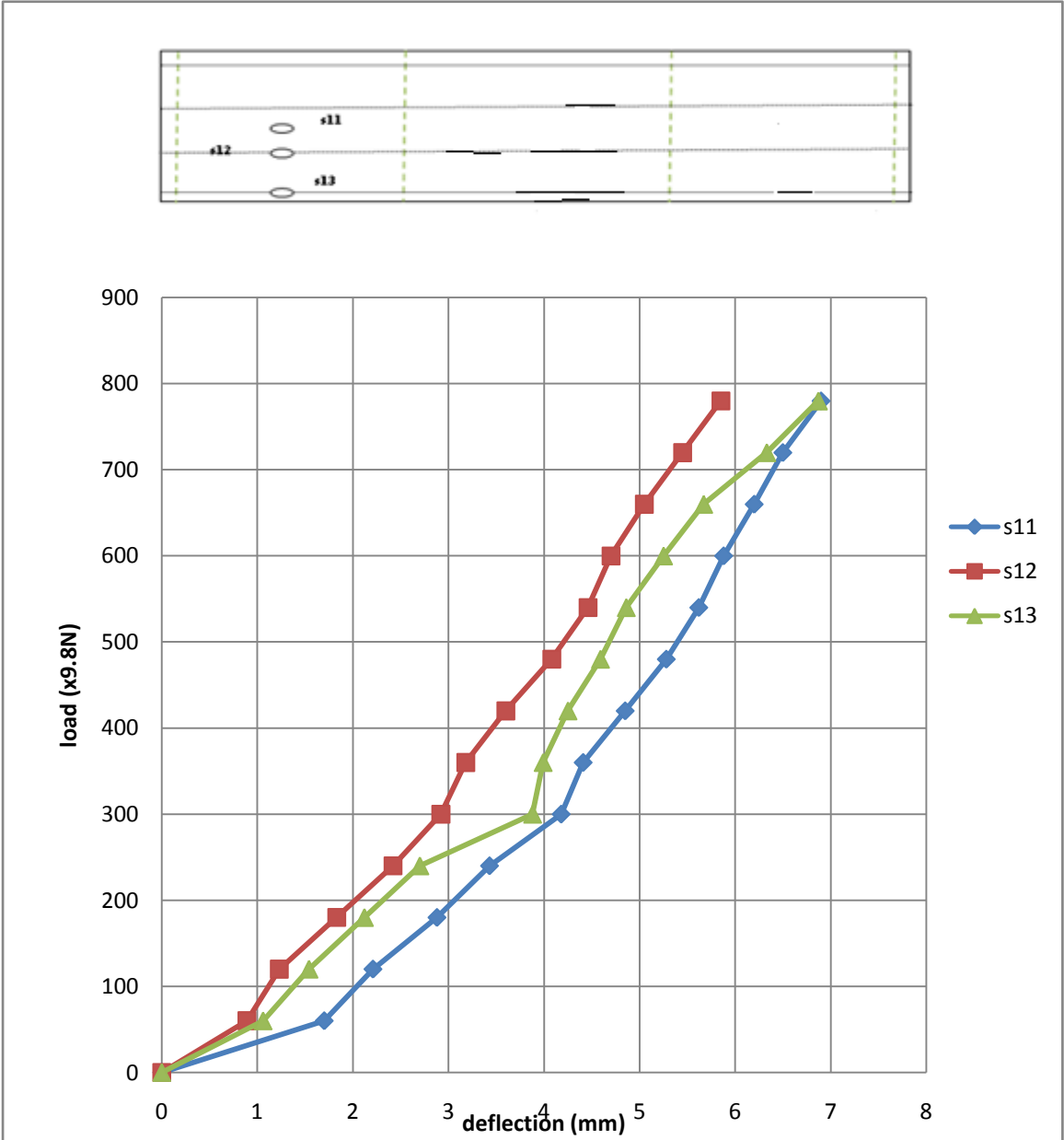


Fig 7.26 Load deflection plot for side forms

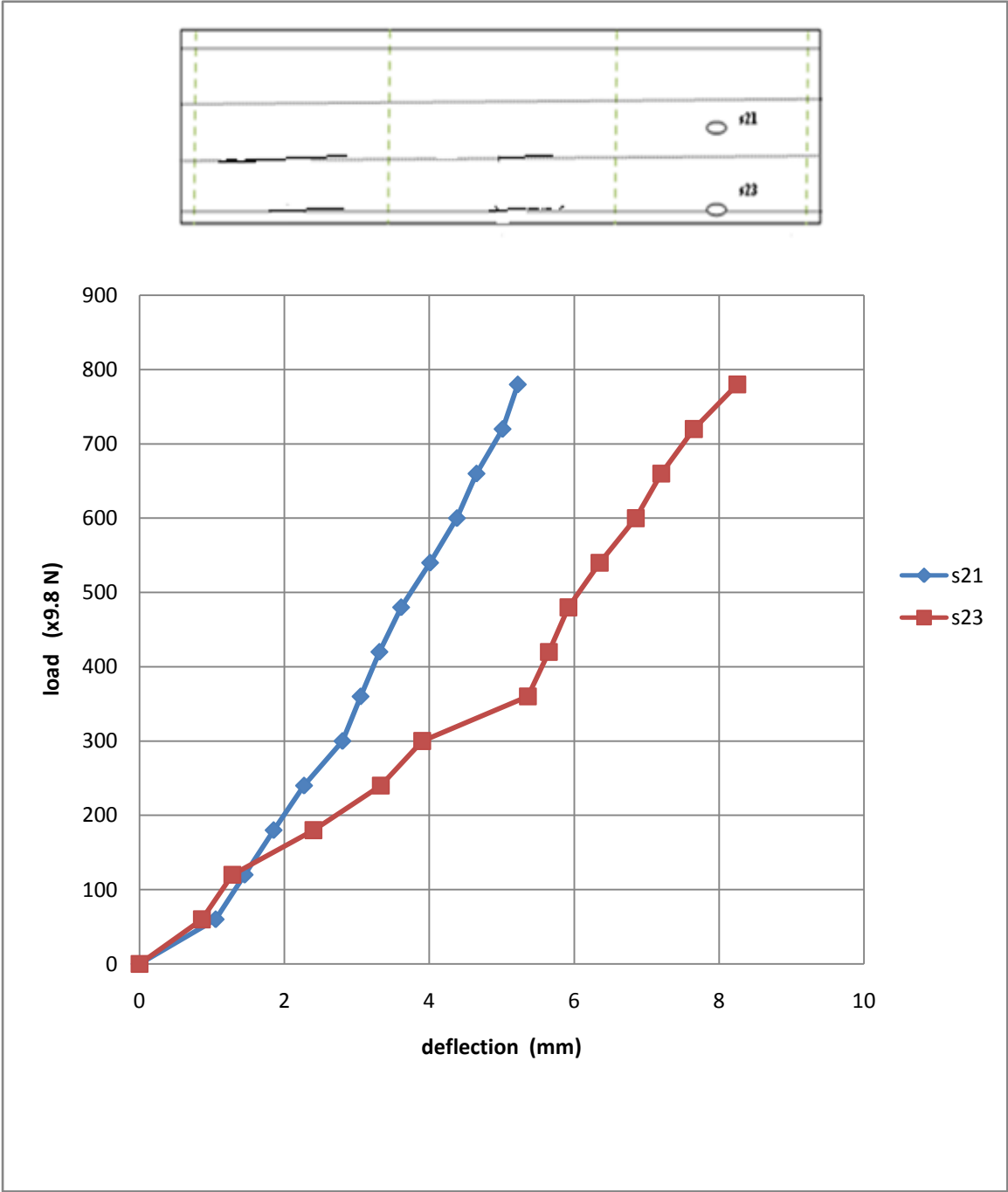


Fig 7.27 Load deflection plot for side span

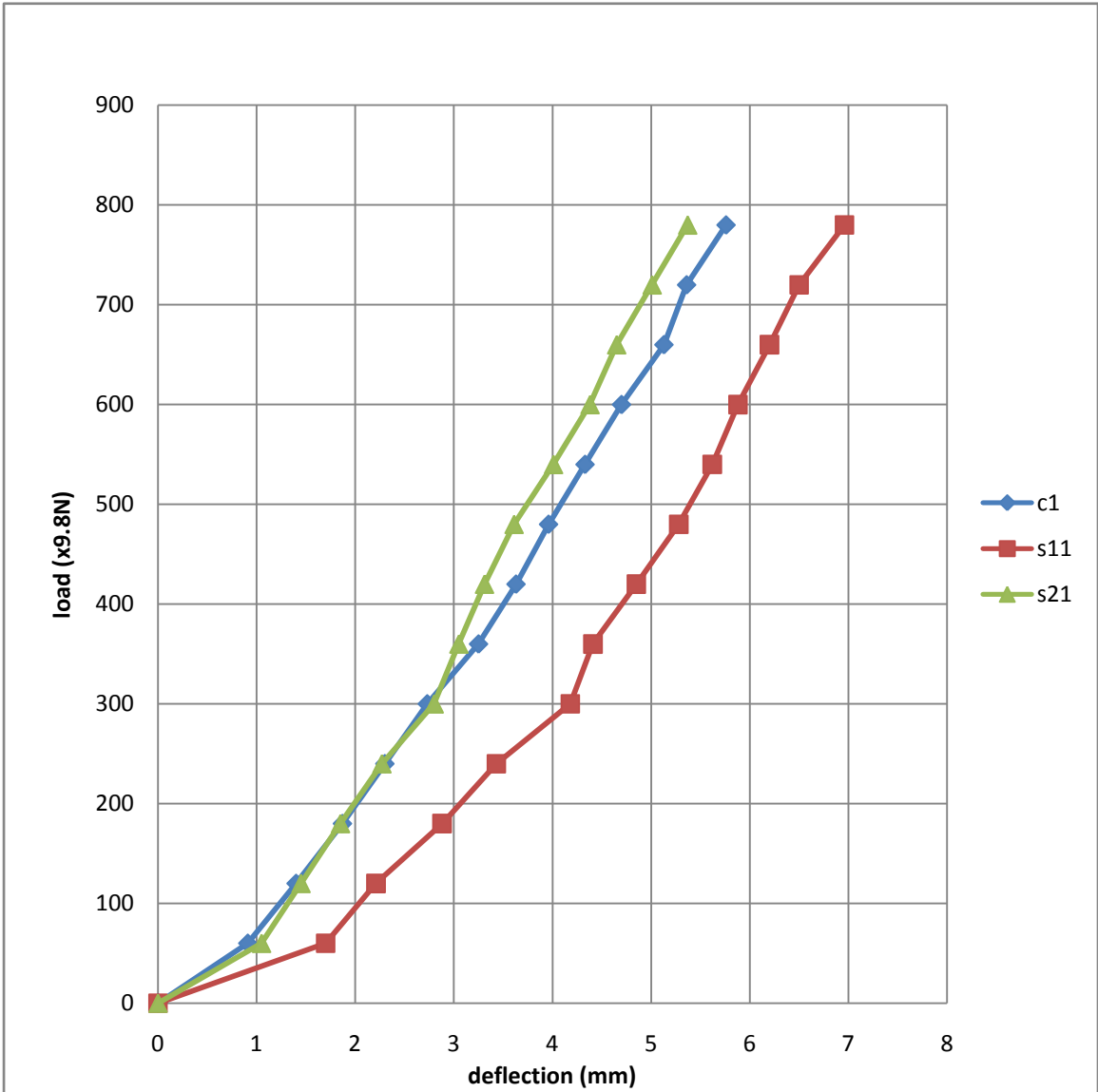


Fig 7.28 Comparison between deflection at central span and side spans

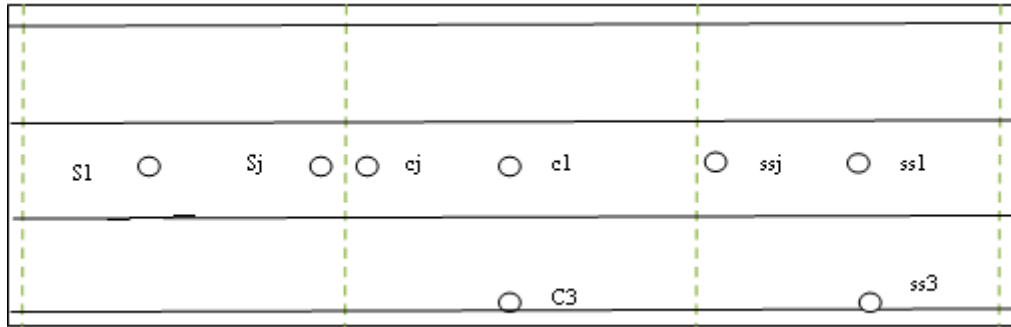


Fig 7.29 Deflection measurement points at the removal of jacks

Table 7.14 Deflection at various points after removal of jacks.

Time	Deflection at							
	c1	s1	ss1	c3	ss3	cj	sj	Ssj
Before	0.00	0.00	0.00	0.00	0.00	0.00	0.00	0.00
After	0.38	0.23	0.17	0.05	0.96	0.35	0.26	0.28
2:00hr	0.52	0.34	0.23	0.20	1.00	0.45	0.42	0.37
4:hr	0.57	0.38	0.22	0.22	0.65	0.55	0.47	0.46
7:hr	0.64	0.41	0.18	0.23	0.65	0.6	0.50	0.56
10:hr	0.64	0.41	0.18	0.23	0.64	0.61	0.59	0.56

7.4 Structural Testing Of Forms

7.4.1 F11 slab

The results of load testing using unstiffened channels on slab casted on form F11 are presented in table 7.15 and Fig.7.31. Fig.7.30 shows points where deflection was measured

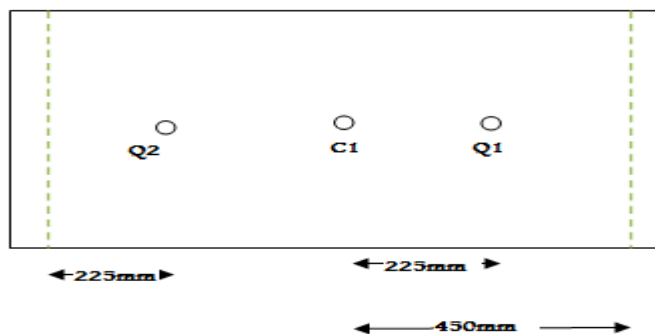


Fig 7.30 Points where deflection was noted during ultimate load test

Table 7.15 Deflection in F11 slab during ultimate load test

S.No.	Load	Deflection		
		Centre	Quarter	Quarter
1	0.0	0.00	0.00	0.00
2	2.0	0.06	0.02	0.03
3	4.7	0.11	0.06	0.10
4	7.0	0.15	0.11	0.13
5	9.0	0.19	0.14	0.18
6	11.0	0.20	0.16	0.20
7	13.0	0.24	0.18	0.24
8	16.0	0.28	0.20	0.28
9	17.7	0.31	0.23	0.30
10	19.5	0.32	0.25	0.34
11	22.5	0.35	0.26	0.36
12	25.7	0.37	0.28	0.38
13	28.0	0.40	0.30	0.41
14	30.0	0.41	0.31	0.43
15	31.5	0.42	0.32	0.45
16	34.2	0.44	0.34	0.45
17	35.5	0.45	0.35	0.47
18	37.3	0.47	0.36	0.48
19	39.5	0.49	0.37	0.49
20	41.5	0.50	0.38	0.50
21	43.5	0.51	0.40	0.51
22	45.5	0.52	0.41	0.53
23	47.7	0.53	0.42	0.55
24	50.24	0.55	0.44	0.56
25	52.7	0.56	0.45	0.57
26	54.8	0.58	0.47	0.59
27	56.5	0.59	0.48	0.6
28	59.0	0.61	0.49	0.61
29	61.0	0.62	0.51	0.62
30	62.7	0.64	0.52	0.64
31	64.5	0.65	0.53	0.65
32	66.5	0.66	0.54	0.67
33	68.5	0.67	0.55	0.68
34	70.5	0.68	0.56	0.70
35	72.5	0.69	0.57	0.70
36	74.5	0.71	0.58	0.72
37	76.0	0.72	0.585	0.74
38	79.2	0.74	0.59	0.75
39	81.2	0.75	0.595	0.76
40	82.5	0.76	0.60	0.78
41	84.5	0.77	0.62	0.79
42	86.5	0.79	0.63	0.80
43	87.2	0.85	1.17	1.20
44	88.0	1.15	1.36	1.35
45	89.5	1.20	1.36	1.38
46	90.5	1.24	1.40	1.38
47	91.5	1.26	1.41	1.39
48	92.7	1.30	1.43	1.40

49	93.7	1.34	1.45	1.42
50	95.0	1.37	1.47	1.43
51	95.7	1.39	1.49	1.45
52	96.7	1.40	1.50	1.46
53	98.0	1.44	1.52	1.48
54	98.5	1.46	1.53	1.49
55	100.7	1.50	1.55	1.52
56	102.5	1.55	1.60	1.55
57	104.0	1.59	1.61	1.57
58	105.2	1.63	1.62	1.59
59	106.5	1.68	1.64	1.60
60	108.0	1.71	1.67	1.62
61	109.2	1.73	1.70	1.64
62	110.5	1.76	1.70	1.66
63	112.2	1.80	1.75	1.68
64	115.0	1.85	1.80	1.70
65	116.5	1.90	1.82	1.73
66	117.8	1.95	1.84	1.75
67	119.5	2.04	1.88	1.78
68	122.5	2.08	1.92	1.80
69	123.5	2.11	1.94	1.82
70	125.5	2.18	1.96	1.85
71	127.5	2.23	2.00	1.90
72	128.7	2.26	2.03	1.92
73	130.7	2.31	2.06	1.95
74	133.5	2.40	2.11	1.98
75	135.7	2.45	2.14	2.00
76	136.5	2.48	2.17	2.02
77	138.0	2.50	2.19	2.04
78	140.2	2.55	2.20	2.06
79	141.0	2.60	2.24	2.09
80	142.5	2.62	2.26	2.12
81	144.0	2.68	2.30	2.14
82	145.5	2.72	2.30	2.18
83	148.0	2.80	2.38	2.20
84	149.2	2.85	2.40	2.22
85	151.0	2.90	2.43	2.25
86	153.5	2.95	2.48	2.28
87	155.2	3.01	2.51	2.30
88	157.5	3.06	2.55	2.35
89	162.7	3.22	2.63	2.42
90	165.2	3.31	2.71	2.48
91	166.5	4.1	3.68	3.00
92	170.0	4.4	3.70	3.10
93	172.5	4.8	3.83	3.50
94	175.5		3.90	
95	178.5		4.00	
96	181.7		4.50	
97	186.0		4.90	
98	189.3			
99	193.3			
100	199.3			

101	212.3			
102	226.0			
103	245.0			

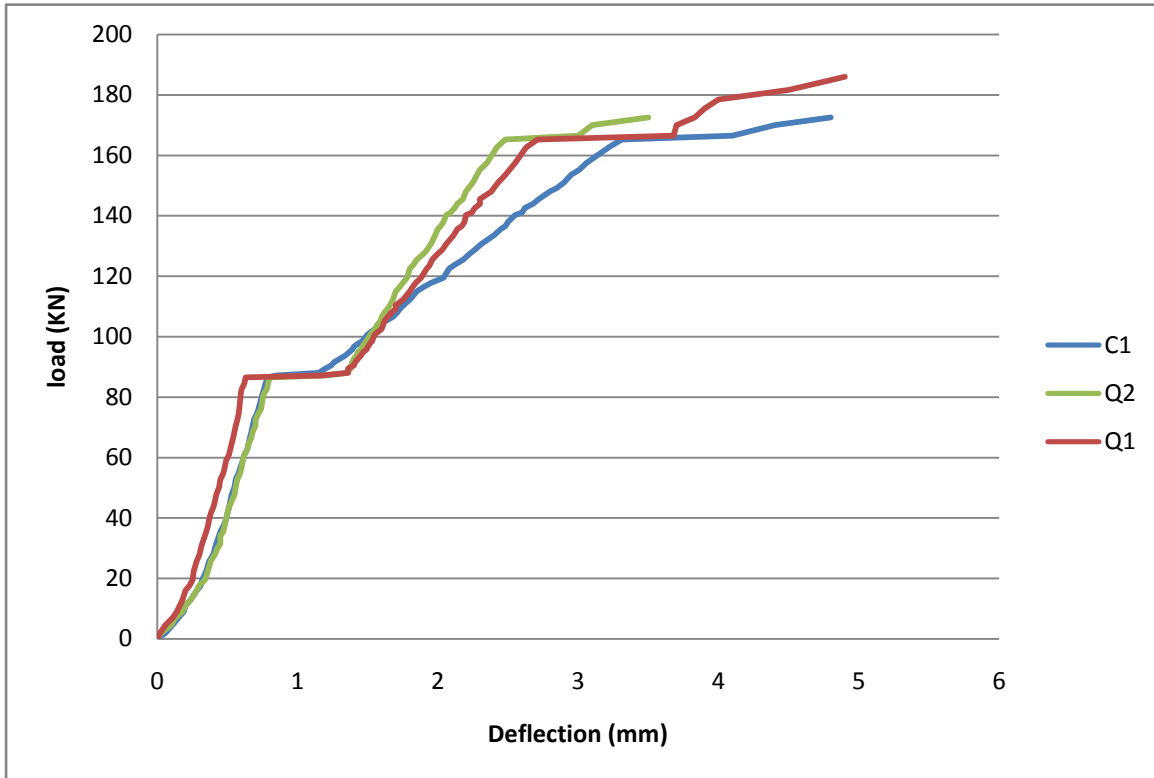


Fig.7.31 Deflection during ultimate load test



Fig.7.32 First crack developed at load level of 89KN

It was observed that first crack appeared at the load level of 89 KN (Fig.7.32). Also a load noise was heard at load level of 89KN. Also there was sudden increase in deflection at 86KN. After this, the load-deflection curve was again linear. There was widening of existing crack and no other crack appeared at this level. One more loud noise was heard at 97 KN and one more crack was observed 136 KN. One more crack was observed at load of 150KN (Fig. 7.33)



Fig.7.33 More cracks at load of 150 KN

After load level of 170KN rate of increase of deflection increased and it was difficult to measure the deflection as it appeared that at any time it will fall down. Q1 and Q2 dial gages were removed at load level of 172.5 KN and C1 dial gage was removed at 186 KN.

A loud noise was again heard on 180 KN

At the load level of 200 KN the cracks reached till the top of the slab. At the load level of 210 KN delamination of form was noticed (Fig.7.34). There was just a slight delamination.



Fig.7.34 Slight delamination at load of 210kN

At load of 200kN the cracks widened (Fig.7.35) and there was sound change after that



Fig.7.35 Widening of cracks at 200kN

At the load of 240 kN there was data acquisition system showed a slight decrease in load and then started increasing again and also there was sudden increase in deflection after that load. There was ultimate failure of slab at load of 245 kN. Slab broke into two pieces and fall down from the loading platform. Failure was also associated with a loud breaking noise. It failed along the central crack. It was a flexural failure. It was observed that the channels were delaminated from the base form.



Fig.7.36 Breakage of form F11



Fig 7.37 Delamination of channels

7.4.2 SLAB F21

Form F21 was having aggregates bonded to it. The results of the loading test performed on the slab casted on this form are shown in &table 7.16 and Fig.7.38a

Table 7.16 Deflection during ultimate load test of form F21

S. No.	Load (KN)	Deflection mm		
		Centre	Quarter Q1	Quarter Q2
1	0.0	0.00	0.00	0.00
2	2.0	0.05	0.01	0.05
3	3.6	0.07	0.02	0.07
4	5.1	0.10	0.03	0.09
5	7.4	0.15	0.05	0.13
6	9.4	0.18	0.07	0.16
7	12.1	0.23	0.09	0.19
8	14.1	0.26	0.10	0.22
9	18.6	0.32	0.13	0.25
10	21.6	0.35	0.14	0.27
11	23.5	0.38	0.16	0.29
12	34.9	0.49	0.25	0.36
13	39.6	0.55	0.29	0.40
14	48.1	0.60	0.34	0.43
15	60.6	0.70	0.41	0.53
16	65.6	0.73	0.44	0.57
17	70.6	0.75	0.48	0.59
18	72.4	0.78	0.49	0.60
19	75.1	0.80	0.51	0.62
20	77.4	0.83	0.52	0.63
21	80.4	0.84	0.53	0.65
22	83.4	0.86	0.55	0.70
23	87.1	0.89	0.57	0.72
24	89.4	0.91	0.59	0.73
25	92.6	0.95	0.61	0.77
26	94.6	0.97	0.63	0.78
27	98.1	2.25		
28	100.0	2.50		
29	102.1	2.60		
30	104.4	2.65		
31	106.6	2.70		
32	107.9	2.72		
33	109.4	2.80		
34	111.4	2.90		
35	114.0	3.30		
36	116.6	3.45		
37	117.9	3.55		
38	118.4	3.71		
39	122.4	3.77		
40	126.0	3.80		
41	128.4	3.92		

42	130.0	3.95		
43	133.6	4.05		
44	138.0	4.18		
45	140.1	4.28		
46	143.1	4.32		
47	145.0	4.44		
48	148.9	4.50		
49	150.0	4.60		
50	153.4	4.67		
51	155.1	4.77		
52	157.9	4.90		
53	161.4	4.95		
54	163.1	5.00		
55	165.1	5.10		
56	167.4	5.18		
57	169.4	5.29		
58	172.1	5.35		
59	173.9	5.40		
60	175.1	5.55		
61	178.4	5.60		
62	181.4	5.70		
63	183.1	5.80		
64	186.9	5.95		
65	190.6	6.08		
66	193.4	6.18		
67	196.9	6.25		
68	198.4	6.35		
69	200.0			
70	202.4			
71	273.6			

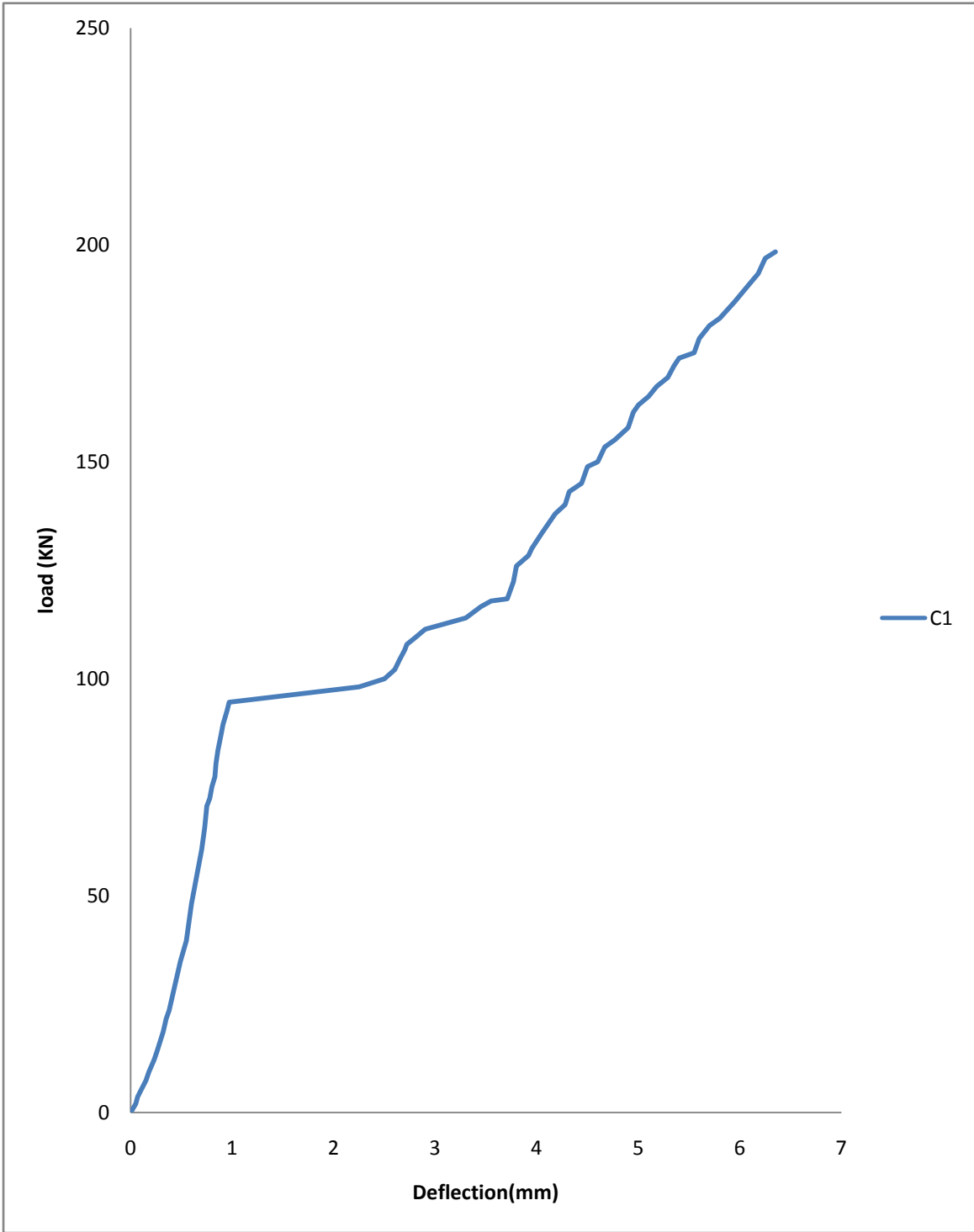


Fig.7.38a Deflection during ultimate load test of form F21



Fig.7.38b First crack in F21 slab

During this test it was found that the first crack was observed at load of 95 KN (Fig.7.38b) and a noise sound was heard at that load. At that load there was sudden increase in deflection. At that point Q1 and Q2 dial gages were removed. After load of 100 KN load deflection curve was again linear.

At the load of 120 KN second crack was observed and there was a horizontal crack development at the form concrete junction. It clearly shows that there is a delamination in the system. A loud noise was also heard at 120 KN.

At load of 200 KN there was a sudden increase in deflection rate and at that point C1 dial gage was removed. At load level of 220 KN, there was a easily noticeable delamination. Crack has not reached to the top at this load. Cracks were widened at the bottom side (Fig.7.39)

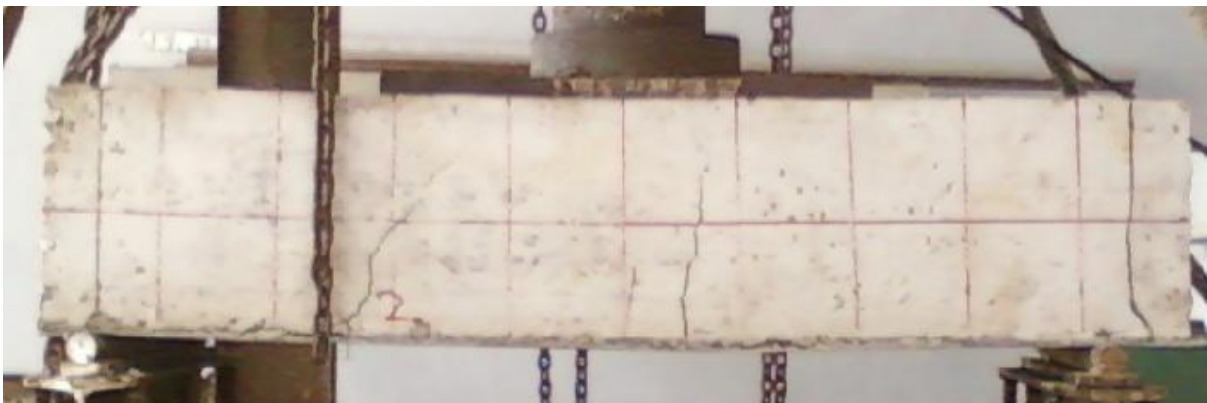


Fig 7.39 Horizontal cracks and delamination in F21 slab

At load level of 273.6 KN there was ultimate failure of the slab. It was broken into two pieces along the crack which was near to the quarter section. Failure was shear failure.

Channels were delaminated from base forms (Fig.7.40) and noticeable delamination of form from concrete was observed



Fig.7.40 Delamination of form F21

From the above two tests on the forms with and without aggregates, it was noted that aggregates increases the initial cracking load and the ultimate strength. Also less number of cracks were developed by using aggregates.

7.4.3 F31 Slab

Results of ultimate load carrying test of form F31 are presented in table7.17 and fig.7.41and 7.42. There was sudden failure of slab without any warning.

Table7.17 Deflection during ultimate load testing of for F31

S.No.	load	Deflection		
		centre	Quarter1	Quarter2
1	0.0	0.00	0.00	0.00
2	2.0	0.03	0.01	0.02
3	4.2	0.06	0.03	0.04
4	6.2	0.09	0.06	0.07
5	8.2	0.10	0.10	0.09
6	10.2	0.12	0.13	0.11
7	12.2	0.15	0.16	0.13
8	14.2	0.19	0.20	0.15

9	16.2	0.22	0.22	0.17
10	18.2	0.24	0.25	0.18
11	20.7	0.30	0.27	0.21
12	28.2	0.33	0.28	0.22
13	42.2	0.35	0.38	0.27
14	52.2	0.50	0.50	0.38
15	56.2	0.60	0.60	0.44
16	60.4	0.65	0.68	0.49
17	64.4	0.68	0.69	0.51
18	70.4	0.72	0.72	0.54
19	72.4	0.79	0.79	0.58
20	74.4	0.81	0.81	0.63
21	74.9	0.85	0.85	0.65

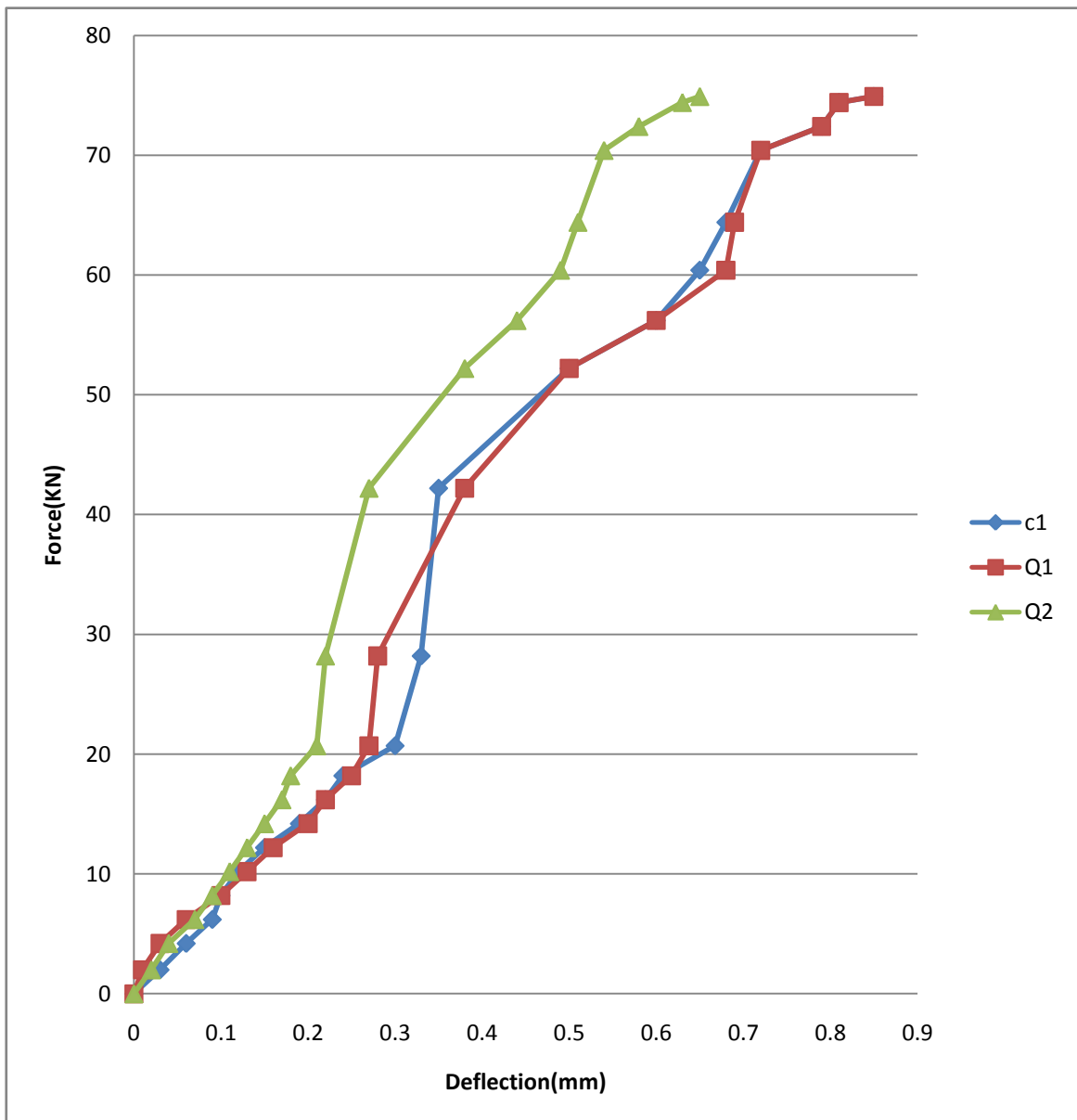


Fig. 7.41 Deflection during ultimate strength testing of form F31

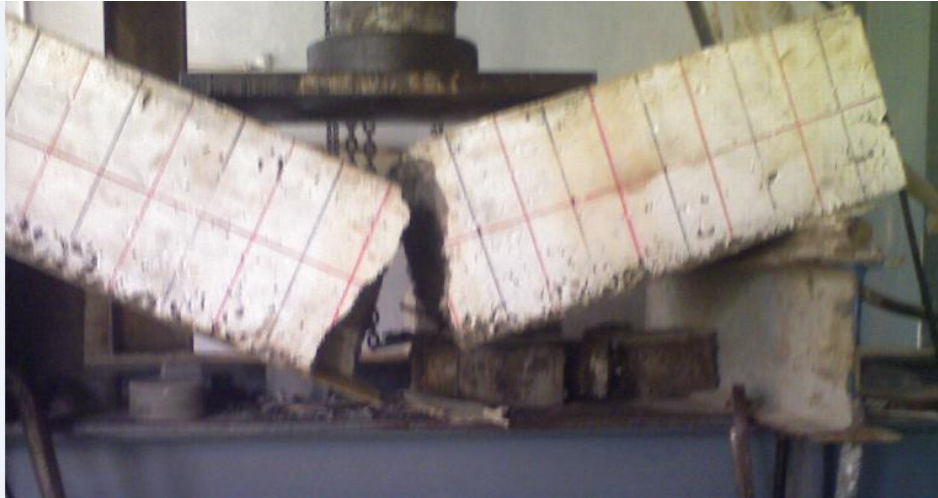


Fig. 7.42 Sudden brittle failure of form F31

From this it was concluded that the fibers used in this form were of poor quality and were not suitable for use in forms.

Chapter 8

CONCLUSION AND SCOPE FOR FURTHER STUDIES

8.1 GENERAL

In the present work GFRP woven roving mat of 450 gsm was used for preparing forms which served the purpose of forms when concrete was in wet state and reinforcement, when concrete has hardened. The conclusions drawn from the present study and scope for further research are discussed in this chapter

8.2 CONCLUSIONS

Following conclusions can be made based upon the laboratory investigations:

1 Hand lay-up GFRP sections can be used as forms. These serve the purpose of forms when concrete is in hardened stage and as reinforcement when concrete has hardened.

2 Four layer base form stiffened with four no., four layer channels is suitable for slab 200mm deep.

3 Aggregate bonding to form increase the initial crack load and increases the load carrying capacity.

4 If connectors are designed properly multiple span FRP forms can be used conveniently.

5 Slabs formed on four layer stiffened forms showed good ultimate strength

8.3 Scope for further work

The use of FRPs in concrete as formwork is relatively a new development in the construction industry and lot of research must go in before these forms are actively used in construction. Further work which should be done is summarised below:

1. Different sections can be tried out to work as forms.
2. Different types of Fibers should be tried to work as forms.

3. Forms prepared by pultrusion method should be tried.
4. Different type of connectors should be assessed, so that multiple span forms can be used.

REFERENCES

ACI 440.XR, (2006), Report on Fiber-Reinforced Polymer (FRP) Reinforcement for Concrete Structures, “Structurally Integrated Stay-In-Place FRP Forms.” Chapter 9, pp.175-200

Bank, L., Oliva, M.G., Russell, J.S., Dieter, A., Berg, A.C., Ehmke, F.G., (2004),“ Bridge -20-133 On US-151 With Fiber Reinforced Concrete Deck.” University Of Wisconsin, Madison

Bank, L., Oliva, M., Bae, H.U., Barker, J., (2006), “Pultruded FRP Plank As Formwork And Reinforcement For Concrete Structures.”Composites 2006 Convention And Trade Show, American Composites Manufacturers Association October 18-20, 2006, St. Louis, MO USA

Bank, L., Ringelstetter, T., Oliva, G.M., Russel , J., Matta, F.,Nanni,A., (2006,) “Development Of A Cost-Effective Structural FRP Stay-In-Place Formwork System For Accelerated And Durable Bridge Deck Construction.” Construction and building materials, Vol. 20, pp. 515-526

Berg,C. A., Bank, L., Oliva, G. M., Russell, J.,(2005), “Construction And Cost Analysis Of An FRP Reinforced Concrete Bridge Deck” Construction And Building Materials, Vol. 20,pp.515–526

Deskovic, N., Triantafillou, T.C., Meier, U., (1995), “Innovative Design Of FRP Combined With Concrete: Short-Term Behavior.” Journal Of Structural Engineering, July 1995, pp. 1069-1078.

Dieter, D.A., Dietsche, J.S., Bank, L.C., Olivia, M.G., And Russel, J.S., (2002), "Concrete Bridge Decks Constructed With Fibre-Reinforced Polymer Stay-In-Place Forms And Grid Reinforcing." Transportation Research Record 1814, 219-226.

Dietsche, J.S.,(2002), "Development Of Material Specifications For FRP Structural Elements For The Reinforcing Of A Concrete Bridge Deck ." ,Thesis ,Master Of Science (Civil Engineering) At The University Of Wisconsin – Madison 2002

Einde, D.V., Karbhari, M.V., Seible, F., (2007), "Seismic Performance Of FRP Encased Concrete Bridge Pylon Connection." Composites: Part B , Vol. 38 ,pp. 685–702

Einde, D.V., Zhao, L., Seible, F., (2003), "Use of FRP in Civil Structural Applications ." Construction And Building Materials, Vol. 17, pp389-403

Fam, A.Z., Honickman, H., (2009) ," Investigating A Structural Form System For Concrete Girders Using Commercially Available GFRP Sheet-Pile Sections" Journal Of Composites For Construction, Vol. 13, No 5, Oct 2009, pp. 455-465

Formwork Code Of Practice, (2007), Workplace Health And Safety Queensland, Department Of Justice And Attorney General FRPRCS-8,2007, "FRP SIP Formwork And Reinforcing For Concrete Highway Bridge Decks." University of Patras, Greece.

Hall, J.E., And Mottram, J.T., (1998) "Combined FRP Reinforcement And Permanent Formwork For Concrete Members" Journal Of Composites For Construction, vol.2, No.2, pp.78-86.

Hanus, P.J., Bank, L., Oliva, G.M., (2009), “ Combined Loading Of A Bridge Deck Reinforced With A Structural FRP Stay-In-Place Form.” Elsevier, Construction And Building Materials , Vol.23 ,pp. 1605–1619

Hanus, P.J.,(2007),“ Investigation Of A Deployable Military Bridge System With A Fiber Reinforced Concrete Deck.” Phd Thesis (Civil And Environmental Engineering) At The University Of Wisconsin – Madison.

Honickman, H.N., (2008), “Pultruded GFRP Sections As Stay In Place Structural Open Formwork For Concrete Slabs And Girders.” Theses For ME, Queens University Kingston,Ontario, Canada.

Jaffery, A.D., (2001),“ Concrete filled glass fiber reinforced shells under concentric compression.” Thesis for Master of Applied Science, University of Toronto.

Li, T., Feng, P., And Ye, L., (2006) “Experimental Study On FRP-Concrete Hybrid Beams.” Third International Conference On FRP Composites In Civil Engineering (CICE 2006) December 13-15 2006, Miami, Florida, USA, pp.343-346.

Li, G., Ji, G., Li, X., Pang, S., Jones, R., (2008),” Experimental Study Of FRP Tube Encased Concrete Cylinders Exposed To Fire.” Composite Structures, Vol. 85 ,pp.149–154

Lu, L.W., Kanatharana, J., (1998) ,“Strength And Ductility Of Concrete Columns Reinforced By FRP Tubes.” Proc. 2nd Int. Conf. Composites In Infrastructure, Tucson AZ, pp. 370-384

Matta, F., Nanni, A., Bank, L., (2004) "Accelerated Construction Of Bridge 1480 2301 Greene Country, Missouri With Prefabricated Stay In Place Glass Fiber Reinforced Polymer Reinforcement." National University Transportation Center At Missouri University Of Science And Technology

Parvatheni, H.K., Iyer, S.L., Greenwood, M., (1996), "Design And Construction Of Test Mooring Pile Using Superprestressing Procedure Of Advanced Composite Materials In Bridges And Structures." Montreal Canada, pp.313-324

Peurifoy, R.L., "Form work for concrete structures" McGraw Hill Book Company

Reising, R., Shahrooz, M.B., Hunt, J.V., (2004), "Performance Comparison Of Four Fiber-Reinforced Polymer Deck Panels." *Journal Of Composites For Construction*, Vol. 8, No. 3, June 1, 2004. pp. 265-274

Schaumann, E., Valle, E.T., Keller, T., (2008), "Direct Load Transmission In Hybrid FRP And Lightweight Concrete Sandwich Bridge Deck." *Composites: Part A* Vol.39 ,pp.478-487

Seible, F., Burgueño, R., Abdallah, M.G., Nuismer, R., (1996) "Development Of Advanced Composite Carbon Shell Systems For Concrete Columns In Seismic Zones." *Proc., 11th World Conf. On Earthquake Engineering*, Pergamon-Elsevier Science, Paper No. 1375, Oxford, U.K.

Seible, F., Karbhari, V.M., Burgueno, R., Seaburg, E., (1998), "Modular Advanced Composite Bridge Systems For Short And Medium Span Bridges." *Proceedings Of Fifth International Conference On Short And Mediumspan Bridges*, Calgary, Canada.

Zhou, Z., Mirmiram, A., Shahway, M., (2005), "Multicellular Fiber-Reinforced Polymer (FRP) Composite Bridge Deck Systems Produced From Adhesively Bonded Pultrusions." Journal Of Compo

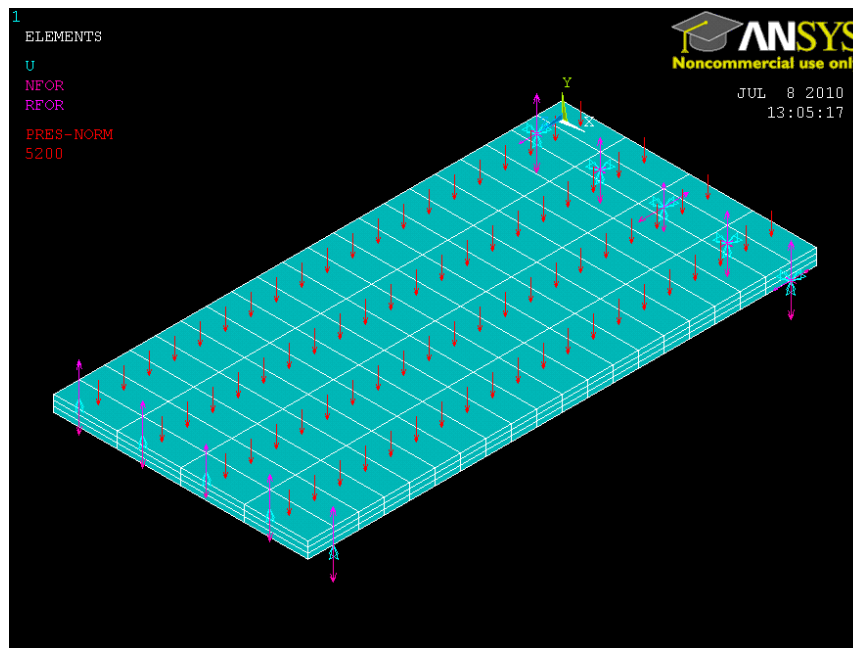
Appendix A

ANSYS Software was used to do the FEM modelling of Forms used. In this analysis FRP forms stiffened with channels were converted into equivalent plates and were modelled as solid shell elements. The basic aim of this analysis was to get idea about the deformed shape of the form during the concrete or sand loading.

A.1 FEM modelling for D11 forms

For D11 forms (double layer base forms stiffened with single layer channel sections) equivalent plate of thickness 18mm. Details about the modelling are presented in Fig.A1 . uniformly distributed pressure load was applied to get deflection due to concrete loading.

Results showed that maximum deflection in this case would be 29.4 mm (Fig. A2)



FigA1. FEM modelling for D11 form

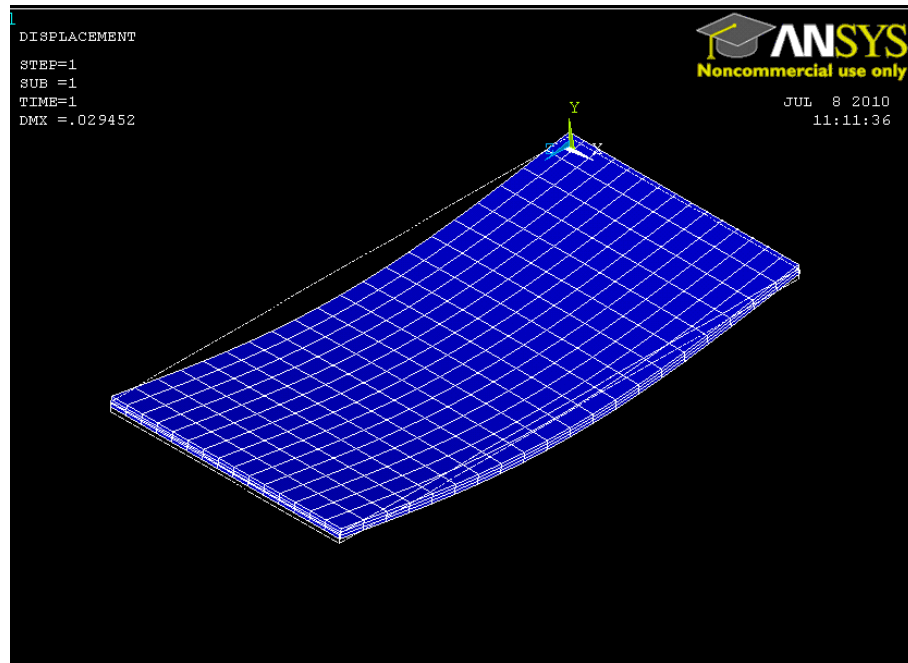


Fig.A2 results obtained for D11 form

A.2 FEM modelling for D13 form

D13 form was a stiffened double layered three span form. FEM modelling for D11 subjected to concrete loading is shown in Fig A3 and results in Fig A4. It was observed that maximum deflection of 17.02 mm is at side forms

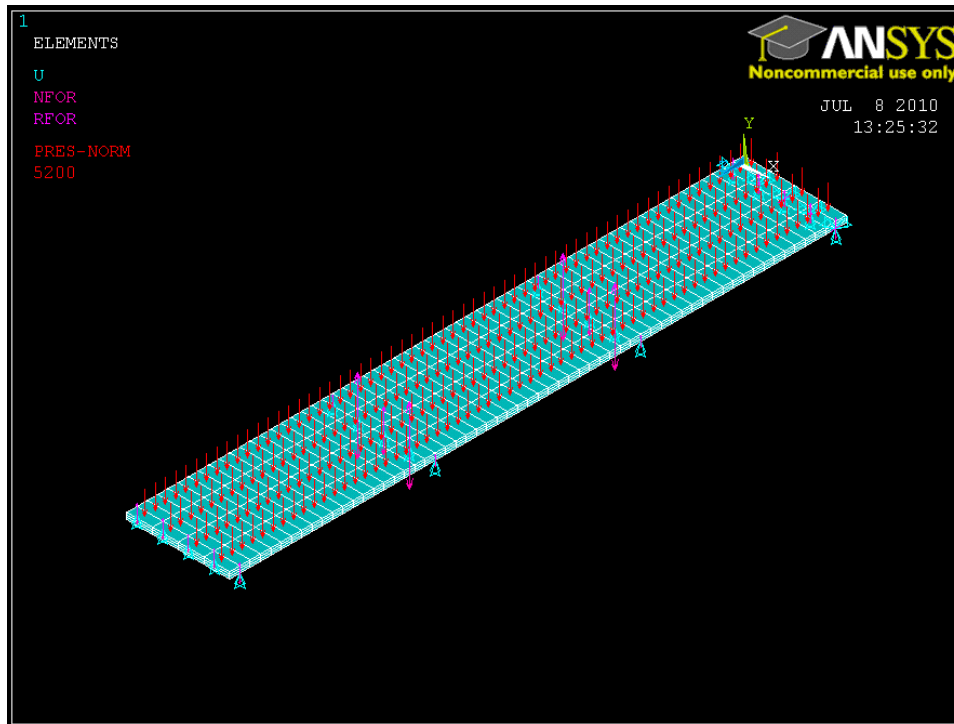


Fig.A3 FEM modelling for D13

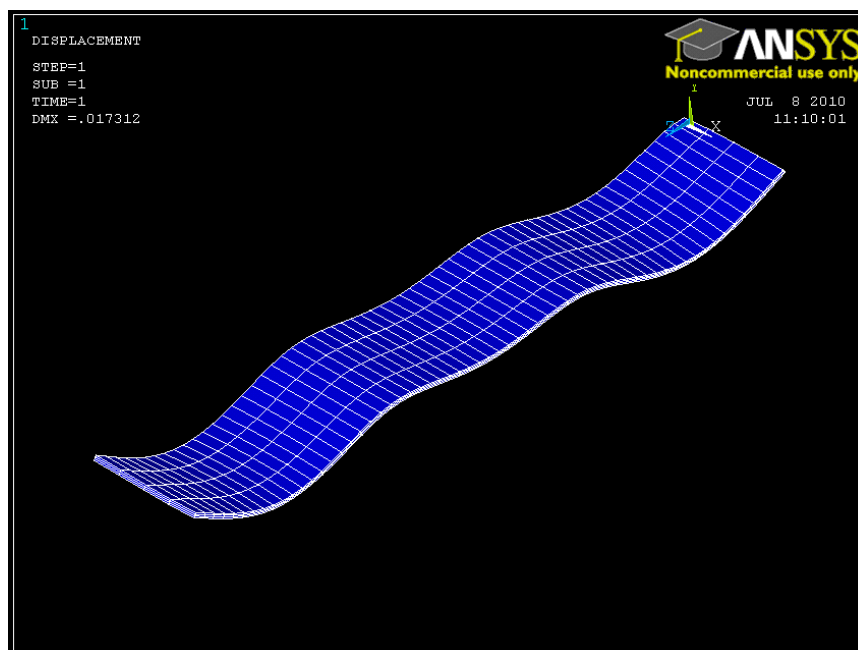


Fig.A4 Results for FEM modelling form D13

A.3 Form F11

For form F11 four layered base form stiffened with channels was converted into equivalent plate with dimension 31mm. Maximum deflection obtained was 5.7 mm . FEM modelling for F11 is shown in fig A5 and results in Fig. A6

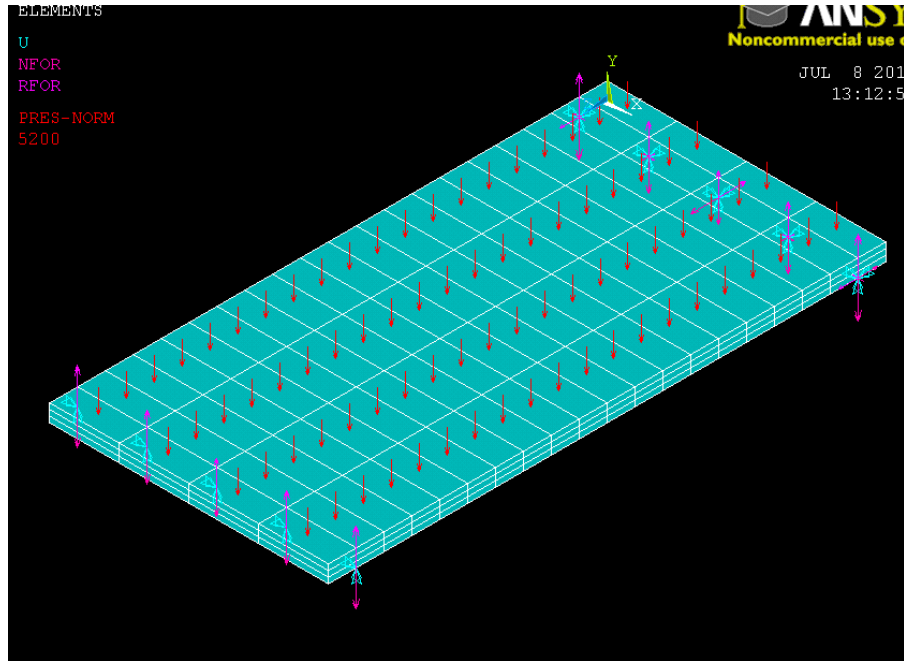


Fig.A5 FEM modelling for F11

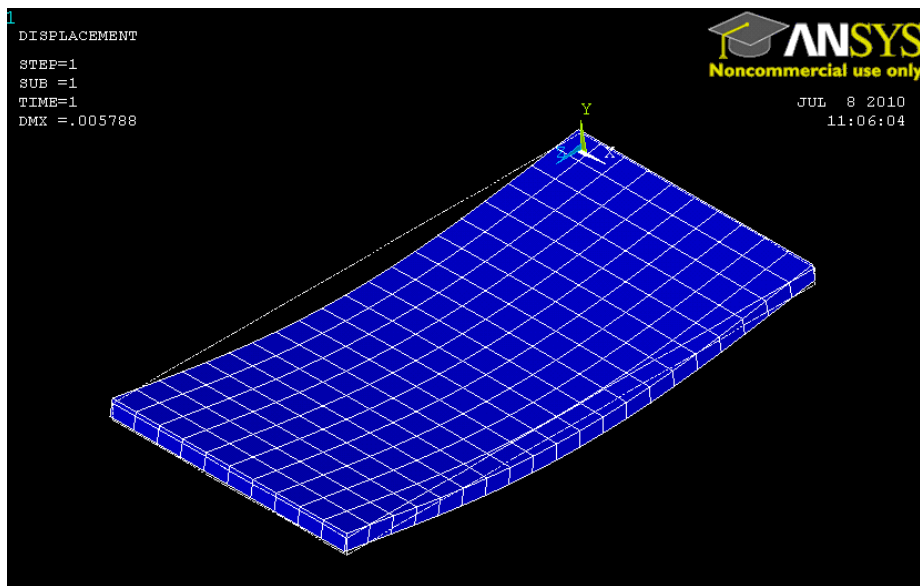


Fig.A6 Results for F11

A.4 Form F23

F31 is a stiffened four layered three span form. This was again converted into equivalent plate of thickness 31mm. Results showed that the maximum deflection will be at side span. FEM modelling for F11 is shown in fig A7 and results in Fig. A8

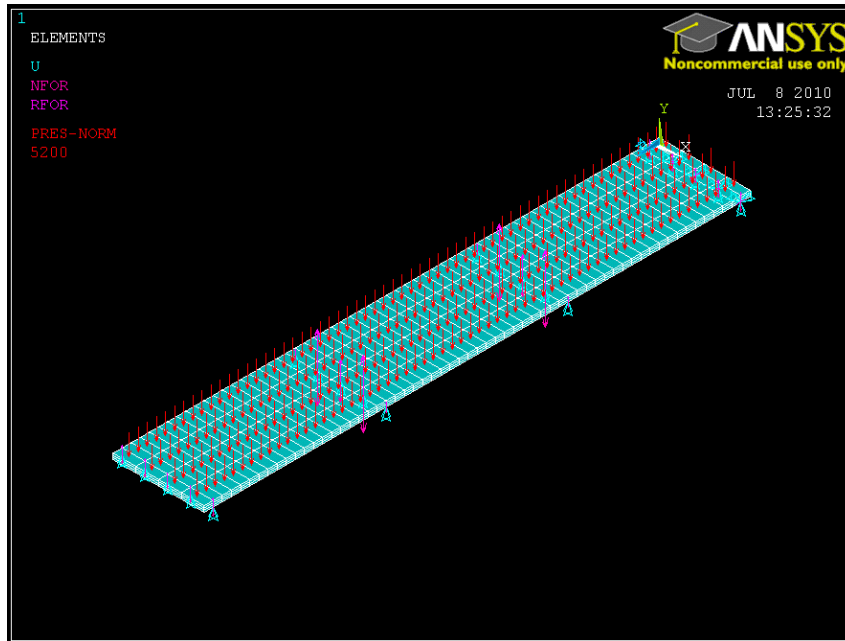


Fig.A7 FEM modelling for form F23

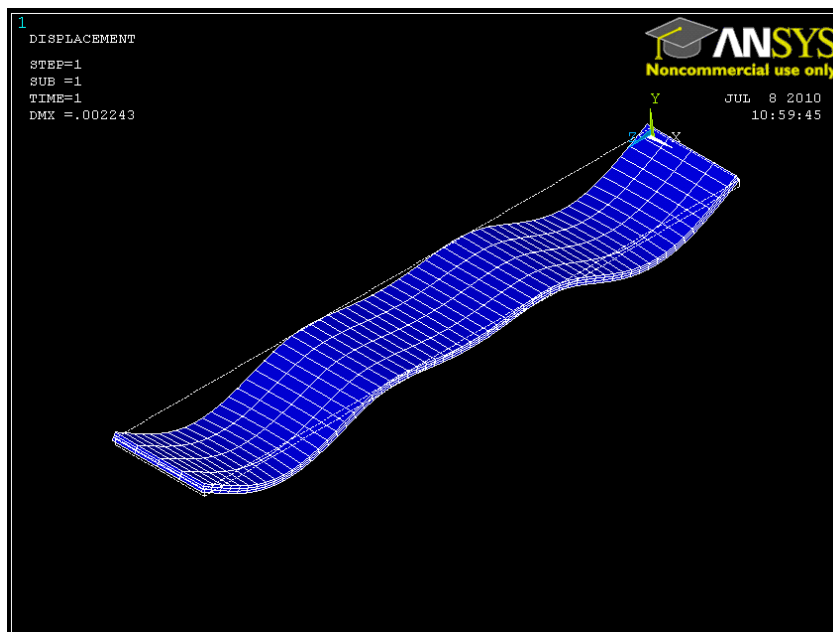


Fig.A8 Results for F23

Appendix B

Tensile testing of FRP iso-resin matrix

For tensile testing of FRP matrix ASTM 3039 D method was used. Firstly single layer FRP strips were prepared having length 500 mm and width 15 mm. Then 150 mm from both the ends, it was converted into five layered strip by placing two single layered strips on each surface of the previously prepared strip. It was done so that the ends do not fail.

Three such strips were prepared and subjected to tensile loading in UTM. Load at failure was recorded. Fig B1 shows FRP strip for tensile testing.



Fig.B1

Table shows the details of the strips

S.No.	Avg width(m)	Avg thickness(mm)	Load (KN)	Tensile strength KN/mm ²
1	14.7	1	1.4	95.23
2	16.5	1	1.8	111.0mm
3	16.0	1	1.5	93.0mm

Avg value of tensile strength i.e 100 N/mm was used in the analysis work.

APPENDIX C

Role of FRP form as reinforcement

In this work four layered GFRP sheet stiffened with four no. four channelled section is used as formwork for slabs. This appendix includes the analysis regarding role of this form as reinforcement.

Concrete used M25

Concrete modulus: $E_C = 4750(25)^{1/2} = 23.750 \text{ GPa}$

Beta factor: $\beta_1 = 0.85$

Area of plate = $4 * 500 = 2000 \text{ mm}^2$

Effective depth of plate: $d_{pl} = 202 \text{ mm}^2$

Area of four channels = $(25 * 4 * 2 + 46 * 4) * 4$

$$= 1536 \text{ mm}^2$$

Effective depth of channels: $d_{ch} = 173 \text{ mm}^2$

Avg. Effective depth: $d_{eff} = (202 * 2000 + 173 * 1536) / (1536 + 2000)$

$$= 189.4 \text{ mm}$$

Area of form $A_{st} = (A_{ch} + A_{pl})$

Avg. reinforcement density: $(A_{st}) / (b * d_{eff})$

$$= 3536 / (500 * 189.4)$$

$$= 0.0373$$

Avg. Modulli ratio: $n_f = \frac{E_f}{E_c} = 3.5 / 23.750$

$$=0.147$$

Ultimate tensile strength of FRP'S $f_{fup} = 100N/mm^2$

Balanced reinforced ratio:

$$\begin{aligned} &=0.85*\beta*(f_c/f_{fup})*((E_f*\epsilon_{Cu})/(E_f*\epsilon_{Cu}+f_{fup})) \\ &=0.85*0.85*(25/100)*((3.5*10^3*0.003)/((3*10^3*0.003)+100)) \\ &=0.1491 \end{aligned}$$

This is over reinforced section as avg. Reinforced density is greater than balanced reinforced ratio.

m= concrete constant

$$\begin{aligned} m &= (E_c*\epsilon_{Cu})/(1.7*\beta_1*f_c) \\ &= (23.750*0.003*10^3)/(1.7*0.85*25) \\ &= 1.972 \end{aligned}$$

Cult= neutral axis depth at ultimate load

$$\begin{aligned} K_{ult} &= ((2*m*p_f*n_f) + (m*p_f*n_f)^2)^{1/2} - p_f*n_f \\ &= ((2*0.147*0.0373*1.972) + (1.972*0.126*0.373)^2)^{1/2} - (0.147*0.0373*1.972) \\ &= 0.1366 \end{aligned}$$

$$\Rightarrow K_{ult} = C_{ult}/d_{eff}$$

$$\begin{aligned} C_{ult} &= 0.1366*189 \\ &= 25.87\text{mm} \end{aligned}$$

Stress in FRP base form

$$\begin{aligned} F_{pla} &= 0.003*3.5*10^3 \frac{202-25.87}{25.87} \\ &= 71.64 \text{ N/mm}^2 \end{aligned}$$

$$\text{Force in FRP plate: } T_{fp} = A_{fp} * E_{fp} * \epsilon_{Cu} * (d_{fp} - x_{ult}) / (x_{ult})$$

$$=71.64*2000$$

$$=143291\text{N}$$

$$\text{Force in FRP channels } f_{ch} = 0.003 * 3.5 * 103 * ((17.3 - 25.87) / 25.87)$$

$$T = 59.7 * 1536$$

$$= 91724$$

$$\text{Moment capacity: } M_n = T_p * \left(d_p - \frac{(\beta_1 * C_{ul})}{2}\right) + T_{ch} * \left(d_{ch} - \frac{(\beta_1 * C_{ul})}{2}\right)$$

$$= 42230219.15$$

This moment corresponds to load of 250 KN when applied to slab through plate of dimension 450mmx250mm